Mitochondrial Dynamics Alteration in Astrocytes Following Primary Blast-Induced Traumatic Brain Injury

Fernanda Guilhaume Correa

Dissertation submitted to the faculty of the Virginia Polytechnic Institute and State University in partial fulfillment of the requirements for the degree of

Doctor of Philosophy
In
Translational Biology, Medicine, and Health

Pamela J. VandeVord, *Thesis advisor*
Alicia Pickrell
Michelle Olsen
Harald Sontheimer

September 8th, 2022
Blacksburg, VA

Keywords: primary blast-induced traumatic brain injury, mild, acute, sub-acute, astrocytes, mitochondrial dynamics, fission

Mitochondrial Dynamics Alteration in Astrocytes Following Primary Blast-Induced Traumatic Brain Injury

Fernanda Guilhaume Correa

Abstract

Mild blast-induced traumatic brain injury (bTBI) is a modality of injury that has been of major concern considering a large number of military personnel exposed to the blast wave from explosives. bTBI results from the propagation of high-pressure static blast forces and their subsequent energy transmission within brain tissue. Current literature presents a neuro-centric approach to the role of mitochondria dynamics dysfunction in bTBI; however, changes in astrocyte-specific mitochondrial dynamics have not been characterized. As a result of fission and fusion, the mitochondrial structure is constantly altering shape to respond to physiological stimuli or stress insults by adapting structure and function, which are intimately connected. Dysregulation of the protein regulator of mitochondrial fission, DRP1, and upregulation in the phosphorylation of DRP1 at the serine 616 site is reported to play a crucial role in astrocytic mitochondrial dysfunction, favoring fission over fusion post-TBI. Astrocytic mitochondria are starting to be recognized to play an essential role in overall brain metabolism, synaptic transmission, and neuron protection. Mitochondria are vulnerable to injury insults leading to the worsening of mitochondrial fission and increased mitochondrial fragmentation. In this study, a combination of *in vitro* and *in vivo* bTBI models were used to examine the effect of blast on astrocytic mitochondrial dynamics. Acute differential remodeling of the astrocytic mitochondrial network was observed, accompanied by an acute (4hr) and sub-acute (7 days) activation of the GTP-protein DRP1. Further, results showed a time-dependent reactive astrocyte phenotype transition in the rat hippocampus. This discovery can lead to innovative therapeutics targets to help prevent secondary injury cascades that involve mitochondria dysfunction.

Mitochondrial Dynamics Alteration in Astrocytes Following Primary Blast-Induced Traumatic Brain Injury

Fernanda Guilhaume Correa

General Population Abstract

Blast-induced traumatic brain injury (bTBI) is a modality of injury that has become prominent considering a large number of military personnel exposed to a blast wave caused by explosives. Blast injury results from the energy transmission of the blast wave to the brain. Within the brain, there are specialized cells, called astrocytes, that help maintain a healthy environment. This work investigates the role that astrocytes play during the injury recovery process. Within the astrocytes, there are organelles called mitochondria, that help maintain the energy for the cell. The number and function of mitochondria can change in response to the brain injury. They can increase in number by a process called fission and they can decrease in number by a process called fusion. These events effect the function of the mitochondria. Researchers have methods that can identify changes in the number and function of the mitochondria. In this work, astrocyte mitochondrial dynamics were examined and compared using models of bTBI. We found significant changes in the mitochondria of astrocytes, which could lead to an unhealthy environment in the brain. This discovery can lead to new treatments for patients that may improve their quality of life following bTBI.

Dedication

I dedicate the result of the effort made throughout this journey to my parents, Fernando Correa and Simone Guilhaume, to my brother, Andre Correa, and to my husband, Juan Camilo Ramirez. Thank you for trusting and believing in my dreams and for all the advice, support, and love. Eu amo voces.

Acknowledgements

I would like to express my gratitude to Dr. VandeVord, who played a big role as my advisor and mentor and has provided me with abundant guidance, knowledge and encouragement helping me to improve and grow as a graduate student. Thank you for letting me be part of your research team and I am humbled by your faith in me. I am grateful for your patience over the last 5 years and appreciate you helping me become more self-assured as a person and scientist.

To my committee members, Dr. Alicia Pickrell, Dr. Michelle Olsen, and Dr. Harald Sontheimer, thank you for taking the time to review this work and offer constructive criticism during our meetings. Your extensive knowledge and feedback served as a solid foundation for my dissertation work.

I want to express my gratitude to my amazing TNT lab colleagues for all of your support, input, and amazing teamwork. I would not be able to successfully complete this journey without you all. I want to especially thank Dr. Susan Murphy for reading all of my protocols, abstracts, and publications and for her assistance in helping me become a better writer. I would like to thank Carly and Caiti-Erin for all the coffee walks, laughs, encouragement. I appreciate Dr. Nora Hlavac for teaching me about *in vitro* models and letting me shadow her during my first year in the lab. Thank you, Dr. Elizabeth McNeil, for all the lessons you taught me in the lab and for being an amazing friend. You all have my sincerest gratitude.

Thank you to the wonderful friends that I met in Roanoke. I am grateful that Carmen, Alessandro, and Roque allowed me to become a member of their family. I appreciate all of the Saturday dinners, constant encouragement, advice, and laughs. Thank you, Carmen, for being the best workout companion I could wish for at 5 a.m. Rachana, I learned so much from you and grew a lot as a scientist. Thank you for being an awesome roommate, friend and especially for the care you took with my baby Zeus. Gabriela

thank you for your great friendship and support. I appreciated the rock climbing lessons! Maybe one day I won't be so scared.

Most importantly, I want to express my sincere gratitude to my family. It is difficult to move to a new country when you have to say goodbye to the people you care and love the most. Mamae, Papai, and Dedeco, thank you so much for all the sacrifices you made so that I could follow all of my dreams. I am grateful for your constant support in helping me to keep fighting, to be brave, to smile, to dream, and, most importantly, to always be a good person in my heart and mind, no matter what. My greatest inspiration will always be you. For my husband, Juan Camilo, thank you for agreeing to be part of this journey with me. I know that spending so many years apart was difficult, but you were always there for me, and I cannot express how grateful I am for that, te amo mi vida. My family unconditional love and support made it possible for this achievement.

Table of Contents

Abbreviations

ATP - Adenosine triphosphate

BBB - Blood-brain barrier

bTBI – blast-induced traumatic brain injury

CA1 - Cornu Ammonis 1

CA2 - Cornu Ammonis 2

CA3 - Cornu Ammonis 3

CCCP - Carbonyl cyanide 3-chlorophenylhydrazone

CDK5 - Cyclin Dependent Kinase 5

CNS – Central nervous system

DG - Dentate gyrus

DOD – Department of defense

DRP1 - Dynamin-related protein 1

GCS - Glasgow Coma Scale

GFAP - Glial fibrillary acidic protein

HOS - High-rate overpressure simulator

ICP - Intracranial pressure

IMM - inner mitochondrial membrane

IMS – Intermembrane space

MiNA - Mitochondrial Network Analysis

MPTP - Mitochondrial permeability transition pore

NF-kB - Nuclear factor kappa B

NOX4 - Nicotinamide adenine dinucleotide phosphate oxidase 4

OMM - Outer mitochondrial membrane

P2 – Two days postnatal

PA – Primary astrocytes

PCNA - Proliferating cell nuclear antigen

pDRP1^{s616} – Phosphorylated-DRP1 serine 616 site

pDRP1^{s637} – Phosphorylated-DRP1 serine 637 site

ROS – Reactive oxygen species

SOD2 - Superoxide dismutase 2

TBI – Traumatic brain injury

TOMM20 - Translocase of the outer mitochondrial membrane complex subunit 20

Chapter 1. Introduction

1.1. Significance

Traumatic brain injury (TBI) is a worldwide public health concern, affecting millions of people every year, and represents one of the major causes of long-term disability and mortality (Dewan et al., 2019). In the United States, approximately 1.7 million people suffer a TBI, with 75% being a mild TBI (mTBI), usually caused by a fall, a motor vehicle accident, an assault, or sports-related injuries (Swanson et al., 2017)**.** Moreover, according to the Department of Defense (DOD), TBI is one of the most common injuries among the military and veteran population, with 82.3% being an mTBI (*DOD TBI Worldwide Numbers | Health.Mil*, 2022). Specifically, mild blast-traumatic brain injury (bTBI) is a prevalent head injury among military combat personnel and veterans due to their exposure to explosives during armed conflict and training.

TBI is a complex and heterogeneous injury, defined by sufficient external physical/mechanical forces acting on the head and brain parenchyma, triggering a secondary insult of cellular and molecular dysfunction leading to a progressive change of the typical architecture and function of the brain. Clinical manifestations of bTBI include ongoing persistent symptoms, including sensory, somatic, neurobehavioral, neuroendocrine, and cognitive deficits, which are driven by underlying cellular and molecular consequences of the injury. Treatments for bTBI remain elusive and are limited to symptom management because the pathophysiology of symptoms is poorly understood. In addition, there is a critical knowledge gap in understanding the cellular and molecular response post-blast exposure.

TBI involves response from both neural and non-neural cells (glia) that interact to maintain the typical architecture and function of the brain. Glial cells, specifically astrocytes, are biochemically and structurally coupled with neuronal cells. Astrocytes are of particular interest in TBI pathology because of their unique ability to respond to insults and their different neuroprotective roles in a healthy (Matias et

al., 2019) and injured brain (Burda et al., 2016; Bylicky et al., 2018; Matias et al., 2019). They can respond to a myriad of CNS insults through morphological, molecular, and functional changes known as astrocyte reactivity (Escartin et al., 2021; Khakh & Sofroniew, 2015)**.** Although astrocyte reactivity does present favorable properties, the prolonged abnormal activation causes detrimental effects on neuronal functionality leading to long-term cognitive issues such as memory impairments (Agoston, 2017; Sajja et al., 2016; Zhou et al., 2020).

Current literature presents a neuro-centric approach to the role of mitochondria dysfunction in focal (blunt or stab wound) and diffuse (blunt or blast) injuries (Arun et al., 2013; Cheng et al., 2012; Fischer et al., 2016)**.** The role of mitochondria in astrocytes during TBI pathophysiology has been overlooked. However, astrocytic mitochondria are starting to be recognized as playing an essential role in astrocytic function (calcium signaling, synaptic transmission, glutamate uptake) and ultimately this is translated to the astrocyte's response in neuron protection. Just like in neurons, astrocytic mitochondria are vulnerable to injury insults leading to altered mitochondrial dynamics and fragments due to an increase in fission and those structural changes can trigger an excessive generation of reactive oxygen species (ROS), among other issues, therefore, further worsening the astrocytes, response to injury (Ishii et al., 2017; Lima et al., 2018; Motori et al., 2013; Sarkar et al., 2018). Changes in mitochondrial dynamics affecting activity and its possible link to astrocyte reactivity have not yet been characterized concerning mild bTBI. Therefore, this dissertation research focuses on characterizing acute astrocytic mitochondrial dynamics, focusing on the unique pattern of the GTP-protein DRP1 and reactive astrocyte phenotype transition in *in vitro* and *in vivo* models of mild bTBI.

1.2. Hypothesis and Specific Aims

The working hypothesis for the study conducted here is: ***Blast-induced traumatic brain injury (bTBI) causes altered astrocytic mitochondrial dynamics leading to an increase in mitochondrial fragmentation by phosphorylated DRP1-mediated mitochondrial fission serine 616*** (Figure 1). The hypothesis was tested using the following specific aims and the characterization within the *in vitro* and *in vivo* models of bTBI.

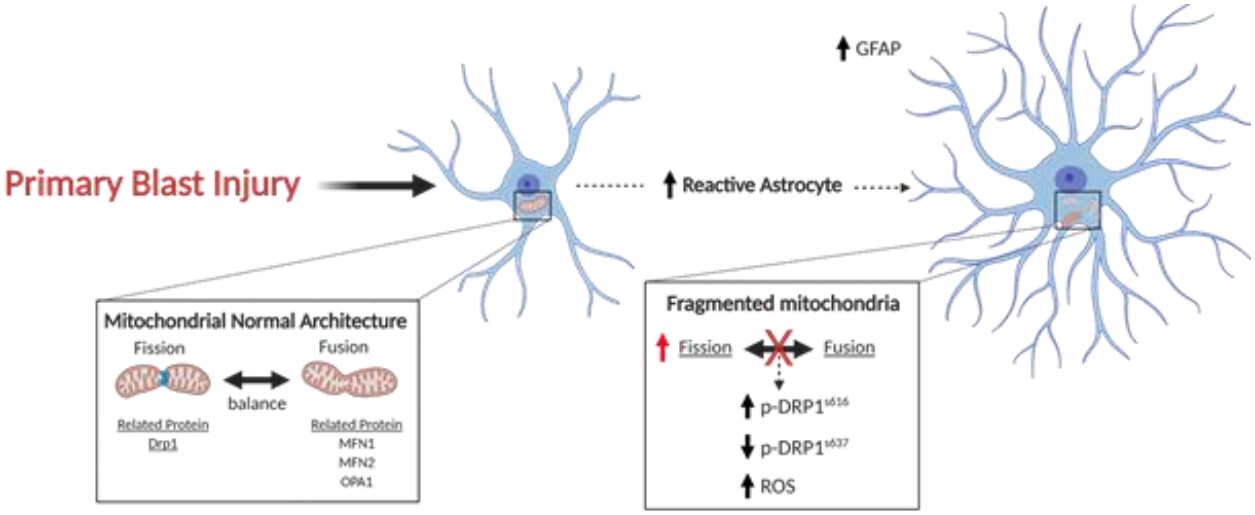

Figure 1.1: Hypothesis. Blast-induced traumatic brain injury (bTBI) causes an acute altered astrocytic mitochondrial dynamic leading to an increase in mitochondrial fragmentation by the phosphorylated DRP1-mediated mitochondrial fission serine 616 ($pDRP1^{s616}$).

I. Specific Aim 1: Characterize the acute effects of bTBI mechanical insult to initiate aberrant astrocytic mitochondrial dynamic alterations.

Aim 1 was divided into three sub-aims:

Sub-aim 1.1: Explore DRP1-mediated mitochondrial fission at 4, 24, and 72 hours in primary astrocyte cell culture post mechanical insult.

Sub-aim 1.2: Determine the role of phosphorylated DRP1 serine 616/DRP1 serine 637 site ratio and the levels of mitochondrial fragmentation at 4, 24, and 72 hours in primary astrocyte cell culture post mechanical insult.

Sub-aim 1.3: Investigate acute astrocyte reactivity phenotypic transition at 4, 24, and 72 hours post mechanical insult.

II. Specific Aim 2: Characterize unique patterns of astrocytic mitochondrial dynamic alteration post single bTBI.

Aim 2 was divided into three sub-aims:

Sub-aim 2.1: Explore DRP1-mediated mitochondrial fission at acute and sub-acute stages of the injury within isolated astrocytes from the hippocampus post single bTBI.

Sub-aim 2.2: Investigate phosphorylated DRP1 serine 616/DRP1 serine 637 site ratio at acute and sub-acute stages of the injury within isolated astrocytes from the hippocampus post single bTBI.

Sub-aim 2.3: Investigate astrocyte reactivity phenotypic transition at the injury's acute and sub-acute stages post single bTBI.

Chapter 2. Background

2.1. Traumatic Brain Injury (TBI)

2.1.2. Clinical Significance

TBI occurs when an external force hits the head resulting in brain damage, and according to the Glasgow Coma Scale (GCS), TBI varies in three categories of severity. The GCS is the most commonly used clinical scoring system to diagnose and describe the early level of impaired consciousness in a person who has suffered an acute head injury. Therefore, the GCS creates a common classification of acute TBIs according to three severity categories: mild, moderate, and severe (Jain & Iverson, 2022). Triaging based only on GCS is not ideal, since the criterial to diagnose and determine the patient TBI severity presents a level of inconsistency (Dong & Cremer, 2011; Fitzgerald et al., 2022). Unfortunately, there is no perfect questionnaire or measure of patient TBI severity; therefore, many practitioners are not solely relying on the GCS but also having a more holistic approach that takes into consideration the patient's post-concussion symptoms and individual experiences.

Compared to moderate and severe TBI, there are challenges to detect mild TBI (mTBI). There is the inability of neuroimaging tests like CT scans or MRI to detect any clear and consistent morphological changes to the brain making early mTBI diagnosis difficult. Instead, mTBI diagnosis is based solely on patient symptoms once in the hospital. For instance, approximately 50% of veterans who suffered a blast-related mTBI reported that they never experienced an immediate loss of consciousness, altered mental status, or immediate temporary amnesia (McGlinchey et al., 2017; Siedhoff et al., 2022). These cognitive symptoms are required for the GCS to classify the severity of neurologic injury in early clinical assessments.

In preclinical studies, mild bTBI can produce subtler morphological changes within the brain's cells, including mitochondrial dysfunction, astrocyte reactivity, synaptic alteration, and neurovascular impairment. Mild TBI, if left untreated for an extended period of time, can cause irreversible cognitive deficits. Blast overpressure exposure has been linked to a variety of cognitive deficits, including memory loss, emotional disorders and anxiety problems such as attention defects, according to clinical reports (Agoston, 2017; Chapman & Diaz-Arrastia, 2014; Higgins et al., 2014; Kashdan et al., 2006; Miles et al., 2017; Theeler et al., 2012). When it comes to long-term memory, the hippocampus play a crucial role and pre-clinical models have shown neuronal death and astrocyte reactivity from mild bTBI in the hippocampus (Cho, Sajja, VandeVord, et al., 2013; Hao et al., 2020; Hernandez et al., 2018; Law et al., 2016; Sajja et al., 2012, 2014). The hippocampus was selected as the focus of this study to learn more about the function of astrocytic mitochondria dynamics because of its association with memory and learning.

2.1.2. Traumatic Brain Injury Etiologies

TBI is a heterogeneous condition whose pathophysiological mechanisms consist of two main etiologies (insults), starting with the primary insult at the moment of the trauma, resulting from the direct biomechanical forces that initiate changes at the cellular level and thus trigger the secondary insult, a cascade of biochemical events that if chronic can be deleterious to the cell.

The initial external mechanical force, the primary insult of TBI, is such as the head colliding or being hit by an object without penetration or the brain being penetrated by a foreign object, rapid acceleration or deceleration of the brain, or in the case of bTBI, the blast overpressure wave causes the primary insult. These insults can lead to elevations in intracranial pressure and swelling, causing low cerebral blood flow and consequently nutrient deprivation, as well as irreparable tearing and stretching leading to secretion of cellular contents into the extracellular

space (Bir et al., 2012; Bolander et al., 2011; Farkas & Povlishock, 2007; Leonardi et al., 2011; Levi et al., 1990; Meythaler et al., 2001; Povlishock & Katz, 2005).

General pathophysiological features of TBI and mechanisms following the primary insult are referred to as the secondary insult. Brain cells attempt to repair the damage after the biomechanical insult but frequently do so with residual damage due to chemical cascades and cellular activation brought on by the primary injury. This secondary insult can happen within minutes, hours or days following the primary insult. It can involve downstream biochemical, physiological, metabolic, and cellular changes, including but not limited to mitochondrial dysfunction, oxidative stress, excitotoxicity, neuroinflammation, blood-brain barrier (BBB) impairment, and glial reactivity (Cash & Theus, 2020; Karve et al., 2016; Munoz-Ballester et al., 2022; Sajja et al., 2014; Sajja, Hubbard, & VandeVord, 2015; Yi & Hazell, 2006)**.** The interrelationship of primary and secondary insults leads to long-term cognitive detrimental outcomes in TBI patients.

A growing collection of pre-clinical and clinical TBI literature has demonstrated that astrocytes are crucial to the pathophysiology of the chronic stages of TBI and long-term cognitive effects could result from chronic astrocytic reactive phenotype that could lead to maladaptive response to the injured brain (Michinaga & Koyama, 2021; Sajja et al., 2014, 2016; Sajja, Hubbard, & VandeVord, 2015). Astrocyte phenotype transition to a reactive state can present neuroprotective functions; however, persistent astrocyte reactivity can lead to prolonged BBB disruption, chronic neuroinflammation, and neurotoxicity (Burda et al., 2016; Casas et al., 2017; Cho, Sajja, VandeVord, et al., 2013; Pekny & Pekna, 2014; Perez-Catalan et al., 2021; Sofroniew & Vinters, 2010; Yi & Hazell, 2006). Both *in vitro* and *in vivo* models of acute TBI and bTBI show that transition between astrocyte reactive phenotypes is highly dependent on injury

mechanism and severity (Bailey et al., 2016; Cullen et al., 2007; LaPlaca et al., 2005; Sajja et al., 2014).

Additionally, research has demonstrated the significance of astrocytes in controlling synaptic transmissions, controlling energy metabolism, maintaining homeostasis, guarding against glutamate toxicity, and shielding neurons from oxidative stress following TBI (Bylicky et al., 2018; Mahmoud et al., 2019; Zhou et al., 2020). Many of those mechanisms by which astrocytes maintain and protect neurons are mitochondrial-associated mechanisms, including buffering excessive ROS, maintaining calcium homeostasis, and providing a metabolic substrate (Gollihue & Norris, 2020; Jackson & Robinson, 2018; Rose et al., 2020; Stephen et al., 2014). Mitochondria are vital organelles for cell physiology, being an essential source of energy, metabolism coordination, regulation of Ca^{2+} signals, and participation in signaling cues for cell survival and death. These organelles have a dynamic nature, constantly remodeling their architecture by combining (fusion) or dividing (fission), facilitating their distribution/migration along the cytoskeleton and homogenization of their content (Liesa et al., 2009). A complex group of guanosine triphosphate (GTP)-binding proteins that carry out either fusion (Mitofusin 1 and 2, MNF1 and MNF2; optic atrophy 1, OPA1) or fission (e.g., dynamin-related protein 1, DRP1; fission 1 protein, FIS1) orchestrate mitochondrial structure (Detmer & Chan, 2007; Liesa et al., 2009). Preserving the balance between these antagonistic forces helps maintain mitochondrial architecture, metabolism, and proper cell physiology.

2.2. Blast-Induced Traumatic Brain Injury

2.2.1. Blast Wave Characteristics

The blast wave is caused by rapid expansion of combustion material that causes supersonic flow of the surrounding air. The blast wave is a fast-moving phenomenon that leaves the

explosion's epicenter as an expanding sphere of compressed gases into the surrounding environment. Far from the explosion's epicenter (far-field blast region), the blast wave is characterized by the Friedlander waveform (figure 2.1). A quick rise in pressure known as overpressure or peak pressure associated with a blast wave characterizes the Friedlander waveform. This peak pressure drops into a short duration of negative pressure (below ambient pressure), followed by a return to normal conditions. These pressure (dynamic) changes happen in milliseconds, and the overpressure or peak pressure duration is the amount of time an object is exposed to the wave pressure.

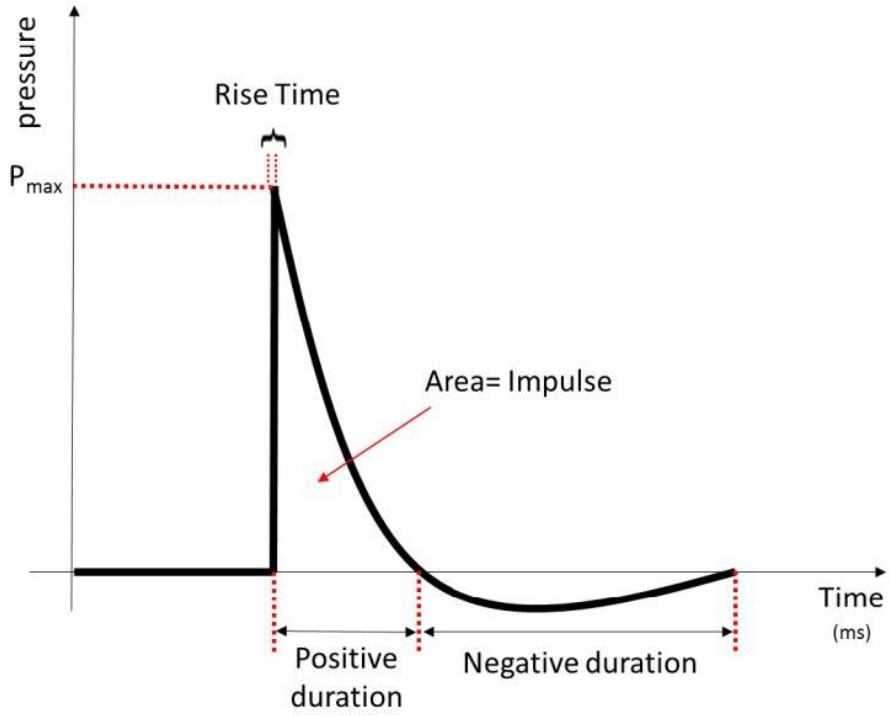

Figure 2.1: The Friedlander waveform represents a shock wave from a far-field blast event. The blast wave profile is characterized by a quick positive duration phase followed by a negative phase. The peak pressure (Pmax), rise time, positive impulse and positive duration define the blast wave. Image acquired from (Hlavac, 2018).

The outward airflow from the blast wave's source is characterized by hydrostatic (static) and dynamic pressures. In the case of the far-field blast region, the static pressure is the pressure felt by an object parallel to the direction of the airflow and is represented by the Friedlander waveform described above. The kinetic energy associated with the airflow is defined as the resulting dynamic pressure, also known as blast wind. The static pressure delivers the compressive, and the dynamic pressure presents the 'drag and lift' forces that push and lift objects or individuals, triggering impact-relevant injuries (Needham et al., 2015). The dynamic pressure (blast wind) effects in studies that isolate primary bTBI are minimized with the idea of better understanding and characterizing how the shock wave itself interacts with the body.

2.2.2. Blast Injury Categories (primary, secondary, tertiary, and quaternary)

There are four types of blast injuries: primary, secondary, tertiary, and quaternary (Figure 2.2**)**. Briefly, immediately after the explosive device is detonated, a high-pressure wave is formed at supersonic velocity into the surrounding medium, which creates a thin outside layer of compressed air. The primary blast injury results from propagation of the high-pressure wave and its subsequent energy transmission within the body. There is a surge in understand this particular type of brain injury; nevertheless, the mechanism behind the injury are still not fully understood and have been the subject of much debate. Secondary brain injury is caused by fragments or debris propelled by the blast wave. Tertiary brain injury is due to acceleration and deceleration of the body by the blast wind (dynamic pressure). Lastly, quaternary injury includes wounds due to burns or post-detonation environmental contaminants.

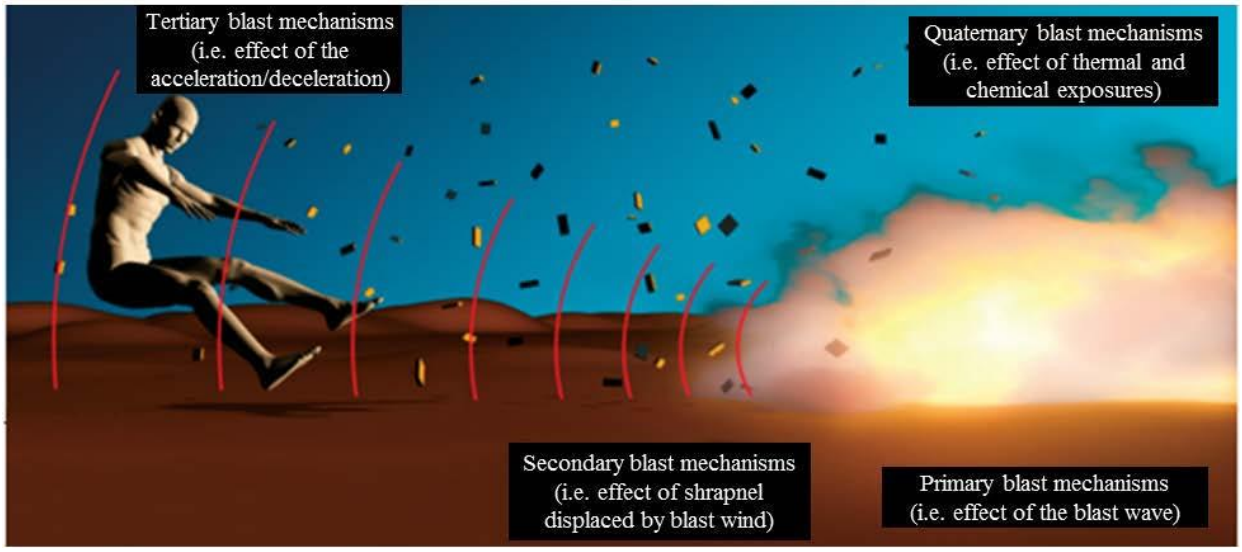

Figure 2.2: Blast injuries can be divided into four categories. After the explosive device goes off, a high-pressure wave expands at supersonic velocity into the surrounding medium. Primary Blast Injury is the injury caused by the blast wave itself. Secondary injury is caused by fragments of debris propelled by the blast wave. Tertiary injury is due to acceleration of the body or part of the body by the blast wind. Quaternary injury is due to burns or post detonation environmental contaminates. Imaged adapted from (Cernak & Noble-Haeusslein, 2010).

2.2.3. Primary Blast-Induced Traumatic Brain Injury

Given the enormous number of service members, primary blast-induced traumatic brain injury (bTBI) is a source of significant worry. bTBI results from the propagation of high-pressure static blast forces and their subsequent energy transmission within brain tissue. Exposure to this overpressure it thought to cause diffuse brain injury that leads to cellular damage. Understanding the physiological and pathological mechanism underlying bTBI is challenging due to the complexity of the blast wave's injurious environment (open-field and closed-field) (Cernak & Noble-Haeusslein, 2010). Therefore, preclinical bTBI models need to make sure to replicate the mechanical properties (intensity, duration and complexity of the blast wave) and clearly identify and reproduce the right components of the blast wave environment that further mimics military blast injuries outcomes.

Mechanical transmission of blast waves into the brain has been described in investigations, leading to pressure abnormalities and tissue level damage (Leonardi et al., 2011; Wang et al., 2014). Unfortunately, how the blast wave travels into and through brain tissue is still a matter of debate. Despite the extensive investigation and offered theories, many gaps remain. Although our understanding of the complicated mechanisms involved in the transmission of blast wave energy to the brain is limited, it is likely that multiple systems are at play (Fievisohn et al., 2018). Some of these mechanisms include the blast wave's direct transmission through the head and brain, while others include the blast wave's action on the skull, resulting in flexure that triggers intracranial pressure oscillations in the brain (Bolander et al., 2011; Ganpule et al., 2013; Hampton & Vandevord, 2012; Moss et al., 2009). An alternative explanation postulates that a pressure wave originating in the thoracic region would travel through the vascular system, resulting in an increase in intracranial pressure. No definitive biomechanical mechanism responsible for bTBI has been established; therefore, these possibilities continue to be discussed.

In an effort to accelerate the process of developing diagnostic tools and therapeutic approaches for bTBI, preclinical animal (*in vivo*) models have been developed. To prove that the pre-clinical models accurately represent human injuries, they must be compared to human data (Cho, Sajja, VandeVord, et al., 2013). Since shock waves are known to have different interactions with brain tissue than other TBIs, it is also crucial to understand how brain cells collectively and singly recognize, respond, and adapt to the primary injury stimulus, the mechanical insult itself, in bTBI. As a result, *in vitro* models can help shed light on these fundamental problems and advance our knowledge of how astrocytes experience, respond and adapt to mechanical overpressure insults (Hlavac et al., 2020; Hlavac & VandeVord, 2019).

2.3. An Astrocytic Approach to TBI Pathophysiology

The most studied cell in the brain is the neuron; however, astrocytes are gaining importance within the TBI field because of their various neuroprotective roles and their unique ability to respond to mechanical and biochemical insults from TBI. In the healthy brain, astrocytes present a spongiform morphology and have many process extensions radially arranged with end-feet enveloping blood vessels and most processes surrounding neurons and the synaptic cleft between the presynaptic and the postsynaptic terminals. In addition, astrocytes can interface with other astrocytes via gap junctions, creating an extensive interconnected network throughout the brain (Khakh & Sofroniew, 2015). This unique anatomical organization permits astrocytes to perform vital roles in the healthy brain, such as helping regulate synaptogenesis, synaptic strength, neurotransmitter regulation levels and brain microcirculation, providing neurons with energetic and antioxidant precursors (Bylicky et al., 2018; Mahmoud et al., 2019; Matias et al., 2019; Perez-Catalan et al., 2021; Sofroniew & Vinters, 2010).

Until recently, astrocytes were considered only as a "glue" for neurons with the idea to solely function as supportive cells within the CNS because of their lack of being electrically excitable like neurons. However, current interest in astrocytes now highlights the importance of these cells in understanding the injury mechanisms and neurodegenerative process that result following injury. The morphologic and biological alterations that astrocytes experience in response to damage is known as astrocyte reactivity. Reactive astrocytes typically have a different appearance than quiescent ones. Characteristics of reactive astrocyte phenotype in clinical and pre-clinical TBI pathology include hypertrophy of their main cellular processes, proliferation, and alterations in protein expression, such as the expression of the intermediate filament protein glial fibrillary acidic protein (GFAP), collectively known as universal hallmarks of astrocyte reactivity

(Ekmark-Lewén et al., 2010; Eng et al., 2000; Escartin et al., 2021, 2021; Khakh & Sofroniew, 2015; Michinaga & Koyama, 2021).

2.3.1. Astrocyte Reactivity, a Finely Graduated Response to TBIs Insult

As we've seen, astrocytes have the potential to contribute significantly to brain health and CNS function. In reaction to injury, astrocyte reactivity may help heal injured tissue and restore homeostasis, or it may have detrimental effects by promoting scar tissue formation and blocking neuronal axon growth. The transitory reactive phenotype is not as simple as it seems and can influence the initial functional response of the astrocytes to an insult and, therefore, leads to the sparking of a growing debate.

The astrocyte reactivity phenotype is primarily characterized by astrocytic proliferation, cellular hypertrophy (body and process), and modification of intermediate filament proteins such as vimentin and GFAP (Ekmark-Lewén et al., 2010; Schwerin et al., 2021), with the latter being the most common marker used to identify astrocyte reactivity. Those characteristics are mainly presented or interpreted as an all-or-none response; however, pre-clinical studies are showing heterogeneity in the astrocyte reactivity phenotype along a spectrum from mild to extreme phenotypic variation which can further varies the cell function and properties (Anderson et al., 2014; Silver & Miller, 2004; Torres-Ceja & Olsen, 2022). In the case of brain injury, the initial reactive phenotype is subtly controlled by primary insult (mechanical) severity and the triggering of a wide array of context-dependent intercellular and intracellular signaling, the so-called secondary insult. Therefore, astrocyte reactivity is not a single stereotypical response (Anderson et al., 2014; Burda et al., 2016; Khakh & Sofroniew, 2015; Sofroniew, 2020). However, it does present a transitory reactive phenotype that can vary by injury severity and inter and intracellular signaling that could be further influenced by time-dependent (acute, sub-acute, and chronic) stages

of the injury. All of this together can play an important role in controlling astrocyte response post-injury as either a positive and helpful response or a more harmful and detrimental response (Buffo et al., 2010; Pekny et al., 2016; Pekny & Nilsson, 2005; Zhou et al., 2020). As a result, according to Sofroniew and colleagues (Sofroniew, 2015a)**,** dividing the astrocyte reactivity phenotype into three groups such as I) Mild, II) Moderate, and III) Severe could help to better understand the astrocyte reactive phenotype and perhaps help to give a better interpretation of astrocyte reactivity response post brain injury (Figure 2.3).

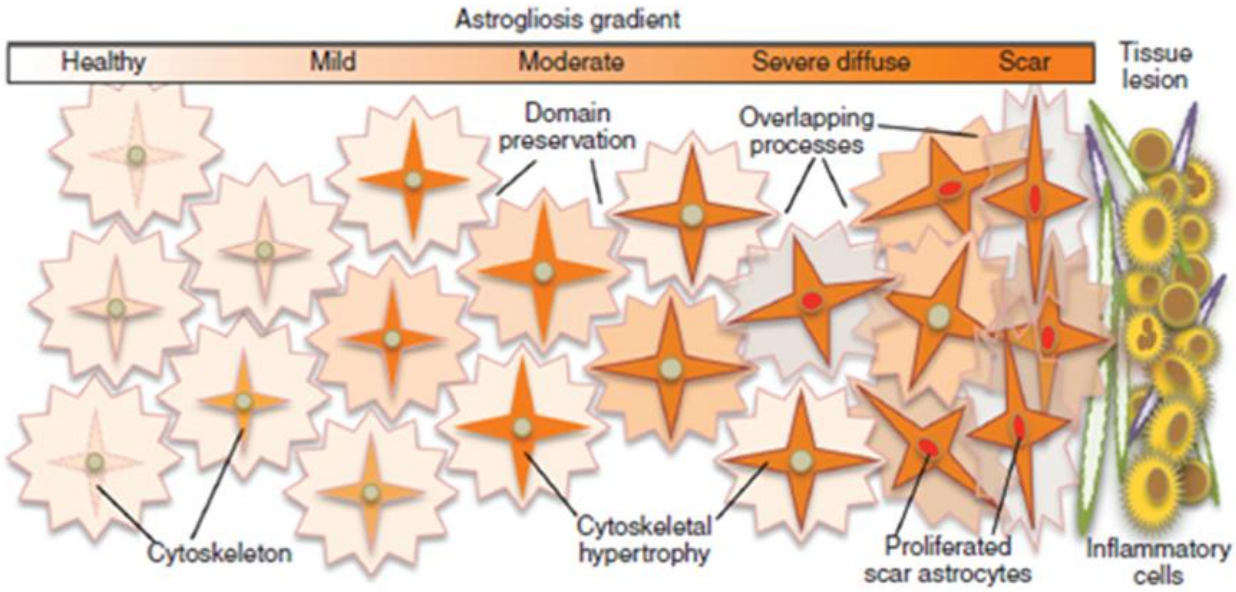

Figure 2.3: Illustration representing astrocyte reactivity phenotype transition from health to injured brain. Post insult, a mild to moderate astrocyte reactivity presents upregulated GFAP protein expression with initial cytoskeleton hypertrophy, however, most of the astrocytic individual domain is maintained. On the other hand, a severe astrocyte reactivity phenotype presents u-regulation of GFAP, cytoskeleton hypertrophy and loss of astrocytic individual domains by increase in proliferation starting to form scar borders around damaged tissue. Image acquired (Sofroniew, 2015a)**.**

I. Mild Astrocyte Reactivity

Focal TBI lesions, even those far from the point of damage, can show signs of mild astrocyte reactivity, which is typically linked with mild non-penetrating and non-contusive trauma. In addition, astrocytes displaying a phenotypic shift, including upregulation of the intermediate

filament protein GFAP, changes in their cytoskeleton such cellular body and process hypertrophy, and minimal to no proliferation, have been linked to mild reactivity of astrocytes (Khakh & Sofroniew, 2015; Sofroniew, 2015a; Sofroniew & Vinters, 2010). Hypertrophy of the cytoskeleton is a feature unique to astrocytes, where it persists in isolation (Sofroniew, 2015a; Wanner et al., 2013). In other words, the independent domains of astrocytes are maintained because their processes do not cross into one another. However, in the context of TBI, the physiological ramifications of subtle changes in astrocyte responsiveness are poorly known.

II. Moderate Astrocyte Reactivity

The presence of moderate astrocyte reactivity is typically linked to chronic neurodegenerative disorders, diffuse TBI, and severe focal TBI in the regions around the focal lesions. Moderate reactivity in astrocytes is characterized by a number of phenotypic features including significant upregulation of the intermediate filament protein GFAP, noticeable alterations in the cytoskeleton via cellular body and process hypertrophy, and considerable astrocyte proliferation. In addition, it's characterized by the early disappearance of certain astrocyte domains, something that happen really minimal in the mild astrocyte reactivity, as a result of significant process extension via overlap with adjacent astrocyte process domains (Sofroniew, 2015a; Sofroniew & Vinters, 2010). This phenotype can initiate a remodeling of tissue architecture without extensive, compact astrocytic scars along borders to necrotic tissue which can be initially beneficial to the injury site by preventing the injury from spreading (Anderson et al., 2014; Silver & Miller, 2004; Zhou et al., 2020).

III. Severe Astrocyte Reactivity.

Penetrating trauma, severe conducive trauma is all implicated to a scar formation phenotype associated with astrocyte reactivity. The exhibited phenotype is highly reminiscent of

severe astrocyte reactivity, as it includes strong upregulation of GFAP, hypertrophy of the cell body and process, and enhanced astrocyte proliferation, which ultimately leads to loss of individual astrocyte domains (Sofroniew, 2009, 2015a; Wanner et al., 2013). Furthermore, extensive tissue damage results in the production of an astrocytic scar, which is nearly exclusively formed from substantial astrocyte growth with elongated forms and processes that overlap and tangle to form compact barriers (Anderson et al., 2014; Silver & Miller, 2004; Zhou et al., 2020).

The data discussed here reveal a considerable reactive phenotypic heterogeneity among astrocytes, which is regulated by potential responses to various external environmental stressors intensity (severity). These differences are likely to be of consequence when considering the functions and impact of astrocyte reactivity on TBI. Lately, research within the TBI field aims to understand the long-term pathophysiology of mild to moderate brain injury. However, it is important to understand the pathophysiology of acute mild to moderate astrocyte reactivity after a TBI. In acute mTBI, astrocyte reactivity is governed by notable upregulation of intermediate filament protein GFAP and cytoskeleton changes (hypertrophy). This response may present protective responses in the acute stages of the injury; however, it can eventually present maladaptive responses since chronic astrocyte reactivity contributes to scar tissue formation which initially helps to separate the injury area from healthy tissue; however, it negatively affects regenerative responses at later stages of the injury (Silver & Miller, 2004; Voskuhl et al., 2009). As mentioned above, mild TBI can lead to an astrocyte reactivity phenotype that display little or no reorganization of tissue architecture characteristics (Sofroniew, 2015a); therefore, in order to deconstruct the molecular processes for both adaptive and maladaptive phenotypes of astrocyte reactivity, it will likely be crucial to understand how astrocytes respond to bTBI in the early phases of the damage because astrocytes morphology and structural alterations are possibly easier to

manipulate back to a homeostatic state or to control its reactive phenotype and avoid long-term detrimental outcomes (Burda & Sofroniew, 2014).

2.4. Mitochondria

2.4.1. Mitochondria Structure, an Intricate Architecture

Adenosine triphosphate (ATP) generation, cell anabolic and catabolic functions, calcium signaling, influencing ROS levels and redox management, cell division and differentiation, and cell death are all significant functions performed by mitochondria, which are remarkable organelles (Chan, 2012; Duchen, 2000; Jacobson & Duchen, 2004; Newmeyer & Ferguson-Miller, 2003; Osellame et al., 2012; Susin et al., 1999). Organelles termed mitochondria present a double membrane-bound structure, forming a complex architecture with four specific compartments that perform various functions (mitochondrial outer mitochondrial membrane (OMM), intermembrane space (IMS), inner mitochondrial membrane (IMM), and the matrix) (Figure 2.4).

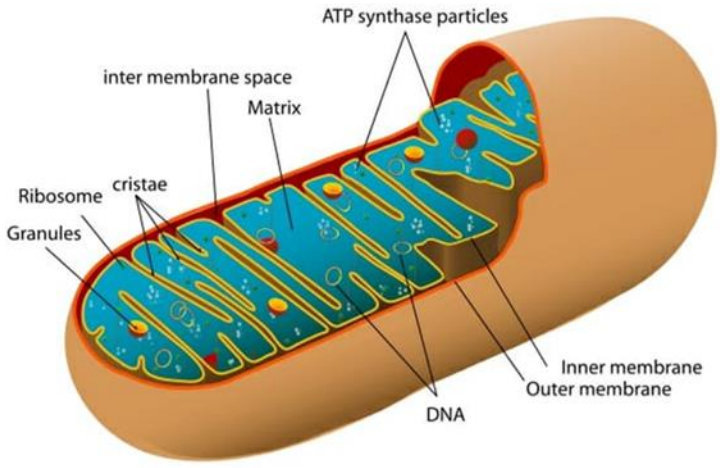

Figure 2.4: Mitochondria structure. Mitochondria are organelles that present a double membrane-bound arrangement creating an intricate architecture with four distinct compartments that present different functions, e.g. mitochondrial outer mitochondrial membrane (OMM), intermembrane space (IMS), inner mitochondrial membrane (IMM), and the matrix.
Image acquired from (https://commons.wikimedia.org/wiki/File:Diagram_of_a_human_mitochondrion_es.jpg)

The OMM forms connections with several cytosolic subcellular organelles, including the plasma membrane, endoplasmic reticulum, lysosomes, peroxisomes, and endosomes. Several porins (VDACs) and translocases (TOMs) are also present in the OMM, allowing unrestricted passage of tiny molecules (5 kDa) into the intermembrane space (IMS). The OMM is also home to proteins and complexes that are involved in a variety of mitochondrial and cellular processes, including protein sorting and assembly (SAMs) and apoptotic signaling (Bak) (Pernas & Scorrano, 2016; Walther & Rapaport, 2009). The OMM can undergo fusion and fission owing to the presence of membrane fusion (Mfn1/2) and four protein fission receptors, including mitochondrial elongation factor 1 (MIEF1/MiD51), mitochondrial elongation factor 2 (MIEF2/MiD49), fission protein 1 (Fis1), and mitochondrial fission factor (Mff); therefore, the OMM exhibits a highly dynamic structure (Chan, 2012; Giacomello et al., 2020; Yu et al., 2020). Furthermore, as a result of fission and fusion, the mitochondrial dynamics system controls how the mitochondria react to different physiological stressors and insults.

The IMS, the area enclosed by the mitochondrial outer and inner membrane, is the most constricted subaqueous compartment in the mitochondrial organelle and is further subdivided by the IMM and cristae compartments, called the intracristae compartment. The IMS presents important functions, such as transporting proteins, ions, and electrons during cellular respiration and other metabolic processes. Furthermore, several apoptotic components, such as cytochrome *c*, are kept in the IMS until their release which initiates programmed cell death (Edwards et al., 2021; Giacomello et al., 2020).

The IMM presents a well-compartmentalized structure known to separate the mitochondrial matrix from the intermembrane space. Furthermore, the IMM is the main site for bioenergetic functions since all the complexes implicated in mitochondrial respiration reside in

numerous IMM invaginations called cristae, the main site for oxidative phosphorylation. Lastly, the innermost compartment within mitochondria is the matrix, which is another subaqueous compartment in the mitochondrial organelle. The matrix space is home to ribosomes, soluble tricarboxylic acid (TCA) cycle enzymes, metabolites, nucleotides, and ions in addition to mitochondrial DNA (mtDNA) (Giacomello et al., 2020).

2.4.2. Regulation of Mitochondrial Dynamics: Mechanisms and Consequences

The term *mitochondrial dynamics* refers to the balance involving fusion and fission events within the cell (Figure 2.5). A family of GTPase proteins that are encoded by genes in the nuclear genome orchestrate this phenomenon. The size and number of mitochondrial, quality control (mitophagy), transport within the cell, and alteration of mitochondrial morphology are all significantly influenced by fission and fusion events (Chan, 2012; Giacomello et al., 2020; Hoitzing et al., 2015; Newmeyer & Ferguson-Miller, 2003; Yu et al., 2020).

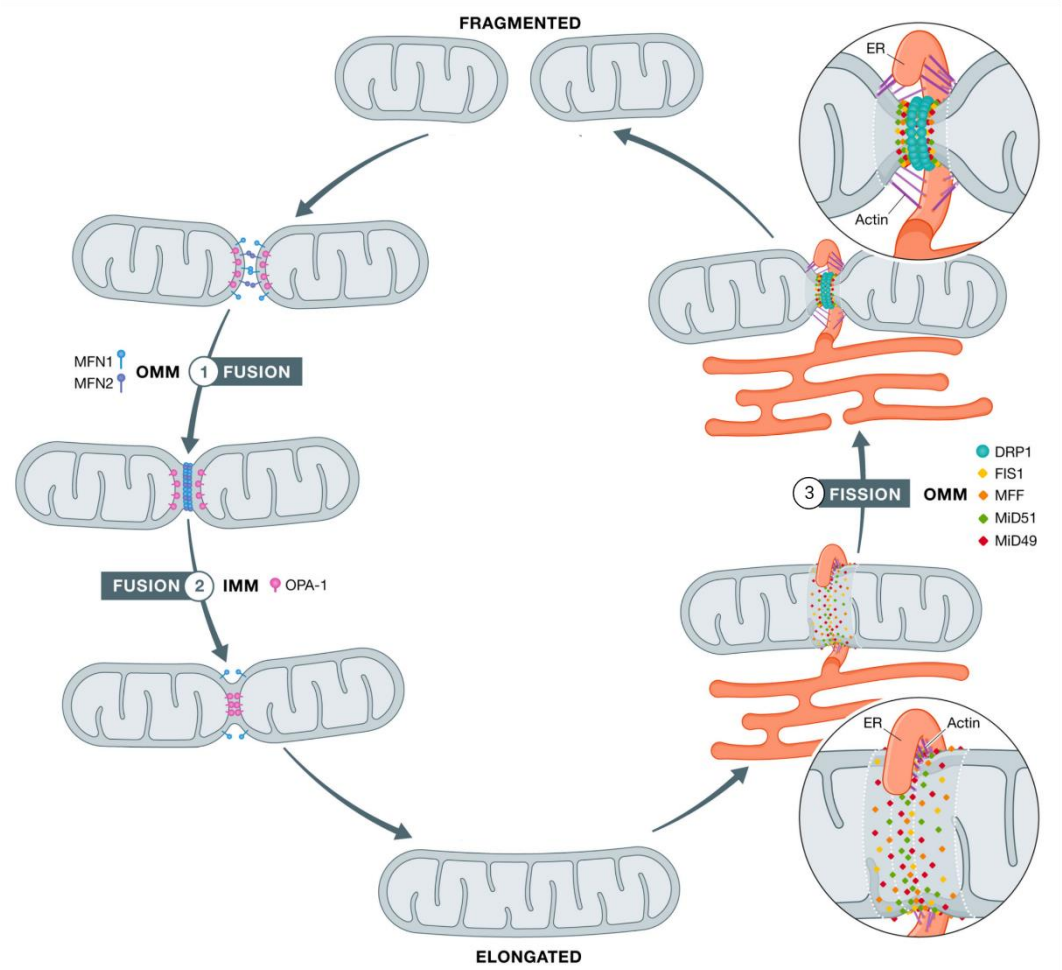

Figure 2.5: Mitochondrial Fusion and Fission. 1-2) Fusion is first initiated by merging the two mitochondrial OMM mediated by the protein receptors Mfn1 and Mfn2. In contrast, their C-termini interact with one another, allowing the tethering of the two OMM with GTP hydrolysis-mediated conformational changes allowing the fusion of the OMM. Finally, fusion of the IMM starts, mediated by the GTPase OPA1, allowing the formation of a new cristae structure and ultimately combining both mitochondrial organelles. **3)** Fission is mediated by the translocation of activated DRP1 from the cytosol to the mitochondria, and binding to the OMM receptors Mff, MiD49, MiD51, and Fis1. Upon recruitment to the OMM, DRP1 forms oligomeric rings. GTPase hydrolysis-mediated conformational changes lead to the rings' construction and promote mitochondrial scission into two new mitochondrial organelles. Imaged adapted from (Cervantes-Silva et al., 2021).

Activated fission can lead to the mitochondrial network breaking into punctuated fragmented (≤1 μm in length), small and rounded mitochondria mainly by the GTPase dynamin-related protein 1 (DRP1). Briefly, fission is mediated by the translocation of activated DRP1 from the cytosol to the mitochondria, and binding to the OMM receptors Mff, MiD49, MiD51, and Fis1. Upon recruitment to the OMM, DRP1 forms oligomeric rings. GTPase hydrolysis-mediated

conformational changes lead to the rings' construction and promote mitochondrial scission into two new mitochondrial organelles. Mitochondrial fission helps to provide sufficient numbers of mitochondria, being important for cell growth and division as well as oxidative functions and the elimination of damaged mitochondria by mitophagy (Giacomello et al., 2020; Wallace, 2005; Yu et al., 2020). On the other hand, by gradually merging the OMM and IMM of two distinct mitochondria organelles, triggered fusion can result in thin, elongated, and highly linked networks of mitochondria (≥ 3μm in length). Briefly, fusion is first initiated by merging the two mitochondrial OMM mediated by the protein receptors Mfn1 and Mfn2. In contrast, their C-termini interact with one another, allowing the tethering of the two OMM with GTP hydrolysis-mediated conformational changes allowing the fusion of the OMM. Finally, fusion of the IMM starts, mediated by the GTPase OPA1, allowing the formation of a new cristae structure and ultimately combining both mitochondrial organelles (Giacomello et al., 2020). Opposite to fission, mitochondrial fusion is important for the connection and exchanging of mitochondrial contents (e.g. mtDNA, ions, and other small molecules), providing a higher energy capability (increased mitochondrial surface), and alleviating oxidative damage (Giacomello et al., 2020; Newmeyer & Ferguson-Miller, 2003; Yu et al., 2020).

The mitochondrial structure is exceptionally dynamic and continually changing shape due to fission and fusion, allowing it to respond to physiologic cues or stress insults by modifying the structure and consequently the mitochondrial function since both are tightly associated. Mitochondrial organelles consist of branching, densely connected networks, which are a byproduct of fusion or punctate, isolated mitochondria, which are a byproduct of fission. As a result, a growing body of evidence suggests that altered mitochondrial dynamics such as disruption of the mitochondrial network, resulting in mitochondrial dysfunction, affects various cellular processes.

Several human neurodegenerative illnesses have been linked to it. Additionally, TBI researchers are beginning to investigate the link between altered mitochondrial dynamics and the development of detrimental TBI outcomes (Arun et al., 2013; Cheng et al., 2012; Fischer et al., 2016; Liesa et al., 2009; Sridharan et al., 2021). The pathophysiology of acute TBIs is characterized by loss of mitochondrial function, and excessive fission in particular has been found to be a major pathogenic event in neuronal death and injury in numerous models of neurodegenerative diseases and TBIs. A specific mechanism linked to excessive fission and neurodegeneration has been identified as dysregulation of the main protein regulator of mitochondrial fission, DRP1 (Balog et al., 2016; Detmer & Chan, 2007; Knott et al., 2008; Liesa et al., 2009).

Mechanical pressures from the original injury and downstream dysregulation from atypical metabolic cascades during the secondary insult can contribute to mitochondrial dynamic changes after TBI (Lifshitz et al., 2003). According to research done on brain tissue from TBI patients, mitochondrial morphology showed a spherical shape and swelling characteristics that could indicate an increase in fission process byproducts close to the injury site (Balan et al., 2013). Alterations in mitochondrial dynamics, such as a higher fission event, cause intracellular calcium to accumulate in the mitochondria, ROS production to excessively increase, and activation of the mitochondrial permeability transition pore (MPTP), which can severely limit the ability of the mitochondria to adapt to changes in the cellular environment and ultimately result in cell death.

2.4.3. Mitochondrial Fission

DRP1 is a guanosine triphosphate (GTPase) family member. It is the key player in mitochondrial fission machinery, mediating mitochondria-related physiological functions such as mitophagy, oxidative respiration chain, and mitochondrial redox status.

I. DRP1 Structure and Machinery:

An N-terminal GTPase domain, a middle domain, a variable domain, and a C-terminal GTPase effector domain can all be found in the crystal structures of DRP1. The GTPase domain controls DRP1's ability to self-assemble, and conformational changes brought on by GTP hydrolysis will encourage DRP1 polymerization. DRP1 self-assembles into dimers, tetramers, and higher-order oligomers in response to the middle domain. The C-terminal GTPase effector domain plays a crucial role in mediating intramolecular and intermolecular interactions, stimulating the GTPase, and assisting in the stability of higher-order complexes (Chang & Blackstone, 2010; Dai et al., 2020; Otera et al., 2013). The GTPase effector domain and DRP1 phosphorylation occur at the variable domain. Through intramolecular and intermolecular interactions, these domains link up to facilitate DRP1 assembly into higher-order spiral-like structures. To aid in membrane constriction, a coordinated rise in GTPase activity and GTPase hydrolysis-mediated conformation changes are critical (Chang & Blackstone, 2010; Dai et al., 2020; Otera et al., 2013).

DRP1 is a cytosolic protein and undergoes several steps to mediate mitochondrial fission (Figure 2.6): 1) DRP1 exists as dimers or tetramers in the cytoplasm, and when mitochondria are destined to divide, DRP1 translocates from the cytoplasm to the outer membrane mitochondria (OMM) fission sites, 2) in the OMM, DRP1 assembles into helical oligomeric spiral-like structures, and it is anchored to the OMM by binding four receptors: Mff, MiD49, MiD51 and Fis1, 3) GTP hydrolysis-mediated conformational changes, arrangement of the DRP1 GTPase domain and GTPase effector domain, which generates a force resulting in mitochondrial membrane deformation, constriction, and ultimately incise mitochondria (Chang & Blackstone, 2010; Dai et al., 2020; Otera et al., 2013; Yu et al., 2020).

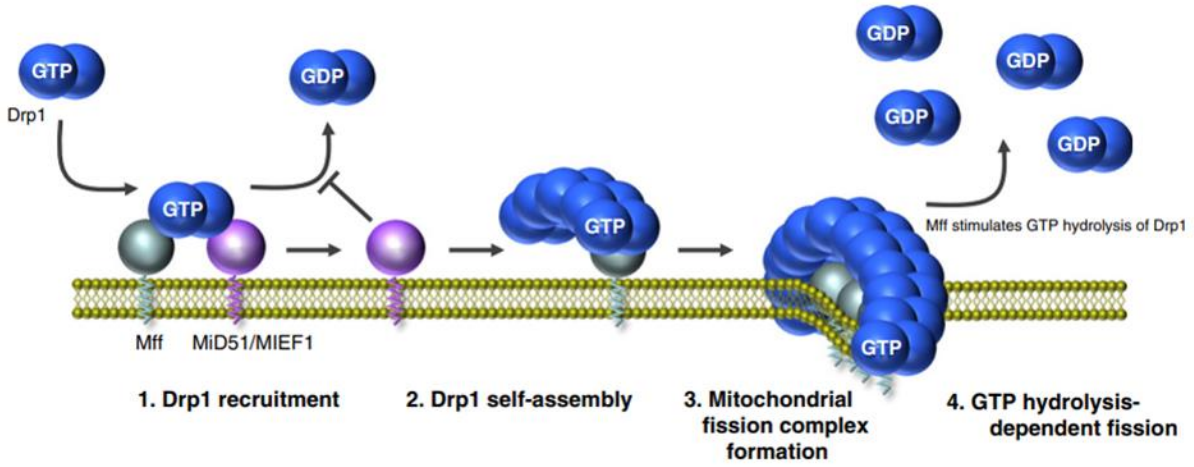

Figure 2.6: DRP1 Mechanism: Model in theory for the construction of DRP1 mediate mitochondrial fission mechanism. To mediate mitochondrial fission, the GTP-Drp1 protein goes through several processes. These include translocation from the cytoplasm to the OMM, which starts a higher order assembly into spirals; GTP hydrolysis, causing a conformational change and causing the mitochondrial membrane to deform; and, finally, disassembly. Image from (Otera et al., 2013).

Only 3% of DRP1 is localized in the OMM since it is predominantly cytosolic (Chang & Blackstone, 2010; Smirnova et al., 2001). Studies have shown that overexpressing the DRP1 protein has no effect on the dynamics of the mitochondria toward an increased number of fission events. Additionally, it has been demonstrated that the activation or inactivation of DRP1 enzymatic activity requires post-translational changes including phosphorylation, SUMOylation, nitrosylation, and ubiquitinylation. The processes governing DRP1's regulation are still unclear, despite the significant research that has been carried out to understand the activity of DRP1 in cells. Phosphorylation is one of the most well-studied post-translational changes of DRP1 that affects how it functions (Serasinghe & Chipuk, 2017).

II. Post-translational Regulation of DRP1: Phosphorylation

Protein phosphorylation is a post-translational modification carried out by protein kinases, which have a wide variety of substrate specificities. Protein phosphorylation is a successful way

used by cells to modify protein function due to the advantage of integrating fast functional changes with cellular signaling pathways. According to the literature, the DRP1 GTPase effector domain contains two serine residues (serine 616 and 637) that are crucial targets for post-translational modification (Liesa et al., 2009; Serasinghe & Chipuk, 2017). Phosphorylation at these two sites present antagonist effects on mitochondrial morphology.

Phosphorylated DRP1-mediated mitochondrial fission at serine 616 ($pDRP1^{s616}$) is an activating event promoting mitochondrial fission by triggering DRP1 translocation from the cytoplasm to the OMM and consequently mitochondrial fragmentation (Liesa et al., 2009; Serasinghe & Chipuk, 2017). The phosphorylation of DRP1 at the serine 616 site has been shown to be promoted by different kinases and enzymes that catalyze the transfer of a phosphate group to other molecules, depending on the physiological stimuli or stress insult conditions. For instance, phosphorylation of DRP1 at serine 616 by Cyclin Dependent Kinase 1 (CDK1/cyclin B) or Cyclin Dependent Kinase 5 (CDK5) happens during mitosis (Taguchi et al., 2007)**,** by Protein Kinase C (PKC) it happens under oxidative stress conditions (Qi et al., 2011), and by extracellular signal-regulated protein kinases 1 and 2 (ERK1/2) under pathological conditions leading to activation of mitochondrial fission (Kashatus et al., 2015; Serasinghe & Chipuk, 2017). On the other hand, phosphorylation of DRP1 at the serine 637 site ($pDRP1^{s637}$) suppresses fission by inactivating DRP1 from being recruited to the OMM (Liesa et al., 2009; Serasinghe & Chipuk, 2017). According to studies, protein kinase A (PKA) phosphorylation of DRP1 at serine 637 prevents DRP1 from translocating to the OMM and also inhibits GTPase function (Chang & Blackstone, 2007; Liesa et al., 2009; Serasinghe & Chipuk, 2017).

Therefore, serine 616 or 637 phosphorylation affects mitochondrial morphology via regulating the translocation of cytosolic Drp1 to the OMM. For instance, the balance of the

pDRP1^{s616}/ pDRP1^{s637} ratio is important for neuronal health, and its imbalance can lead to acute programmed neuronal necrosis. Moreover, its balance ensures stable oxidative phosphorylation, and the imbalance toward a higher level of pDRP1^{s616} leads to disruption of the oxidative status and, ultimately, an increase of reactive oxygen species (ROS) levels (Dai et al., 2020; Tsushima et al., 2018). Furthermore, the balance of pDRP1^{s616}/ pDRP1^{s637} ratio correlates with regional specific astrocyte death and inhibition of CDK5 following status epilepticus improving the balance of pDRP1^{s616}/ pDRP1^{s637} ratio. This ameliorates astrocytic apoptosis and astrocyte reactivity (Hyun et al., 2017).

2.4.4. Astrocytic Mitochondrial and TBI

Despite this neuronal bias, it is beginning to become clear that synaptic transmission, general brain metabolism, and neuron protection are all significantly influenced by mitochondrial function in glial cells, particularly astrocytes (Bylicky et al., 2018; Gollihue & Norris, 2020; Joshi et al., 2019; Rose et al., 2017, 2020). Astrocytic mitochondrial metabolism is crucial for astrocyte bioenergetics, neurotransmission, and redox equilibrium even though research has demonstrated that astrocytes primarily use glycolysis to meet their bioenergetic needs (Bylicky et al., 2018; Rose et al., 2020).

Through fluctuations in intracellular calcium levels controlled by their mitochondrial organelles, astrocytes exhibit excitability. Furthermore, neuronal activity and astrocyte activity are interrelated. In order to fit the local energy provision and calcium buffering requirements due to neuronal signaling as astrocyte calcium elevation promotes the release of neuroactive chemicals that can influence synaptic transmission and plasticity, increasing neuronal activity produces transitory mitochondrial remodeling in astrocytes by encouraging the immobility of mitochondria

in their tiny processes near highly neuronal synaptic activity (Agarwal et al., 2017; Bélanger et al., 2011; Lovatt et al., 2007; Stephen et al., 2015). Furthermore, fine astrocytic processes have been found to include a lot of mitochondria, and an astrocytic transcriptome study revealed the requisite molecular equipment for carrying out oxidative metabolism (Agarwal et al., 2017; Bélanger et al., 2011; Lovatt et al., 2007; Stephen et al., 2015). All of these findings highlight the significance of mitochondrial function in astrocytes and show how closely related mitochondrial dynamics are to healthy mitochondrial function.

Recent studies highlight the importance of proper astrocytic mitochondrial dynamics in a healthy brain and how altered mitochondrial dynamics could lead to both detrimental and protective astrocyte reactivity phenotypes in CNS degenerative diseases and TBI pathologies (Bantle et al., 2021; Ishii et al., 2017; Rahman & Suk, 2020; Rose et al., 2017; Sarkar et al., 2018; Zehnder et al., 2021). Furthermore, it has been suggested that astrocytic mitochondrial dysfunction, which favors fission over fusion post-TBI, is largely caused by dysregulation of DRP1, the main protein regulator of mitochondrial fission, as well as an increase in the phosphorylation of DRP1 at the serine 616 site (p-DRP1s616), the activated form of DRP1 (Motori et al., 2013; Rahman & Suk, 2020; Shih & Robinson, 2018; Stephen et al., 2014). This is supported by studies conducted *in vitro* and *in vivo* that observed changes in the mitochondrial morphology (fragmented mitochondria) of astrocytes, which resulted in the loss of proper mitochondrial function and caused cellular stress by increasing ROS production. This in turn activated various signaling pathways, including nuclear factor kappa B (NF-kB), which in eventually caused to an inflammatory astrocyte phenotype and higher levels of astrocyte proliferation. Additionally, inhibiting astrocytic mitophagy, a function regulated by mitochondrial dynamics, prevented the

mitochondrial network from being established and increases astrocytic cell death (Motori et al., 2013).

The coordination of neuronal metabolism, survival and synaptic maintenance in a healthy brain is recognized to be significantly influenced by astrocytes. Therefore, understanding the effects of altered astrocytic mitochondrial dynamics leading to changes in mitochondrial morphology and functionality could help to determine the impact not only on astrocyte phenotype transition but also on the mechanisms contributing to the progression of maladaptive astrocytes phenotypes and consequently chronic detrimental cognitive outcomes in TBI.

Chapter 3. Characterize the acute effects of bTBI mechanical insult to initiate aberrant astrocytic mitochondrial dynamic alterations

The text within Chapter 3 are adapted, in part, from Hlavac, N., **Guilhaume-Corrêa, F**., & VandeVord, P. J. (2020). Mechano-stimulation initiated by extracellular adhesion and cationic conductance pathways influence astrocyte activation. *Neuroscience letters*, *739*, 135405.

3.1 Introduction

Mild bTBI can produce more subtle morphological changes within brain cells, including mitochondrial dysfunction, astrocyte reactivity, synaptic alteration, and neurovascular impairment. Long-term, mild bTBI can lead to permanent cognitive deficits for which no consistently effective treatments exist. It is noteworthy that bTBI pathophysiology mechanisms consist of a primary insult (external mechanical forces) followed by secondary injury cascades that are deleterious to the cells. This interrelationship between primary and secondary insults leads to chronic neurological dysfunction and consequently long-term cognitive detrimental outcomes in bTBI patients.

The ability of individual brain cells to detect, react to, and adjust to damage stressors is poorly understood. It is crucial to comprehend the direct cellular mechanisms connected to specific forms of trauma mechanics. It is unclear how the mechanical overpressure insult transmits signals that cause certain astrocyte reactivity and how the astrocytic mitochondrial dynamics responds to it. This is particularly true for bTBI since, compared with other TBI, shock waves interact differently with the brain parenchyma. *In vitro* models that can mimic a primary bTBI insult can provide important information about mechanistic questions.

3.1.1 Significance

Understanding the mechanical forces impinge on the brain is crucial for treating all forms of TBI (Keating & Cullen, 2021). Cells sense external forces or mechanical stimuli and translate them into intracellular biochemical signals, known as mechanotransduction. An *in vitro* bTBI model found alterations in transient intracellular calcium signaling within CNS human cells only when shear forces were induced during a shock wave. This model used a pneumatic device (pressurized air gun) that produced a transient shock wave where the magnitude of the shear forces was controlled by manipulating the cell media volume and pressure magnitude (Ravin et al., 2012). Astrocytes were found to have a larger

influence on increased intracellular calcium and presented increased GFAP expression after 24 hours post-shock wave exposure (Ravin et al., 2012, 2016). Moreover, another study of bTBI *in vitro* model used military explosives to study the effects of shock waves of approximately 10-14 psi in submerged 2D mixed cell culture from two days postnatal (P2) Sprague-Dawley rat pups (Zander et al., 2016). The study found an increase in membrane damage and ROS formation 24 hours after exposure to an explosive blast (Zander et al., 2016). These *in vitro* models of bTBI were created to investigate the interactions of shock waves with brain cells. Although those studies do present outcomes seen in the *in vivo* bTBI models, the mechanics of the wave is important to consider. For instance, differences in medium limits and dependencies exacerbate the mechanics of blast waves. Therefore, a shock wave could be greatly altered when traveling from air into the fluid, which may cause the injury to be overstated. In the *in vivo* model, the air-gas boundary does not exist. Therefore, it is more translational to replicate the mechanics of shock wave propagation through a shock wave fluid medium device (Sawyer et al., 2017). As a result, our lab created a one-chamber fluid-filled device *in vitro* bTBI model by taking this into account (Hampton et al., 2013). The main pathogenic reactions following shock wave exposure to cell cultures revealed that there is a mechanical basis for astrocyte responsiveness, notwithstanding the limitations of current *in vitro* bTBI models (Canchi et al., 2017; Hlavac et al., 2015; Ravin et al., 2016; Sawyer et al., 2017; VandeVord et al., 2008).

New research reveals that functioning mitochondria are essential for several astrocytic processes, including glutamate metabolism, calcium signaling, fatty acid metabolism, antioxidant generation, and inflammatory activation (Gollihue & Norris, 2020; Rahman & Suk, 2020; Stephen et al., 2014). The structure of the mitochondria is extremely dynamic and changes shape frequently as a result of fission and fusion events. This allows the mitochondria to respond to physiologic cues or stress insults by adjusting their structure and function. The ability of the mitochondria to adapt to changes in the cellular environment

is severely hampered by altered mitochondrial dynamics toward a higher fission state, which causes intracellular calcium accumulation, an excessive rise in the level of ROS generation, and activation of the mitochondrial permeability transition pore (MPTP). Studies on astrocytes conducted *in vitro* and *in vivo* have demonstrated the participation of DRP1-mediated mitochondrial fission events. A change in the balance of the pDRP1^{s616}/pDRP1^{s637} ratio results in a disruption of the oxidative status. As a result, there is an increase in ROS levels and consequent activation of numerous signaling pathways, including nuclear factor kappa B (NF-kB), which results in an inflammatory phenotype and increased astrocyte proliferation (Motori et al., 2013; Rahman & Suk, 2020; Shih & Robinson, 2018; Stephen et al., 2014).

A recent study from our laboratory using an *in vitro* model of bTBI unveiled mechanisms of astrocyte activation with a significant increase in proliferating cell nuclear antigen (PCNA) followed by metabolic and structural reactivity changes via glial fibrillary acidic protein (GFAP) increases at 48 hours post-mechanical insult (Hlavac & VandeVord, 2019)**.** Furthermore, our *in vitro* bTBI model unveiled changes in mitochondrial membrane integrity seen as early as 15 minutes post-mechanical insult, and at 24 hours, they were followed by altered mitochondrial redox balance towards a pro-oxidative environment by upregulation of nicotinamide adenine dinucleotide phosphate oxidase 4 (NOX4) (Hlavac et al., 2020). The mitochondrial structure, which is altered by fission and fusion events, is closely related to changes in mitochondrial membrane integrity and oxidative state. Together, our findings support the hypothesis that a single mechanical injury has the capacity to change mitochondrial dynamics toward a fission state and serve as a potential indicator of mitochondrial dynamics failure.

3.1.2 Specific Aim 1 Summary:

For this specific aim, an *in vitro* model of bTBI was used to investigate how astrocytic mitochondrial dynamics respond to controlled mechanical perturbations. The goal was to characterize GTP-protein DRP1 levels and the role of their post-translational phosphorylation forms, pDRP1^{s616}, and

pDRP1^{s637}, in DRP1-mediated mitochondrial fission. The high-rate overpressure simulator (HOS) used for the *in vitro* model presented in this aim was designed to simulate intracranial pressure (ICP), which was measured using an *in vivo* model of bTBI (Leonardi et al., 2011). The HOS provides a novel tool to study ICP effects on cultured cells.

In order to isolate the effects of extracellular signaling from other cells, which is known to further affect astrocytes' reactive response following brain injury, primary rat astrocytes were cultured. Astrocytes were then exposed to a single directed mechanical insult (primary insult) to understand how astrocytic mitochondrial dynamics are affected by the pressure mechanics itself. Assessments were designed to help investigate whether altered mitochondrial dynamics towards activated fission are linked to the activation of the GTP-DRP1 protein by its phosphorylation at the serine 616 site (e.g., 4 hours, 24 hours and 3 days) following the mechanical insult.

3.2 Methods

3.2.1. Primary Astrocyte Cultures: Purification Technique

In accordance with protocols approved by the Virginia Tech Institutional Animal Care and Use Committee, brain cortices were isolated from two days post-natal (P2) Sprague-Dawley rats (Envigo; Indianapolis IN) by enzymatic digestion within 0.05% trypsin for approximately ten minutes. Seven days after isolation, astrocytes were mechanically purified by gently shaking for 24-48 hours, helping remove the other resident cells from the culture. Mixed cortical cells were cultured for up to 14 days allowing the cells to reach confluence before initial passage. Astrocytes were maintained in Dulbecco's modified Eagle's medium (Gibcos DMEM/F12; Cat#: 11320) with 10% fetal bovine serum (Millipore sigma; Cat#: F2242) and 1% antibiotic-antimycotic (ThermoFisher; Cat#: 1540062). Primary astrocyte (PA) cultures were stained with anti-GFAP (Abcam; Cat#: ab7260) to ensure astrocyte purity and a homogenous astrocyte population (Figure 3.1).

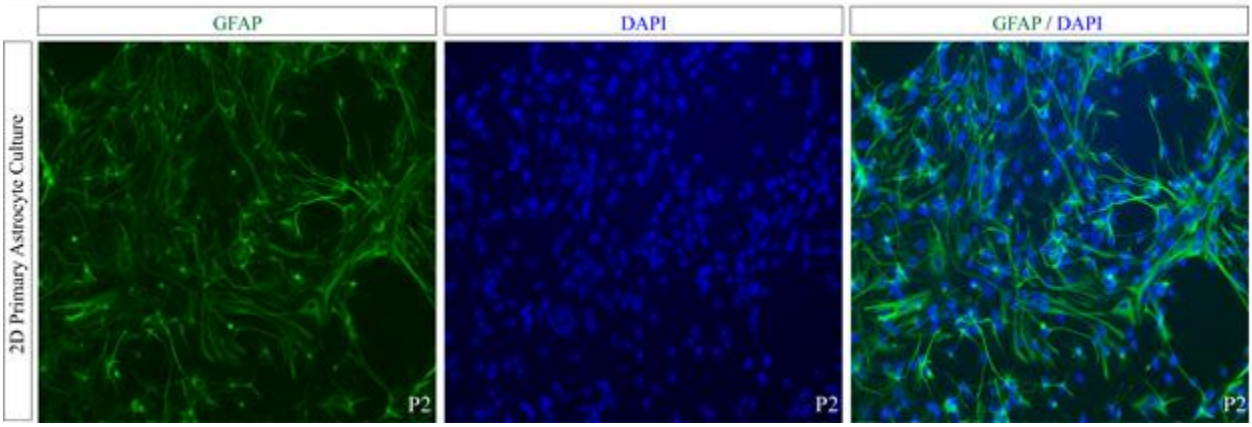

Figure 3.1. Primary astrocytes cultures. Image of GFAP-positive primary astrocyte cell culture. Two days post-natal (P2) Sprague-Dawley primary astrocytes were stained with GFAP antibody to make sure the study population was purified.

3.2.2. Primary Astrocytes Cell Culture: Testing Preparation

According to (Hlavac et al., 2020)**,** astrocyte density and confluence were conducted. Prior to undergoing mechanical exposure, all PA cells were seeded at a density of $1x10^5$ cells per well, forming a 2-D monolayer model, and cultured for six days. Astrocyte counting and viability were conducted using Countess III Automated Cell Counter (ThermoFisher). PA cultures were assigned to either: *Group I)* Primary astrocytes culture used for protein quantification were seeded into a standard six-well plate (Corning; Cat#: CLS3506), and *Group 2)* PA cultures used for immunocytochemistry analysis were seeded in a treated 25mm round coverslip (CellTreat; Cat#: 229174) added to a standard six-well plate with a total of three PA culture per group. The coverslip treatment was conducted in a sterile environment, treated in 1M of hydrochloride acid (1M HCl) overnight, followed by a wash in sterile ultrapure water. A final rinse with 100% ethanol for ten minutes was conducted and dried overnight. Finally, the coverslip was coated with collagen type I rat tail (Corning; Cat#: 354236), incubated for one hour in the cell incubator (at 37°C), and washed with sterile Dulbecco's Phosphate-Buffered Saline (DPBS Gibco; Cat#: 14-190-250).

3.2.3. High-Rate Overpressure Simulator for In Vitro Mechanical Exposure

A high-rate overpressure simulator (HOS) (Figure 3.2 a) was designed (Hampton et al., 2013) based on studies conducted using ICP data from an *in vivo* blast TBI model using rodents (Leonardi et al., 2011). The HOS is a one-chamber fluid-filled device that works through an exploding bridge wire mechanism by using a source of high electrical current in a closed electrical circuit containing a thin wire tightly suspended in two angled plates. This part of the circuit is submerged at the simulator's small end. A capacitor and a voltage source act as the driver for the energy required, and upon discharge, a high current flows through the circuit up to the bridge wire leading to its vaporization, creating a high-rate compression wave that propagates through the conical section of the device exposing the cell culture plate. The peak overpressure data is recorded from a piezoelectric transducer (Meggitt-Cat# 8350C) sensor located in the device's wall directly above and adjacent to the cell culture (Figure 3.2 b).

PA cultures were exposed to a single isolated, transient overpressure with an average of 20 psi (138 kPa) and approximately one-millisecond positive phase duration (Figure 3.2 b). These metrics have been correlated to mild injury outcomes seen in our rodent models (Sajja et al., 2014; Sajja, Hubbard, & VandeVord, 2015; Säljö et al., 2010). Briefly, prior to the test, the HOS was first filled with reverse osmosis water at 37°C. In a sterile environment, PA cultures were filled entirely with Dulbecco's Modified Eagle Medium (Gibco; Cat#: 310530) with no added fetal bovine serum and sealed with sterile parafilm membrane to maintain sterility during injury. Cell plates were gently submerged in the HOS and exposed to a single high-rate overpressure. Sham groups underwent the same steps without exposure to overpressure. PA cultures, post-overpressure exposure, and sham groups were gently removed from the HOS. The parafilm membrane was removed in a sterile environment, and new DMEM/F12 media were added. Finally, PA cultures were returned to the incubator, and upcoming data analyses were performed at 4 hours, 24 hours, and 3 days post-overpressure exposure.

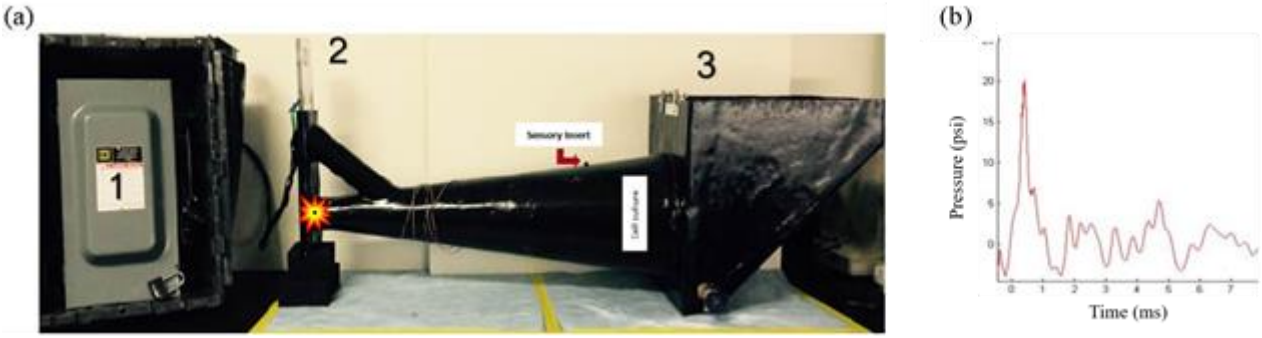

Figure 3.2 High-Rate Overpressure Simulator - *In Vitro* Injury Model of bTBI. (a) The HOS is a water-filled chamber that exposes in vitro samples to high-rate overpressure via an exploding bridge wire mechanism. 1) Driver for the energy required (high electrical current); 2) Bridge wire mechanism (wire holder), and 3) Cell culture plate location and sensory insert. Upon wire vaporization, the wave front travels down the test section of the cell culture plate denoted by "Cell Culture." **(b)** Pressure profile: The high-rate compression waves, as represented in the pressure profile, is meant to mimic an intracranial high-rate overpressure.

3.2.4. Immunocytochemistry and Mitochondrial Morphology Analysis

I. Immunocytochemistry:

Immunocytochemistry was performed to analyze PA mitochondrial morphology post-overpressure exposure. Prior to mechanical exposure, PA cultures were seeded in a coverslip introduced to a six-well plate as described in Section *3.2.2.* under *"group 2"*. Post-overpressure insult, PA cultures underwent fixed immunocytochemistry at each data collection time point (4hr, 24hr, and 3d). First, cultures were washed three times with cold DPBS, fixed in warm (37℃) 4% paraformaldehyde (pH 8) for 20 minutes, washed three times with DPBS at room temperature, and incubated in a solution of blocking buffer containing 10% normal goat serum (ThermoFisher; Cat#:50062Z) and 0.5% Triton-x 100 (Millipore Sigma; T9284) for 45 minutes at room temperature, helping to minimize non-specific hydrophobic interactions. Fixed cells were incubated, for three hours at 4℃, in blocking buffer with primary antibody TOMM20 at 1:100 dilution (Novus; Cat#: NBP1-81556) and GFAP at 1:100 dilution (ThermoFisher; Cat#: 13-0300), this step was carefully conducted by placing the coverslip with upturned cells into a humidified chamber. PA was washed four times with DPBS to remove unbounded primary antibody and

then incubated for one hour at room temperature in blocking buffer with secondary antibody AlexaFluor 555 donkey anti-rabbit at 1:500 dilution and AlexaFluor 488 goat anti-mouse at 1:500 dilution. Post incubation, cells were gently washed three times with DPBS and incubated for ten minutes with DAPI in DPBS (1ug/mL) to visualize nuclei, followed by one wash with DPBS and one wash with ultra-pure water. Finally, the coverslips were mounted with Slowfade-antifade reagent (Invitrogen; Cat#: S36963) with downturned cells onto a tissue slide.

As a positive control, carbonyl cyanide 3-chlorophenylhydrazone (CCCP; ab141229) was used. CCCP is a potent chemical inhibitor of mitochondrial oxidative phosphorylation. Furthermore, CCCP as a mitochondrial uncoupling reagent, leads to rounded and fragmented mitochondria, therefore, being a good positive control for our morphology analysis study. PA cultures that did not undergo blast or sham treatment were treated with 10µM CCCP for ten minutes. Immunohistochemistry for the outer mitochondrial membrane TOMM20 was conducted as described above.

II. Mitochondrial Morphology Analysis:

Fluorescence images were acquired using (Zeiss, Jena, Germany) with a 63x/1.40 oil objective lens, and the Z-stack series consisted of 0.25 µm slice intervals with 12 slices per sample. Images were stacked into a single 2D image using the Zeiss Zen blue 2 software processing tool called "extended depth of focus." A total of four images per PA culture were acquired with approximately three cells per image area, therefore, a total of ~36 cells per group (sham, blast, and CCCP) were analyzed.

As previously mentioned, additional measurements of mitochondrial morphological characteristics were made using Fijian (ImageJ) (Valente et al., 2017). An image macro toolset called Mitochondrial Network Analysis (MiNA) software uses existing Fiji (ImageJ) plugins to help with a semi-automated analysis of mitochondrial morphology in cultured cells (Bakare et al., 2021; Meshrkey et al., 2021; Zehnder et al., 2021). In addition, MiNA software presents optional pre-processing settings to help

to enhance image quality prior to analyses. For analysis, MiNA starts by binarizing and then skeletonizing (figure 3.3 a) the original image to obtain a morphology skeleton to calculate parameters to quantitatively capture the mitochondrial morphology. Finally, MiNA finishes with a summary of data parameters that classify the mitochondrial morphology as individuals, networks, and mitochondrial footprint. Individual mitochondria (rods, punctate, and large/round shapes) and all other objects in the image without a junction pixel are recognized by the MiNA software. All items in the image that have at least one junction are categorized as networks (figure 3.3 b). Results for mitochondrial morphology quantifications were displayed as normalized relative to the sham average.

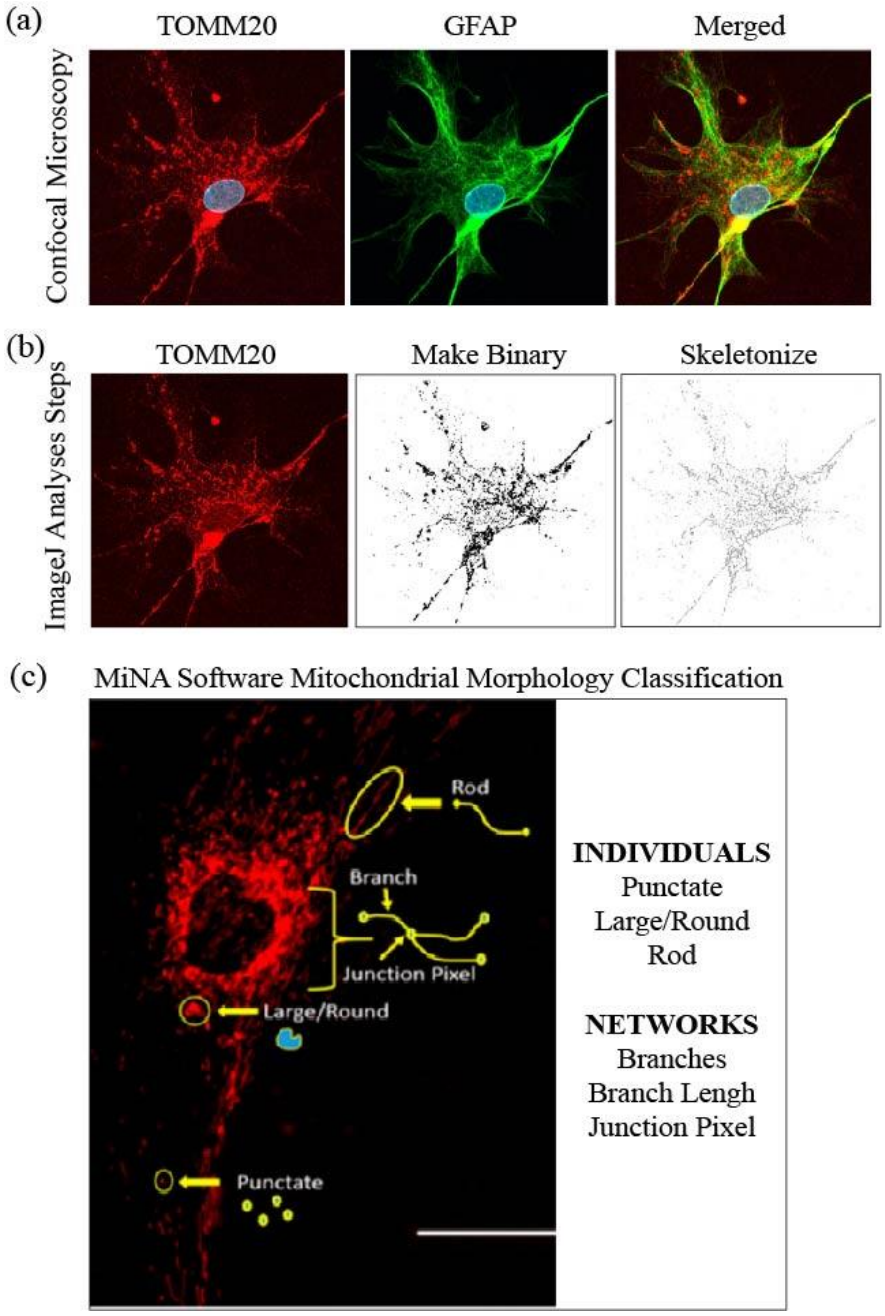

Figure 3.3: Mitochondrial Network Analysis (MiNA) software description and image acquisition. a) Representative images from the 4-hour time point 2D primary astrocytes stained for TOM20 (red) marking an outer mitochondria membrane protein, GFAP (green) a marker for astrocytes and DAPI (blue) to determine the number of nuclei. All pictures were acquired by a 63x/1.40 oil objective. Z- stack series considered of 0.25 µm slice intervals with 12 slices per sample. Images were stacked into a single 2D image using the Zeiss Zen blue 2 software processing tool called "extended depth of focus." Mitochondrial morphological parameters were further measured using Fiji as previously (Image J) disclosed (Valente et al., 2017).**b)** This figure shows how a 2D picture of primary astrocytes at the 4hr time point was processed such that mitochondrial network features could be obtained. The original image is processed on ImageJ and then binarized and skeletonized for data acquisition. **c)** Mitochondrial morphology descriptors by using MiNA toolset. The mitochondria morphology is classified as individuals or networks. Individuals consist of structures without a junction pixel, while networks contain branches with one or more junction pixels. The imaged was from (Bakare et al., 2021).

3.2.5. Protein Isolation and Western Blotting Analysis

Phase separation with chloroform was followed by Trizol (ThermoFisher; Cat# 15596018) treatment on the samples. After extracting RNA and DNA, proteins were recovered from the Trizol phenol phase. The first step in protein precipitation was isopropanol treatment, followed by three 20-minute washes with a 0.3 M guanidine hydrochloride in 95% ethanol solution and one wash with a 20-minute 100% ethanol solution. The protein was re-suspended in a 1:1 solution of 1% sodium dodecyl sulfate solution and 8M urea in 1M Tris-HCl (pH 8). The protein was then further homogenized by sonicating for an additional ten seconds, followed by ten minutes of incubation at 55°C. BCA assay (Pierce; Cat#: 23225) was used to measure the total protein in the samples in preparation for Western Blotting analysis.

To analyze molecular alterations related to astrocyte reactivity, quantification of GFAP (Abcam; Cat#: ab7260) protein levels were chosen. To analyze mitochondrial mediate fission dynamics, protein levels for DRP1 (Novus; Cat#: NB110-55288) and its post-translational phosphorylation at serine 616 ($pDRP1^{s616}$; Cell Signaling; Cat#: 4494S), and serine 637 ($pDRP1^{s637}$; Cell Signaling; Cat#: 4867S) sites were chosen. Target proteins were analyzed at four hours, 24 hours, and three days post-overpressure exposure. Protein samples were produced in accordance with the manufacturer's instructions, and a capillary-based automatic Western system (Wes, Protein Simple) was used for the protein quantification of each studied marker. Wes supplies purchased from Protein Simple were separation modules (Cat#: SW-004), anti-rabbit (Cat#: DM-002), and anti-mouse (Cat#: DM-001) detection modules. Protein levels were calculated using Compass for SW software v.6.1 (Protein Simple) from area measurements obtained from electropherograms at the same exposure period for all data plates. The Wes software determines target protein levels by computing the area under the curve using uniform peak fits across all data. Therefore, the Wes bands shown in the data are digitized images meant to be a qualitative visual comparison of how the target protein traveled through the Wes capillary-based automatic system. According to the target

protein, samples were loaded with the same protein concentration (mg/mL) in each well, normalized to that total protein, and then averaged to the sham value. Protein quantification results are represented as normalized protein expression in comparison to the sham average.

3.2.6. Statistical Analysis

Statistical comparisons were conducted between groups using GraphPad Prism 9 software. A two-way ANOVA was conducted to analyze overall significant differences amongst groups, followed by a Tukey's honestly significant difference (Tukey's HSD) test to analyze which specific group's average differed. For group comparisons within a single individual, a student's t-test was used. Levene's tests were employed to evaluate the equality of variances, and the Kolmogorov-Smirnov test was used to check the assumptions for normality (homoscedasticity). A logarithmic adjustment was carried out to undertake statistical comparisons in the case that the data were not normal. A p-value of 0.05 or less was regarded as statistically significant, and residual analysis was used to identify statistical outliers. The letter "n" stands for the total number of cells. The means and standard errors of the means are presented for all data values (S.E.M.). The figure legend reports the test for each experiment, the n value, and the p-value.

3.3 Results

3.3.1 Acute overpressure mechanical insult induces differential remodeling of astrocytic mitochondrial morphology.

It's crucial to comprehend mitochondrial morphology in order to assess the health of the cell. Descriptors such as fragmented, tubular, and hyper-fused are used to characterize mitochondrial morphology. MiNA software was used to quantify astrocytic mitochondrial morphology by targeting the outer mitochondrial membrane TOMM20. Mechanical-insult significantly increased the number of

fragmented astrocytic mitochondrial ($p = 0.0052$) with a significantly decrease of the number of mitochondrial network ($p = 0.0312$) at 4 hours (Figure 3.4). Furthermore, at 24 hours the amount of fragmented mitochondrial was still significantly increased ($p = 0.0221$); however, the number of networks and the mitochondrial footprint was decreased ($p = 0.0754$, $p = 0.0619$) (Figure 3.5) although not statistically significant. However, by three days, the astrocytic mitochondrial network started to restore to sham levels as the number of individual mitochondrial visible decreased in the blast group, and the number of networks was not significantly different from sham levels (Figure 3.6).

Positive control samples demonstrated that astrocytic mitochondrial treated with CCCP were severely fragmented with significantly increased fragmented mitochondrial ($p < 0.0001$) with significantly reduced total mitochondrial footprint ($p < 0.0001$) (Figure 3.7). This data helps to further show that MiNA software successfully identified and characterized morphological features of astrocytic mitochondrial morphology.

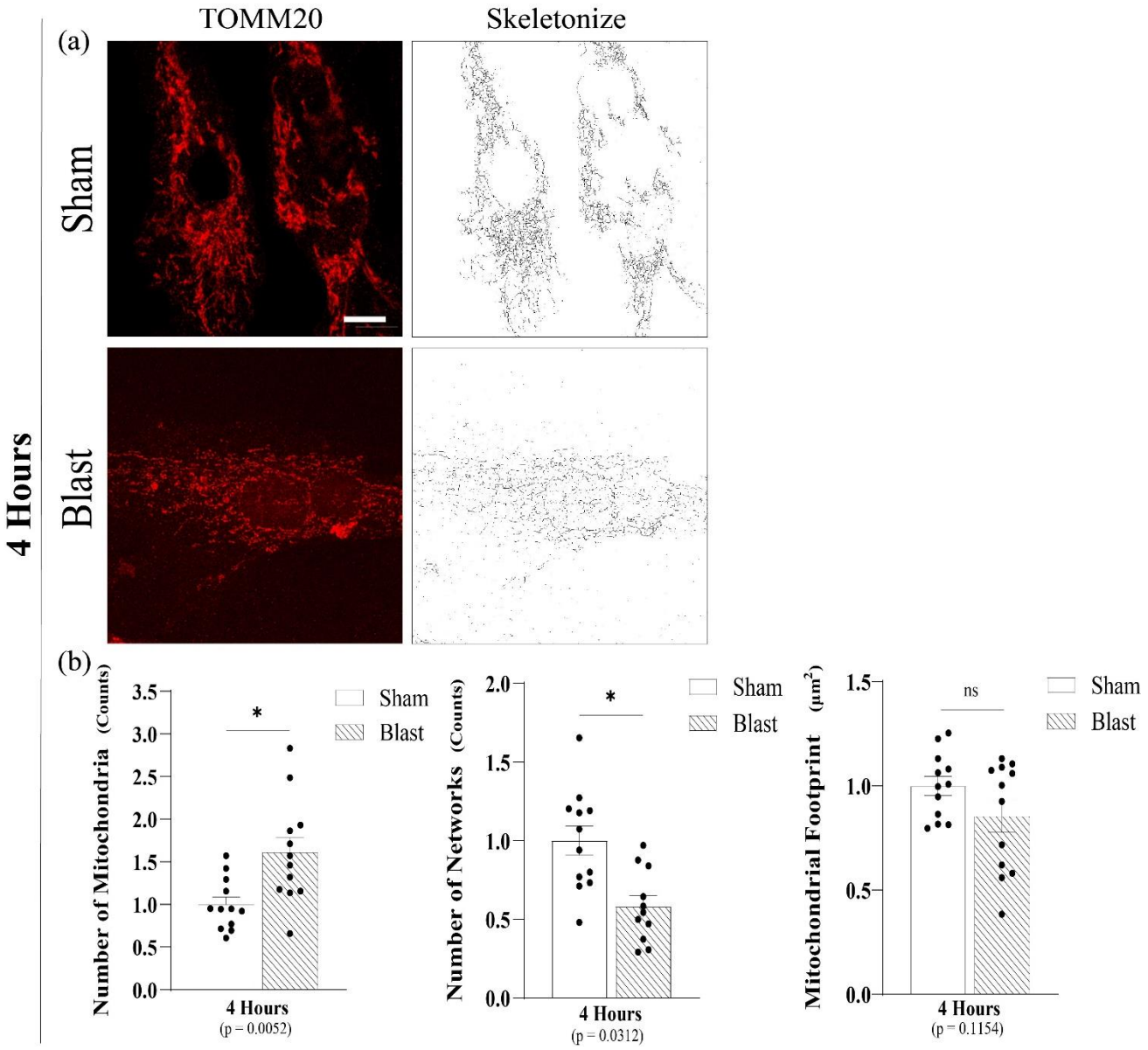

Figure 3.4: Mitochondrial Network Analysis (MiNA) software descriptors show differences in astrocyte mitochondrial morphology in Sham and single overpressure (blast) groups at 4 hours.

a) Representative images of TOMM20 and skeletonized for data acquisition. **b)** At 4 hours post single overpressure, astrocytes increase fission by presenting a significant increase in the number of individuals (puncta and rod) and a small number of networks. ((Each point represents average of 3 cells per image with a total of 3 culture per group; data are mean ± SEM; *p-value represents ≤ 0.05; Scale bar in a = 10 µm).

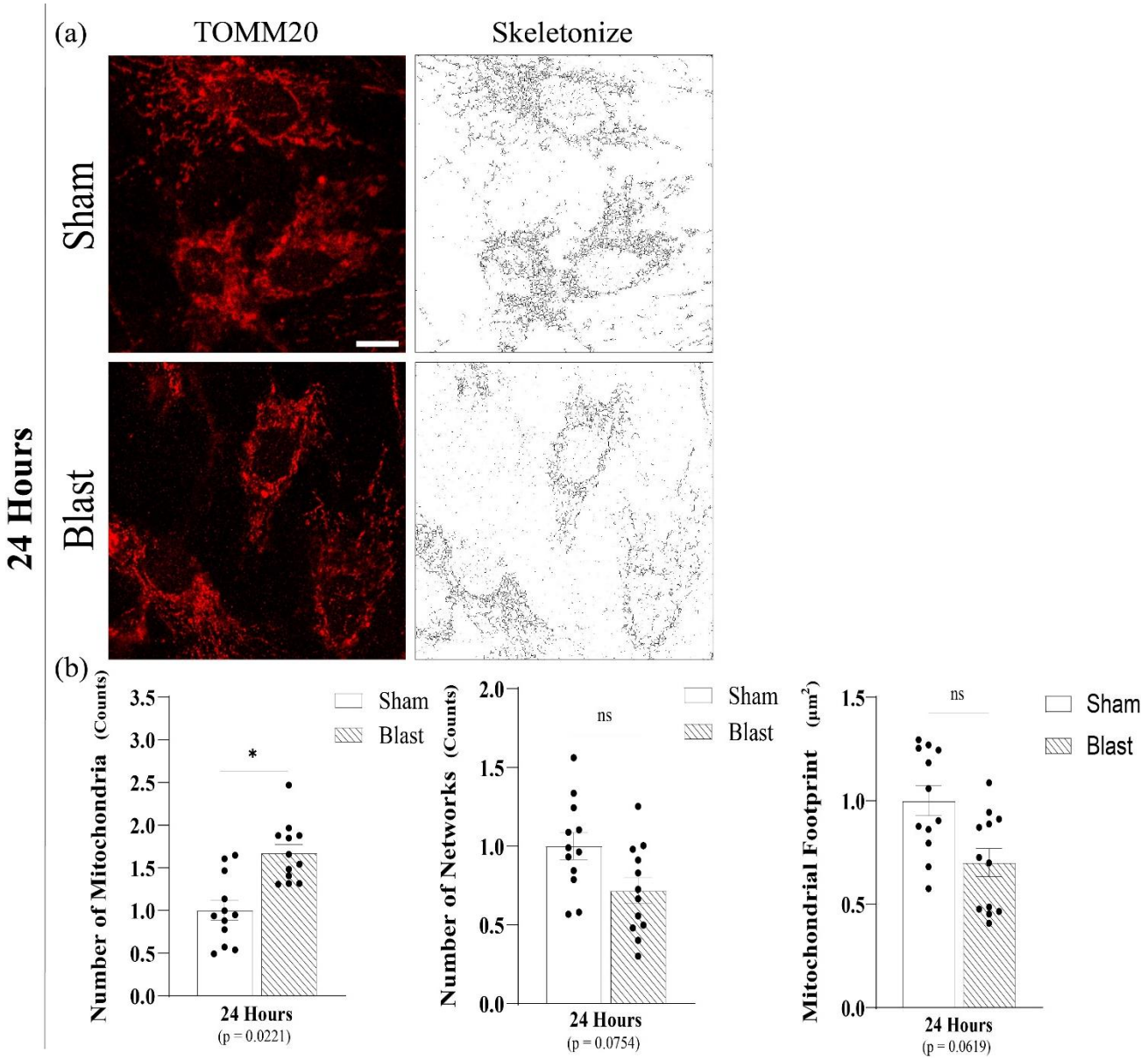

Figure 3.5: Mitochondrial Network Analysis (MiNA) software descriptors show differences in astrocyte mitochondrial morphology in Sham and single overpressure (blast) groups at 24 hours.

a) Representative images of TOMM20 and skeletonized for data acquisition. **b)** At 24 hours post single overpressure, astrocytes still presented a significant increase in the number of individuals (puncta and rod), displayed lower number of networks and mitochondrial footprint (the total area in the cell expressing mitochondrial marker TOMM20) although not statistically significant. (Each point represents average of 3 cells per image with a total of 3 culture per group; data are mean ± SEM; *p-value represents ≤ 0.05; Scale bar in a = 10 µm).

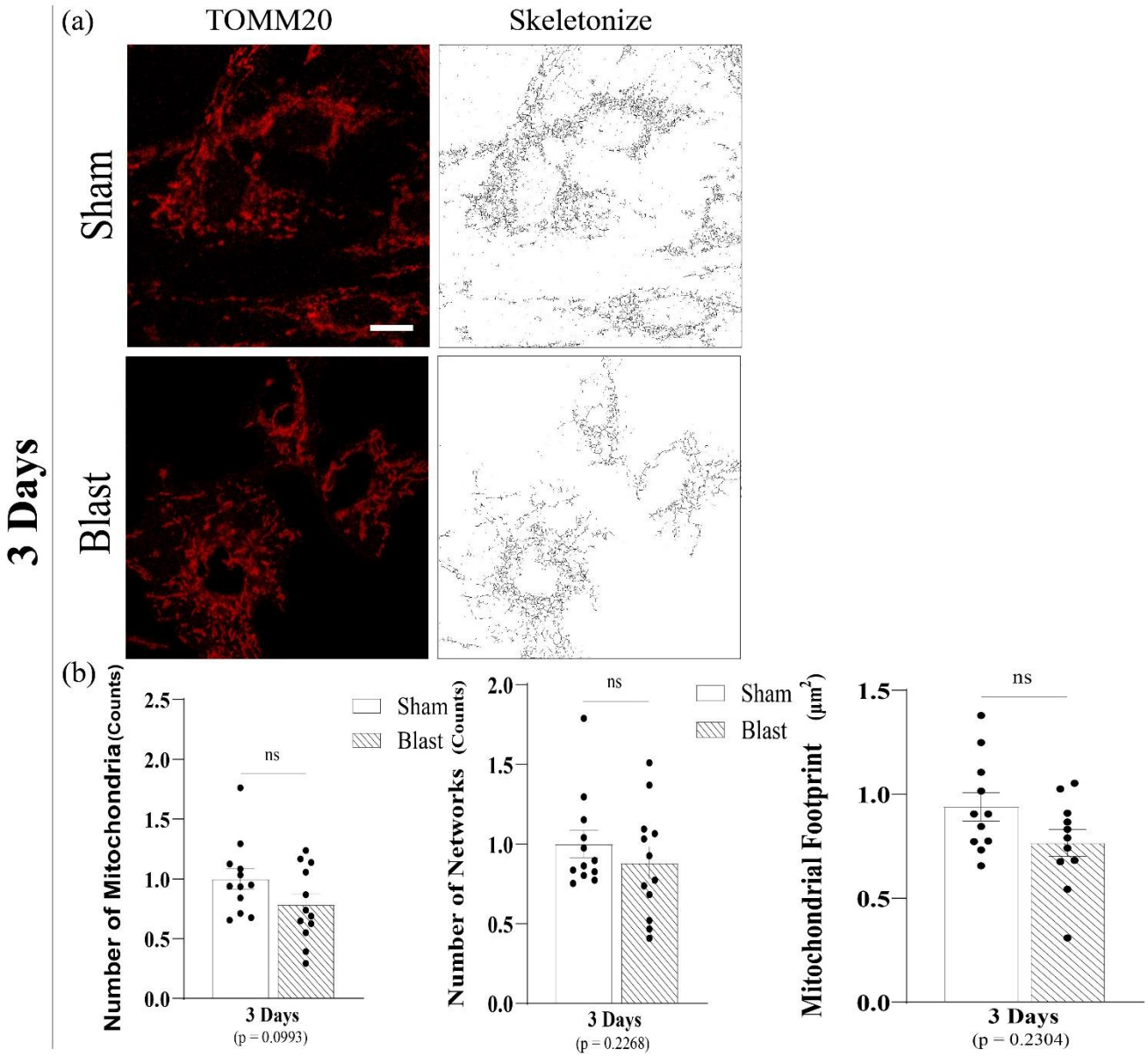

Figure 3.6: Mitochondrial Network Analysis (MiNA) software descriptors show differences in astrocyte mitochondrial morphology in Sham and single overpressure (blast) groups at3 days.

a) Representative images of TOMM20 and skeletonized for data acquisition. **b)** At 3 days, there is no significant difference in the number of individuals, networks, and mitochondrial footprint between sham and overpressure groups**.** ((Each point represents average of 3 cells per image with a total of 3 culture per group; data are mean ± SEM; *p-value represents ≤ 0.05; Scale bar in a = 10 µm).

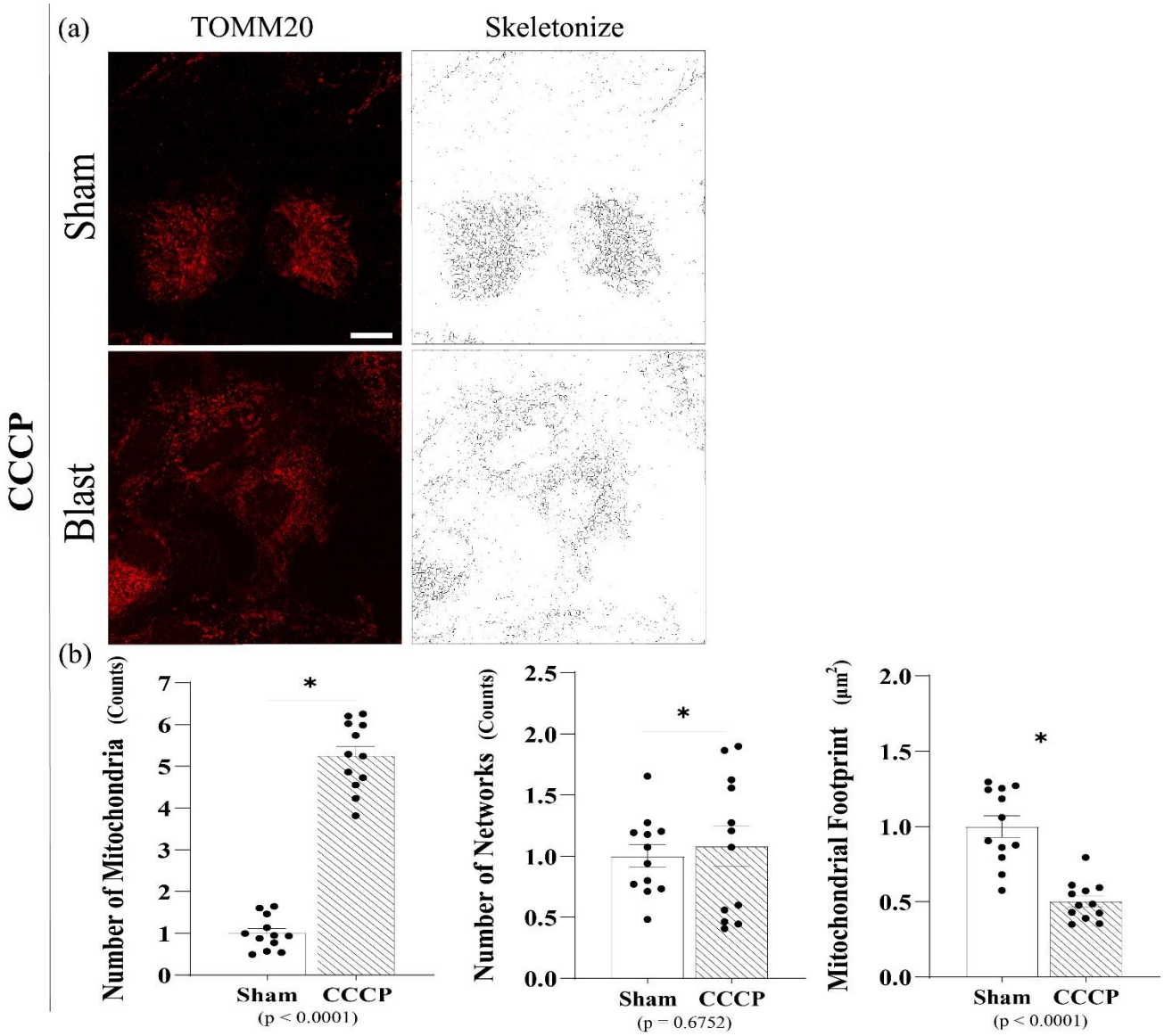

Figure 3.7: Mitochondrial Network Analysis (MiNA) software descriptors show differences in astrocyte mitochondrial morphology in Sham and CCCP positive control groups.

a) Representative images of TOMM20 and skeletonized for data acquisition. **b)** Astrocytic mitochondria treated with 10 µM CCCP (positive control) were severely fragmented with significantly reduced mitochondrial fragment length and total mitochondrial footprint. It further shows that MiNA successfully identified and characterized morphological features of mitochondrial networks. ((Each point represents average of 3 cells per image with a total of 3 culture per group; data are mean ± SEM; *p-value represents ≤ 0.05; Scale bar in a = 10 µm).

3.3.2 Exploring DRP1 protein levels post mechanical insult at acute and sub-acute stages.

Due to an increase in the fragmented mitochondrial organelle, we assessed if this astrocytic mitochondrial phenotype was due to the participation of the GTPase DRP1 protein, known to coordinate

mitochondrial fission dynamics. Western blotting analyses were performed to determine if exposure to the mechanical insult altered DRP1 protein levels at four hours, 24 hours, and three days following the mechanical-insult. Results presented in figure 3.8 indicate no significant changes in PA cultured cortical total DRP1 levels between groups (blast vs. sham).

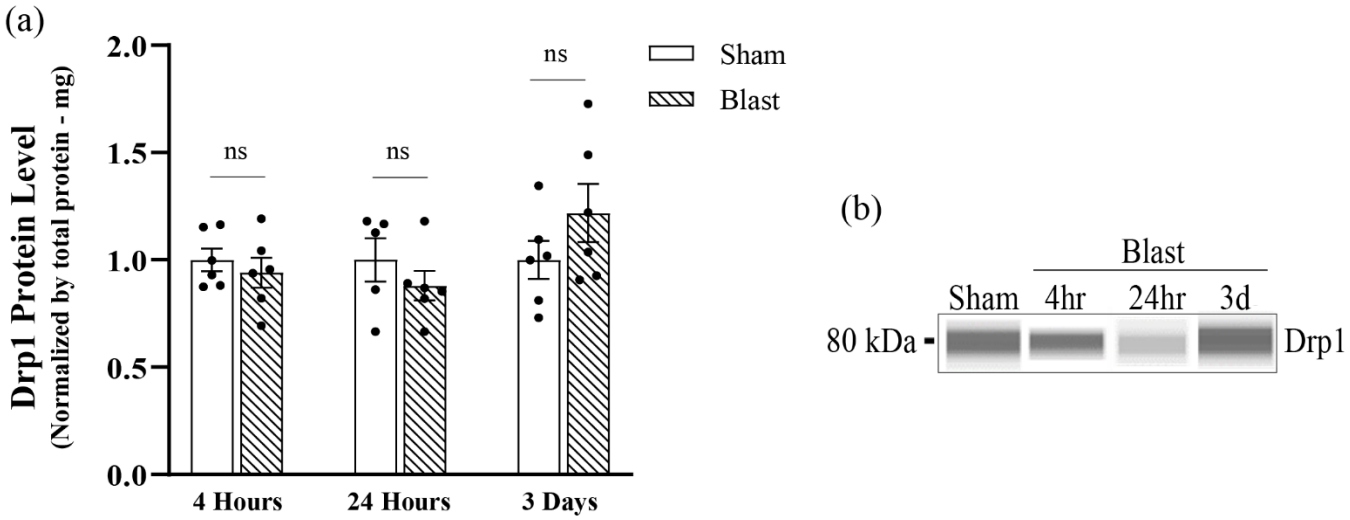

Figure 3.8: Analysis of Total Mitochondrial Fission GTP-DRP1 Protein post single overpressure exposure. Western Blotting was conducted using an automatic capillary-based system (Wes, Protein Simple) to look at relative protein quantification to identify possible fission post-overpressure exposure.
a) There were no significant changes in DRP1 protein levels at 4 hours, 24 hours, and 3 days following the mechanical-insult. **b)** Only for qualitative visual comparison, digitized bands illustrate how proteins moved through the capillary system on the Wes. (n=6/group; data are mean ± SEM; *p-value represents ≤ 0.05).

3.3.3 Post-translation phosphorylation state of DRP1-mediated mitochondrial fission plays a role in astrocytic mitochondrial fragmentation at acute states of the mechanical insult.

To better understand the potential role of DRP1-mediated fission protein, its post-translational phosphorylation state at serine 616 and serine 637 sites, hereafter referred to as pDRP1^{s616} and p-DRP1^{s637}, were analyzed. Since pDRP1^{s616} triggers mitochondrial fission by activating DRP1 translocation from the cytoplasm to the OMM, p-DRP1^{s637} suppresses mitochondrial fission by stopping the translocation of DRP1 protein to the OMM; we quantified both. pDRP1^{s616} total protein levels were found to be significantly increased ($p = 0.0309$) at four hours post-mechanical insult (Figure 3.9 a). This indicates an

increase in the activity of DRP1-mediate mitochondrial fission by its translocation to the OMM since no significant changes were seeing in total p-DRP1^{s637} (Figure 3.9 b) and a non-statistically significant increase in pDRP1^{s616}/ pDRP1^{s637} ratio was observed (p = 0.0786) (figure 3.9 c). Levels of total pDRP1^{s616} started to decrease at 24 hours and were returned to sham levels at three days post-mechanical insult. Furthermore, levels of pDRP1^{s637} were maintained at sham levels at 24 hour and 3 days in the mechanical insult group (Figure 3.9 a-c).

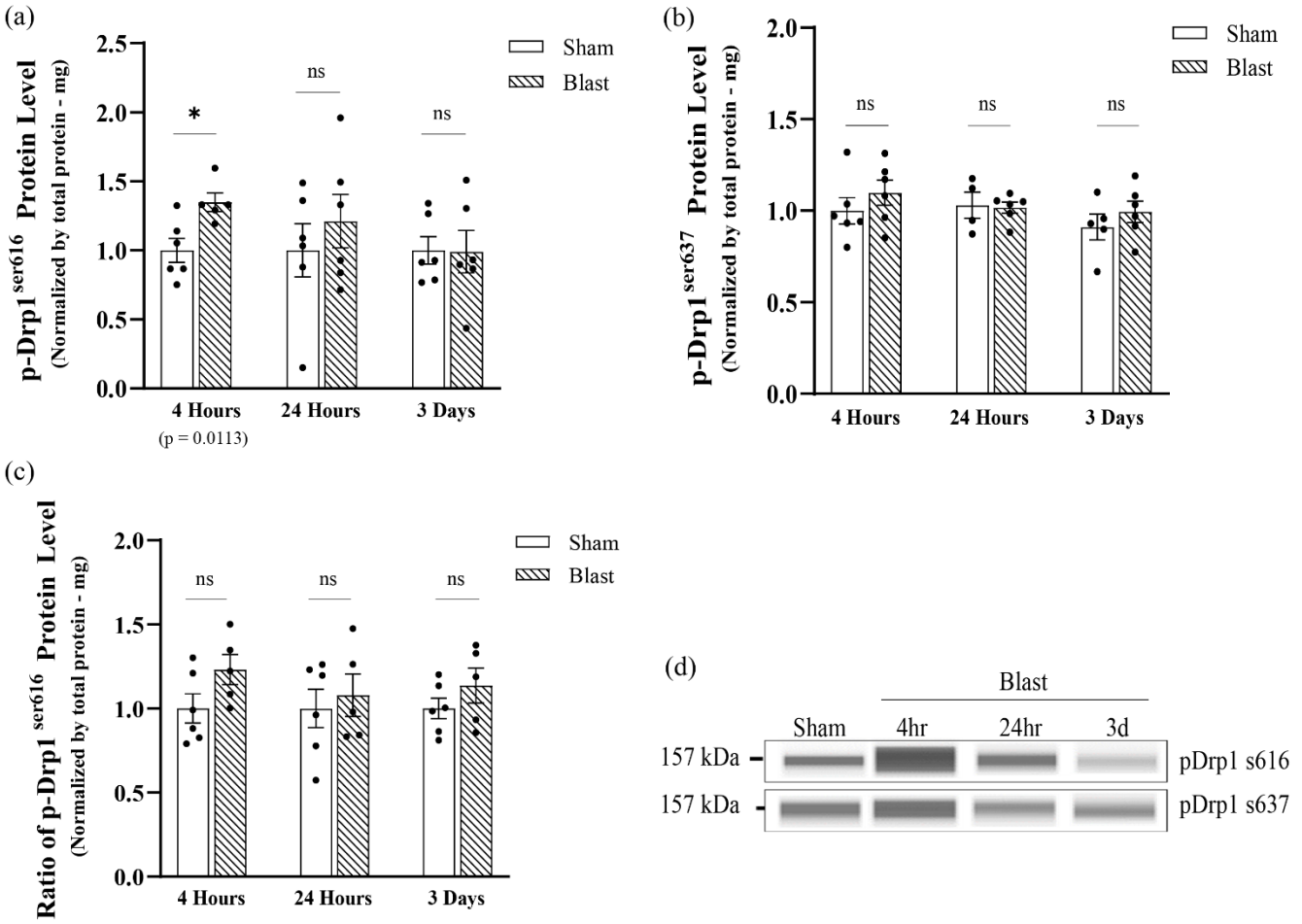

Figure 3.9: Analysis of total DRP1 post-translational modification protein by it phosphorylation at serine 616 and serine 627 post single overpressure exposure. Western Blotting was conducted using an automatic capillary-based system (Wes, Protein Simple) to look at relative protein quantification to identify possible fission post-overpressure exposure. **a)** The total levels of p-DRP1^{616} protein were acutely increased by 4 hours and returned to physiological levels by 3 days post mechanical insult. **b)** The total levels of p-DRP1^{637} protein were maintained at physiological levels at all-time points. **c)** The pDRP1s616/ pDRP1s637 ratio was analyzed and presented no significant difference across groups and time points. **d)** Only for qualitative visual comparison, digitized bands illustrate how proteins moved through the capillary system on the Wes. (n=6/group; data are mean ± SEM; *p-value represents ≤ 0.05).

3.3.4 Investigating astrocyte reactivity phenotypes at acute and sub-acute stages following mechanical insult.

From the samples used to observe the levels of mitochondrial mediated fission proteins, the astrocyte reactive phenotype was assessed by quantifying GFAP protein levels via western blotting technique. Results presented in figure 3.10 indicated no significant changes in total protein levels of GFAP between groups (blast vs. sham) at all-time points post-mechanical insult.

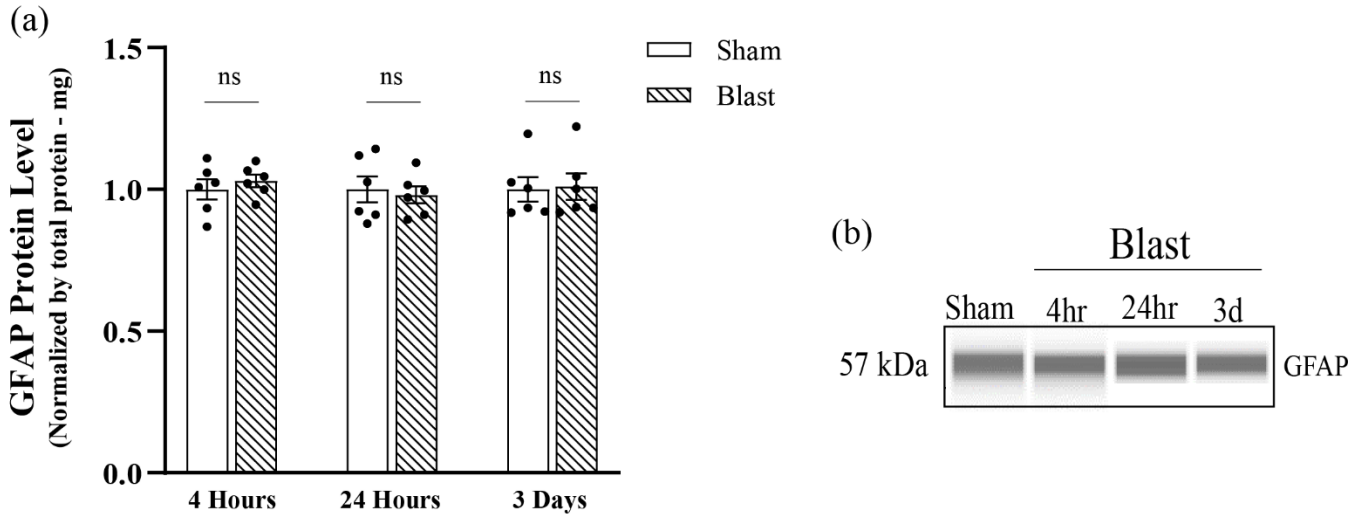

Figure 3.10: Analysis of total GFAP protein post single overpressure exposure. Western Blotting was conducted using an automatic capillary-based system (Wes, Protein Simple) to look at relative protein quantification to identify possible fission post-overpressure exposure.

a) Total levels of GFAP protein were maintained at physiological levels at all-time points. **b)** Only for qualitative visual comparison, digitized bands illustrate how proteins moved through the capillary system on the Wes. (n=6/group; data are mean ± SEM; *p-value represents ≤ 0.05).

3.4 Discussion

The mitochondrial balance of fission and fusion events is known as *mitochondrial dynamics*. It is orchestrated by a family of large GTPase proteins encoded by genes in the nuclear genome. Fission and fusion events play a key role not only in altering mitochondrial morphology (shape changes) but also in size, number, distribution, quality control (mitophagy), and transport of mitochondria in cells (Giacomello et al., 2020; Newmeyer & Ferguson-Miller, 2003; Yu et al., 2020). Growing evidence in the literature indicates the importance of proper astrocytic mitochondrial dynamics in a healthy brain and how altered mitochondrial dynamics could lead to both detrimental and protective astrocyte reactivity phenotypes in TBI pathologies (Bantle et al., 2021; Ishii et al., 2017; Rahman & Suk, 2020; Rose et al., 2017; Sarkar et al., 2018; Zehnder et al., 2021), shedding light on a novel therapeutic route for TBI. In Specific Aim 1, primary astrocytes were directly exposed to an overpressure mechanical insult, simulating the bTBI primary insult etiology, and it was characterized mitochondrial dynamics changes, presenting a higher fission state, and further examined whether DRP1 post-translational phosphorylation modification was closely related to these outcomes.

Under physiological conditions, a study showed that astrocytic mitochondria from acute cortical slices present an even split of mitochondrial dynamics with half fission and half fusion events (Motori et al., 2013). Results of this Specific Aim 1 have shown that the mechanical insult was capable of disrupting the mitochondrial dynamic balance by remodeling the astrocytic mitochondrial network as early as four hours post-overpressure exposure. Results revealed a significantly higher amount of punctate/rod-like individual mitochondria as well as a smaller number of individual networks, perhaps due to breakdown into fragmented mitochondria. This event persisted at 24 hours post-insult, presenting the same characteristics, however with the addition of non-statistically significant decrease in mitochondrial footprint, indicating decreased expression of the mitochondrial marker TOMM20 presumably relating to

a possible decrease in mitochondrial mass. Under the MiNA software classification, fragmented mitochondrial is referred as any rods, punctate and large/round shape of mitochondrial morphology. Therefore, the mitochondrial footprint data could perhaps indicate a more punctate (smaller) fragmented mitochondria at 24 hours versus four hours post-mechanical insult. In addition, at three days post-mechanical insult in our study, astrocytes presented with fewer numbers of fragmented mitochondria as well as the number of networks being close to sham level. Therefore, our result presented a possible initiation of recovering mitochondrial dynamic balance to physiological conditions.

Due to an increase in fragmented mitochondrial organelles, we assessed whether this astrocytic mitochondrial phenotype was due to the participation of the GTPase DRP1 protein, known to coordinate mitochondrial fission dynamics. Our results revealed that at four hours, 24 hours, and three days, the overpressure insult did not change total DRP1 protein levels. Rather, DRP1-mediated fission was due to changes in DRP1 activation status. Changes in DRP1 activity happens by post-translational modification with the phosphorylation of two serine residues (serine 616 and serine 637). This two serine sites' phosphorylation have opposing impacts on mitochondrial morphology. DRP1 translocation to the OMM is known to be activated by phosphorylation at the serine 616 site ($pDRP1^{s616}$), and DRP1 activity in translocating to the OMM is known to be inhibited by phosphorylation at the serine 637 site ($pDRP1^{s637}$), which prevents mitochondrial fission (Liesa et al., 2009; Serasinghe & Chipuk, 2017). Our results indicated that at four hours post mechanical insult, there was a significant increase in $pDRP1^{616}$ protein levels, and there were no changes in the protein level of $pDRP1^{s637}$. These results indicate a higher activity of DRP1-mediated mitochondrial fission by its translocation from the cytoplasm to the OMM. Furthermore, although not significant, there was a higher $pDRP1^{s616}/pDRP1^{s637}$ ratio at four and 24 hours, and by three days the $pDRP1^{s616}/pDRP1^{s637}$ ratio returned to sham levels. These results are consistent with the increase of astrocytic fragmented mitochondria seen at four and 24 hours and with the possible

initiation of restoring mitochondrial integrity and mitochondria network observed by three days post-mechanical insult.

It has been demonstrated that the oxidative respiratory chain and mitochondrial redox state are disrupted by DRP1-mediated mitochondrial fission and excessive mitochondrial fragmentation, which results in a significant increase in ROS generation (Balaban et al., 2005; Flippo & Strack, 2017; Glancy et al., 2020; Jezek et al., 2018; Sprenger & Langer, 2019). Superoxide anions (O_2^-), hydroxyl radicals (OH^-), and hydrogen peroxide (H_2O_2) are only a few of the chemicals that make up ROS, which are a natural byproduct of mitochondrial respiration. Overproduction of ROS following injury leads to oxidative stress, a state of lost balance between anti-oxidative and pro-oxidative enzymes that can significantly affect the severity and progression of brain injury. Additionally, consistent oxidative respiration is ensured by the harmony of Drp1 phosphorylation at serine 616 and serine 637. For instance, when under stress, the $pDRP1^{s616}/pDRP1^{s637}$ ratio rises, the oxidative state is disrupted and excessive quantities of ROS are subsequently produced in neurons (Tsushima et al., 2018). According to an *in vitro* study, neurons rely on astrocytes' redox buffering to protect them from oxidative stress (Desagher et al., 1996). Additionally, an adult *in vivo* model revealed that astrocytes possess the redox buffering ability required for neuronal survival and homeostasis under physiological circumstances (Schreiner et al., 2015). Therefore, this indicate the importance of a proper mitochondrial in the astrocytes.

Published data from our laboratory used an *in vitro* bTBI model to demonstrate acute perturbations in astrocytic redox status by a significant increase of NADPH oxidase 4 (NOX4) protein levels (Hlavac et al., 2020). NOX4 is a member of the NOX family of oxidases and it is highly expressed in astrocytes (Xie et al., 2020) and has been linked with multiple detrimental outcomes of TBI, including protein peroxidation, neuronal survival, and neurodegeneration (M. W. Ma, Wang, Dhandapani, & Brann, 2018; M. W. Ma, Wang, Dhandapani, Wang, et al., 2018; Xie et al., 2020). NOX4 changes were not seen at four

hours, but they started to be elevated at 24 hours post-overpressure mechanical insult (Hlavac, 2018; Hlavac et al., 2020)**,** whereas superoxide dismutase 2 (SOD2) did not change at either time point (Hlavac, 2018). SOD2 is located in the mitochondrial matrix and it is an important antioxidant that helps clean up ROS. Moreover, at four hours, significantly lower levels of endogenous ATP were observed, perhaps indicating enzymatic dysfunction associated with impaired mitochondrial function (Hlavac et al., 2020).

The current Specific Aim 1 data showed a significantly higher amount of astrocytic fragmented mitochondria at four hours. This higher fragmented mitochondria level coincided with the lower levels of endogenous ATP also seen at four hours post-mechanical insult (Hlavac et al., 2020). At 24 hours, astrocytes still presented high levels of fragmented mitochondria, but of interest, levels of endogenous ATP had returned to the sham level at 24 hours (Hlavac et al., 2020). This could be happening because astrocytes can shift their metabolism between mitochondrial oxidative phosphorylation and glycolysis to maintain normal central nervous system functions. In addition, although not significant, our current data also presented a visible increase in the pDRP1^{s616}/pDRP1^{s637} ratio with a significant increase of pDRP1^{s616} protein levels at four hours, which start to decrease by 24 hours post-insult, reaching a balance in pDRP1^{s616}/pDRP1^{s637} ratio at three days post-overpressure mechanical insult. Our current study is the first to characterize astrocytic DRP1 protein in mediating mitochondrial fission by its post-translational modification (pDRP1^{s616} and pDRP1^{s637}) following mechanical insult. These results together identify a possible mechanism that triggers astrocyte mitochondrial dynamics changes towards a higher fission state by the increase in activated DRP1-mediated mitochondrial fission, and the imbalance in post-translational modifications of the pDRP1^{s616}/pDRP1^{s637} ratio can further lead to a break in the astrocytic mitochondrial redox status, consequently leading to high production of ROS, which is an outcome reported in the *in vivo* bTBI models (Cho, Sajja, VandeVord, et al., 2013; Kochanek et al., 2013; Kuriakose et al., 2019; Sajja, Hubbard, & VandeVord, 2015; Toklu et al., 2018). Our current data suggest a post-injury temporal

window within which mitochondria dynamics was altered by the mechanical insult. This could be associated with the beginning of a pro-oxidative environment in astrocytes (Hlavac et al., 2020) and perhaps a pro-inflammatory phenotype (Motori et al., 2013). Therefore, further research should be conducted to correlate mitochondrial dynamics dysfunction and the DRP1-mitochondrial fragmentation-ROS pathway in the astrocytic response to overpressure mechanical insult.

Lower ATP levels, a lack of inner membrane polarization, and higher mitochondrial ROS generation are all signs of mitochondrial malfunction in astrocytes. This dysfunction has been linked to an increase in astrocyte responsiveness to pro-inflammatory states (Joshi et al., 2019; Motori et al., 2013). Astrocytes that are reactive typically differ morphologically from astrocytes that are at rest. Astrocytes exhibit hypertrophy of their process and body, proliferation, and changes in protein expression in the injured brain. One such change is the upregulation of GFAP, which is a universal marker of the reactive astrocyte phenotype in pre-clinical and clinical TBI pathology (Escartin et al., 2021; Michinaga & Koyama, 2021; Sofroniew, 2015b). Our results revealed that at four hours, 24 hours, and three days, overpressure mechanical insult did not change total GFAP protein levels in cortical astrocytes. Published data from our laboratory with the same *in vitro* bTBI model have shown changes in astrocytic GFAP protein occurring at 48 hours (Hlavac & VandeVord, 2019) but not at 24 hours and 3 days. In addition, our laboratory unveiled a significant increase in proliferating cell nuclear antigen (PCNA) at 24 hours, 48 hours, and three days post mechanical insult (Hlavac & VandeVord, 2019). Since PCNA directly recruits and interacts with numerous DNA replication proteins, it has previously been employed as a possible reparative characteristic (Dieckman, 2012), moreover, PCNA is used as a marker for proliferating cells, including astrocytes (Di Giovanni et al., 2005; Kato et al., 2003). It is thought that acute stages of astrocyte proliferation, with phenotypes of mild astrocyte reactivity, could present reparative characteristics (Sofroniew, 2020). However, if persisting, this might cause a phenotypic change into a severe reactive

state, where it can develop into a highly proliferative, scar-forming phenotype as a result of chronic-state injury (Buffo et al., 2008; Pekny & Nilsson, 2005; Pekny & Pekna, 2014). Mechanical insults first initiated the astrocytic mitochondrial fission as early as 4 hours, followed by an astrocytic increase in PCNA at 24 hours and a delayed response of increased GFAP protein levels by 48 hours. Those results show that the same stimuli that trigger a mild astrocyte reactivity also lead to astrocytic mitochondrial dynamics changes, and those changes are seen first. In addition, according to current data in the Specific Aim 1, at three days post-mechanical insult, the astrocytic mitochondrial network and GFAP protein levels were restored to physiological (sham) levels. In contrast, PCNA protein levels were still significantly high at three days post-mechanical insult (Hlavac & VandeVord, 2019).

These results, in conjunction with the current study data, suggest that astrocytes have an autologous robust ability to respond to a bTBI mechanical insult by presenting acute mild astrocyte reactivity with possible reparative characteristics. Furthermore, it was accompanied by early mitochondrial fission that were restored to physiological (sham) levels by three days, perhaps playing a role as one of the initial triggers and to help to maintain a possible initial astrocyte reparative phenotype. The highly dynamic mitochondrial organelle constantly changes shape in response to physiologic cues or stress insults by modifying structure and function, which are intimately connected, and helping to maintain cellular homeostasis activity. Nevertheless, it is noteworthy that the astrocytes were cultured without other resident brain cells, and secondary insults from other cells are known to contribute to a detrimental phenotypic transition in astrocytes and further contribute to later bTBI pathology. Therefore, the second part of this dissertation has worked to translate those findings to an *in vivo* bTBI model and characterize astrocytic mitochondrial dynamics and the participation of DRP1 and its post-translational modification (phosphorylation) in isolated astrocytes from hippocampus adult rats post single bTBI.

Chapter 4. Characterizing unique patterns of astrocytic mitochondrial dynamic alteration post single bTBI.

4.1 Introduction

Mild bTBI may result in morphological and functional alterations in the brain's cells, such as mitochondrial dysfunction, astrocyte reactivity, synaptic modification, and neurovascular damage. Mild bTBI that is left untreated over time might result in lasting cognitive impairments (Sajja et al., 2016). Clinical studies have demonstrated that exposure to blast overpressure causes cognitive impairments include memory loss, anxiety and depression disorders (Agoston, 2017; Chapman & Diaz-Arrastia, 2014; Higgins et al., 2014; Kashdan et al., 2006; Miles et al., 2017; Theeler et al., 2012). The hippocampus serves as the entry point for emotions and memory enhancement. It is a part of the limbic system and is crucial for spatial navigation and long-term memory. The hippocampus is a structure found in the medial temporal lobe of humans and other primates, just below the cortical surface. Furthermore, mice and humans share a very similar hippocampal organizational structure (Clark & Squire, 2013).

The hippocampus is the primary region that plays a role in emotion and memory potentiation, long-term memory, and special navigation. It is a common region where neuronal death and astrocyte reactivity are reported following mild bTBI in preclinical models (Cho, Sajja, VandeVord, et al., 2013; Hao et al., 2020; Hernandez et al., 2018; Law et al., 2016; Sajja et al., 2012, 2014; Säljö et al., 2010), with correlations between adverse cognition effects and hippocampal dysfunction; however, the injury mechanisms underlying those outcomes still remain unclear. Furthermore, pre-clinical studies of bTBI have shown injury to the hippocampus and subsequently cognitive impairment (Sajja et al., 2014; Sajja, Hubbard, Hall, et al., 2015)**.** A recent focus of chronic TBI outcomes has been on mitochondrial function (Fischer et al., 2016; Hubbard et al., 2021). Therefore, given the significant cognitive effects of clinical bTBI and the central role of the hippocampus in cognition, this current study aims to characterize hippocampal astrocytic mitochondrial dynamics and astrocyte reactive phenotype post single mild bTBI at the acute and sub-acute stages of the injury.

By producing a combination of pro-inflammatory and anti-inflammatory mediators, astrocyte reactivity can play many functions in a damaged brain, either aggravating or relieving TBI pathology. Astrocyte reactivity has a range of potential modifications that can happen in different contexts depending on a variety of distinct signaling events that change depending on the type and severity of the particular brain injury. Recent research suggests that a wide range of intracellular and intercellular signaling and regulatory molecules can control particular elements of astrocyte response to an insult. Combinatorial exposure to several stimuli can significantly change the astrocyte transcriptome profiles and result in different phenotype characteristics that are not anticipated by exposure to a single stress stimulus (Hamby et al., 2012).

Therefore, translating our *in vitro* study to our *in vivo* study is crucial to help translation to the clinic. For Specific Aim 2, we will characterize the time-dependent response of astrocytic mitochondrial dynamic, now in combination with the primary and secondary etiologies triggered by bTBI. As mentioned before, mitochondrial dynamics act upon physiological insults and stress insults by governing mitochondrial structure remodeling and adapting it to the environment at the moment. Mitochondrial structure remodeling is linked with mitochondrial functionality, therefore, protecting mitochondrial by maintaining its dynamic balance is extremely important to avoid a loop of detrimental intercellular signaling in the astrocytes, such as lack of proper calcium buffer, increase in ROS, and consequently an increase in the oxidative stress environment. Moreover, the second part of this Specific Aim 2, further characterizes at a time-depending manner an astrocytic reactive phenotype transition of adult male rat hippocampal following single mild bTBI.

4.2. Methods

The described study was carried out in accordance with protocols approved by the Virginia Tech Institutional Animal Care and Use Committee.

4.2.1. Advanced Blast Simulator for In Vivo Blast Wave Exposure

A custom Advanced Blast Simulator (ABS) (200 cm × 30.48 cm × 30.48 cm) (Figure 4.1 a) located at the Center for Injury Biomechanics (Virginia Tech University, VA, USA) was used to generate a single blast wave. To produce, develop, and dissipate the blast wave, the ABS is divided into three parts. First, helium is compressed in the driver chamber using calibrated acetate membranes (located at the area denoted "compression chamber"). Once passively ruptured, the blast wave is generated as it propagates through the transition chamber and reaches the animal in the "testing chamber" area. The blast wave continues to flow and will dissipate once reaching the end-wave eliminator located downstream of the testing chamber. As a final result, the animal was exposed to a single peak blast wave, recreating a free-field blast exposure. Pressure measurements were collected at 250 kHz using a Dash 8HF data acquisition system (Astro-Med, Inc, West Warwick, RI, USA) (Figure 4.1 b). A customized Matlab script was used to analyze pressure profiles and determine the impulse, duration, and rising time of the positive and negative phases. Rankine—Hugoniot relations and observed wave speed at the sensors within the ABS's animal testing chamber were used to calculate the peak overpressure.

(a)

(b)

	Time Point	Treatment	Peak pressure (psi)	Positive duration (ms)
Group I (MACS)	4 hours	1 x Blast	17.76 ± 0.72	2.28 ± 0.06
	24 hours	1 x Blast	18.82 ± 0.45	2.27 ± 0.06
	3 days	1 x Blast	17.96 ± 0.26	2.28 ± 0.06
	7 days	1 x Blast	20.30 ± 0.75	2.46 ± 0.02

	Time Point	Treatment	Peak pressure (psi)	Positive duration (ms)
Group II (Histology)	24 hours	1 x Blast	17.58 ± 0.5	2.49 ± 0.05
	3 days	1 x Blast	16.6 ± 0.6	2.28 ± 0.06
	7 days	1 x Blast	18.06 ± 0.4	2.35 ± 0.04

Figure 4.1: Preclinical Model: Blast-induced Traumatic Brain Injury.
a) Advanced blast simulator (ABS) consist of three distinct sections to create, develop, and dissipate the blast wave. Acetate membranes are ruptured following pressurization by helium gas located in the driver section. **b)** 10-week old Sprague Dawley rats (male, 250–300 g) were exposed to a single blast wave. The average peak pressure resulted in a blast wave magnitude of ~17-20psi which induces a mild TBI in rodents. *Group I)* Hippocampal astrocyte cell isolation by Magnetic-activated Cell Sorting (MACS) technique for protein quantification and gene expression analysis. The group was divided into four-time points: 4 hours, 24 hours, 3 days, and 7 days post single bTBI exposure; *Group II)* Brain tissue collection for microscopy analysis. The group was divided into three-time points: 24 hours, 3 days, and 7 days post single bTBI exposure.

4.2.2. Animal Care and Preparation for Single Blast Wave Exposure

Adult male Sprague Dawley rats, aged 10 weeks and weighing approximately 250-300 g (Envigo, Dublin, VA, USA), were acclimated for several days before the blast experiment (12 hours light/dark cycle) with ad libitum access to food and water. Prior to a single blast wave exposure, animals were anesthetized with 3% isoflurane and carefully placed in the ABS testing chamber. In there, animals were

positioned in a prone position within a mesh sling designed to minimize flow hindrance and isolate primary blast injury with the elimination of acceleration/deceleration insult. Animals were then exposed to a single blast wave of approximately 17-20psi (Figure 4.1 b), characterizing a mild bTBI. Sham animals received the same procedures except for the blast wave exposure. Following the sham or blast procedure, animals were removed from the ABS and observed through injury and anesthesia recovery stages. Animals were assigned to two groups according to data collection: *Group I)* Hippocampal astrocyte cell isolation by Magnetic-activated Cell Sorting (MACS) technique for protein quantification and gene expression analysis. The group was divided into four-time points: four hours, 24 hours, three days, and seven days post single bTBI exposure; *Group II)* Brain tissue collection for microscopy analysis. The group was divided into three-time points: 24 hours, three days, and seven days post single bTBI exposure.

4.2.3 Magnetic-activated Cell Sorting Technique: Hippocampal Astrocyte Cell Isolation

Hippocampal astrocyte cells were isolated by magnetic-activated cell sorting (MACS) protocol adapted from Dr. Michelle Olsen's laboratory located at Virginia Tech (Holt et al., 2019). All material used is listed in Table 1. Following injury, rats were euthanized according to time points (e.g., 4hr, 24hr, 3d, and 7d) with exposure to carbon dioxide in an enclosed chamber and decapitation. Following decapitation, brains were immediately removed, and the hippocampus was isolated. The isolated tissue was minced in the dissection media solution (Earl's minimal essential media with 20mM glucose and 500 µL of antibiotic-antimycotic and bubbled with gaseous carbogen (95% O2: 5% CO2) for up to five minutes). Using the Worthington Papain Dissociation Kit, solutions such as papain, resuspension media, and albumin density gradient were prepared according to the manufacturing protocol. The minced hippocampus was transferred to a 50mL conical tube containing papain. The tissue-papain mixture was incubated for 20min in a 37°C water bath. At the same time, the solution was exposed to carbogen airflow, enough to agitate the solution but not enough to make the solution bubble or splash. After incubation, the

tissue-papain mixture was titrated until homogenous and centrifuged. The resulting cell pellet was immediately resuspended in the resuspension media. Next, the cell-resuspension mixture was carefully layered on the albumin density gradient solution and centrifuged.

The resulting cell pellet was suspended in a buffer solution made of 0.5% bovine serum albumin in phosphate-buffered saline and then filtered through a 70 mm BD Falcon cell strainer to remove any non-dissociated tissue. Before isolating the astrocytes from other brain resident cells, a "whole" hippocampal fraction containing all cells was first collected to be used as input control for the hippocampal astrocytes purity test. Astrocytes were purified by the MACS technique (Holt et al., 2019), which used superparamagnetic nanoparticles to tag the target cells. Then, it retains the labeled cells (target population) in a column containing ferromagnetic steel wool placed in a potent magnetic separator such as QuadroMACS. In contrast, the non-target cell population was removed once washing the magnetic column with the buffer solution. To increase the astrocytic fraction purity, microglia and oligodendrocytes precursor cells were removed first by incubation with MACS $Cd11b^{+}$ microbeads and MACS Myelin beads, respectively. The remaining cell mixture was incubated with Glt-1 antibody, a marker for astrocytes, followed by a secondary incubation with MACS anti-rabbit beads, allowing retention of astrocytes on a magnetic column positioned on the magnetic stand in the QuadroMACS. The purified hippocampal astrocytes cells were immediately stored at -80°C for later processing for protein quantification and gene expression analysis (purification test).

Table 1. List of supplies used for study.

Reagent	Vendor	Catalog Number
Carbogen (95% O2: 5% CO2)	AirGas	X02OX95C2003102 (CGA 296)
Papain dissociation system	Worthington	LK003150 (PDS)
Falcon cell strainers (70 mm)	Fisher Scientific	08-771-2
QuadroMACS	Miltenyi Biotec	130-091-051
LS columns MACS	Miltenyi Biotec	130-042-401
MACS $Cd11b^+$ microbeads	Miltenyi Biotec	130-093-634
Myelin isolation microbeads	Miltenyi Biotec	130-104-257
Anti-rabbit IgG microbeads	Miltenyi Biotec	130-048-602
Anti-EAAT (GLT-1) antibody	Alomone Labs	AGC-022
Taqman GFAP qPCR primer	Thermo Fisher Scientific	Rn00566603_m1
Taqman MBP qPCR primer	Thermo Fisher Scientific	M01399619m1
Taqman Rbfox1 qPCR primer	Thermo Fisher Scientific	Rn01464214_m1
Taqman Itgam qPCR primer	Thermo Fisher Scientific	Rn00709342_m1

4.2.3. Tissue Collection, Immunohistochemistry, and Microscopy Analysis

I. Tissue Collection:

Adult male Sprague Dawley rats were anesthetized with 5% isoflurane and perfused transcardially with saline followed by 4% paraformaldehyde (pH 7.5) at either 24 hours, three days, and seven days post sham or single blast exposure. Post perfusion, brains were extracted and stored for 24 hours at 4°C in 4% paraformaldehyde solution to ensure proper brain fixation. Following the post-fixation period, brains were dehydrated in 30% sucrose and embedded in optimal cutting temperature (OCT) embedding medium

(Sakura Finetek USA, Inc., Torrance CA) and frozen at −80°C for cryostat sectioning. Coronal sections (40 μm) were prepared in a cryostat microtome (Thermo Scientific Inc, Waltham, MA) and stored in phosphate-buffered saline (PBS) with sodium azide at 4˚C prior to staining procedures. Two random coronal sections (~Bregma -4.16mm) were chosen per animal for immunohistochemistry analysis of the intermediate filament protein called glial fibrillary acidic protein (GFAP).

II. GFAP Immunohistochemistry:

For the immunohistochemistry procedure, all tissue samples were rinsed three times for five minutes with PBS and were incubated in a blocking buffer solution containing 10% neutral goat serum (NGS) (ThermoFisher; Cat#:50062Z) and 0.5% Triton-x 100 (Millipore Sigma; T9284) for 1 h at room temperature. Tissue samples were incubated for 16–18 h at 4°C in blocking buffer with primary antibody GFAP at 1:1000 dilution (Invitrogen; Cat#: 13-0300). The following day, tissue samples were washed three times for five minutes in PBS and incubated for 1.5 h at room temperature in a blocking buffer with secondary antibody AlexaFluor 488 goat anti-mouse at 1:1000 dilution. Following the incubation, tissue samples were washed three times for five minutes with PBS and incubated for 10 minutes with DAPI in PBS (1ug/mL) to visualize nuclei, followed by one wash with PBS. Finally, tissue samples were mounted and coverslipped with Slow Fade Reagent.

III. Fluorescence Microscopy and Image Processing:

All tissue samples were imaged using a Zeiss Fluorescence microscope at a 20X objective lens to comprehensively analyze the astrocyte reactivity phenotype. Images of hippocampal sections containing all four sub-regions: Dentate gyrus (DG) and Cornu Ammonis 1, 2, and 3 (CA1, CA2, and CA3) were acquired for further GFAP analysis. All images were processed and quantified using Fiji (ImageJ) software. First, the background was subtracted using the built-in function on the software. Then, a threshold value was determined and applied equally to all images to isolate GFAP expression from any

background fluorescence. After preparing all images, ImageJ software quantified GFAP fluorescence by three specific parameters: I) *Integrated density of fluorescence* which measures the level of GFAP fluorescence positive signal using gray pixel intensity. Higher fluorescence intensity may indicate astrocyte activation following bTBI as upregulation of GFAP is a well-represented marker for astrocyte reactivity in TBI; II) *Area fraction* quantifies the percentage of GFAP positive signal within the region of interest. Increased GFAP area fraction may indicate the proliferation of astrocytes to the injured region; and III) *Mean area per cell,* which is acquired by the "analyze particles" function with the pixel area size threshold of 0.004, excluding slight pixel noise and extract objects of interest. Mean area per cell provides detail to the average cell soma size normalized to the area, giving the average area of the cell. Increased GFAP per cell area may indicate changes in astrocyte cytoskeleton by hypertrophy of its cellular body. Data were acquired from the average of the replicate images, two coronal sections per animal with four images per sub-region. The final data was determined per animal for each hippocampal sub-region and a total hippocampal expression by adding the data averages from each sub-region.

4.2.4. RNA Isolation and Gene Expression Analysis

Samples underwent Trizol treatment following phase separation using chloroform, allowing simultaneous extraction of RNA and proteins from the same biological sample. RNA was isolated and re-suspended using the PureLink RNA Mini Kit (Invitrogen; Cat#: 12183018) manufacturer's protocol. First, RNA aqueous phase was washed with an equal volume of 70% ethanol, and the lysate-ethanol mix was added to a spin cartridge and washed one time with Wash Buffer 1 and two times with Washed Buffer 2. A final centrifuge was done to dry the spin cartridge membrane. Purified RNA was re-suspended with 25 µL of DEPC-treated water (Invitrogen; Cat#: 4387937). Total purified RNA was quantified using NanoDrop, and an A260/A280 ratio between 1.8 and 2 was used for quantitative reverse transcription

polymerase chain reaction (RT-qPCR) analysis. Purified RNA was converted to cDNA using the iScript reverse transcription supermix (Bio-Rad; Cat#: 1708840). Total cDNA was quantified using NanoDrop.

RT-qPCR analysis of 32 endogenous control (housekeeper) gene expressions was conducted with cDNA samples from hippocampal astrocyte cells isolated from adult male rats by MACS technique at 24 hours and 3 days post sham or single blast exposure. Samples from both time points were processed and analyzed the same. Firstly, cDNA from four animals per experimental group was pooled together to increase the quantity of starting material. Then, 32.5ng of cDNA was combined with Applied Biosystem Taqman Fast Advanced Master Mix (ThermoFisher; Cat#: A44359) and loaded, in triplicate, into a pre-designed endogenous control plate (ThermoFisher; Cat#: 4426698). Quantitative qPCR was performed on the QuantStudio III Real-Time PCR System under the cycling parameters of 95°C for 20 seconds, 40 repeats of 95°C for 1 second, and 60°C for 20 seconds. Data has represented a comparison of fold change [log2 (Blast/Sham)] of the levels of expression of 32 reference genes between 24hrs and three days. The expression level of the 32 reference genes was calculated using the Delta Ct method, and the results are presented as relative fold changes. Mean positive log2 fold changes correspond to an increase in gene expression. In contrast, negative values correspond to a decrease in gene expression.

4.2.5. Protein Isolation and Western Blotting Analysis

Phase separation with chloroform was followed by Trizol (ThermoFisher; Cat# 15596018) treatment on the samples. After extracting RNA and DNA, proteins were recovered from the Trizol phenol phase. The first step in protein precipitation was isopropanol treatment, followed by three 20-minute washes with a 0.3 M guanidine hydrochloride in 95% ethanol solution and one wash with a 20-minute 100% ethanol solution. The protein was re-suspended in a 1:1 solution of 1% sodium dodecyl sulfate solution and 8M urea in 1M Tris-HCl (pH 8). The protein was then further homogenized by sonicating for

an additional ten seconds, followed by ten minutes of incubation at 55°C. BCA assay (Pierce; Cat#: 23225) was used to measure the total protein in the samples in preparation for Western Blotting analysis.

To analyze molecular alterations related to astrocyte reactivity, quantification of GFAP (Abcam; Cat#: ab7260) protein levels were chosen. To analyze mitochondrial mediate fission dynamics, protein levels for DRP1 (Novus; Cat#: NB110-55288) and its post-translational phosphorylation at serine 616 ($pDRP1^{s616}$; Cell Signaling; Cat#: 4494S), and serine 637 ($pDRP1^{s637}$; Cell Signaling; Cat#: 4867S) sites were chosen. Target proteins were analyzed at four hours, 24 hours, and three days post-overpressure exposure. Protein samples were produced in accordance with the manufacturer's instructions, and a capillary-based automatic Western system (Wes, Protein Simple) was used for the protein quantification of each studied marker. Wes supplies purchased from Protein Simple were separation modules (Cat#: SW-004), anti-rabbit (Cat#: DM-002), and anti-mouse (Cat#: DM-001) detection modules. Protein levels were calculated using Compass for SW software v.6.1 (Protein Simple) from area measurements obtained from electropherograms at the same exposure period for all data plates. The Wes software determines target protein levels by computing the area under the curve using uniform peak fits across all data. Therefore, the Wes bands shown in the data are digitized images meant to be a qualitative visual comparison of how the target protein traveled through the Wes capillary-based automatic system. According to the target protein, samples were loaded with the same protein concentration (mg/mL) in each well, normalized to that total protein, and then averaged to the sham value. Protein quantification results are represented as normalized protein expression in comparison to the sham average.

4.2.6. Statistical Analysis

Statistical comparisons were conducted between groups using GraphPad Prism 9 software. A two-way ANOVA was conducted to analyze overall significant differences amongst groups, followed by a Tukey's honestly significant difference (Tukey's HSD) test to analyze which specific group's average

differed. For group comparisons within a single individual, a student's t-test was used. Levene's tests were employed to evaluate the equality of variances, and the Kolmogorov-Smirnov test was used to check the assumptions for normality (homoscedasticity). A logarithmic adjustment was carried out to undertake statistical comparisons in the case that the data were not normal. A p-value of 0.05 or less was regarded as statistically significant, and residual analysis was used to identify statistical outliers. The letter "n" stands for the total number of animals per group. The means and standard errors of the means are presented for all data values (S.E.M.). The figure legend reports the test for each experiment, the n value, and the p-value.

4.3 Results

4.3.1. Magnetic-Activated Cell Sorting Technique Efficiently Isolated Pureed Hippocampal Astrocytes from Adult Male Rat Brains.

Using the “whole” hippocampus fraction as a control, RT-qPCR was used to determine the purity of the isolated astrocyte population. Taqman probes (Table 1 under *“section 4.2.3*) for GFAP (astrocytes), ITGAM (microglia), RBFOX3 (neurons), and MBP (oligodendrocytes) were used to determine enrichment or depletion of cell type-specific genes with GAPDH as a housekeeping gene. Relative gene expression was calculated using ΔΔCt fold-change expression of mRNA. Therefore, the RT-qPCR revealed purified astrocyte isolation from the hippocampus of adult rats by showing enriched expression of GFAP compared to hippocampal fraction sample with depletion expression of ITGAM, RBFOX3, and MBP genes (Figure 4.2). Results are displayed as normalized target gene expression relative to the “whole” hippocampal fraction sample average.

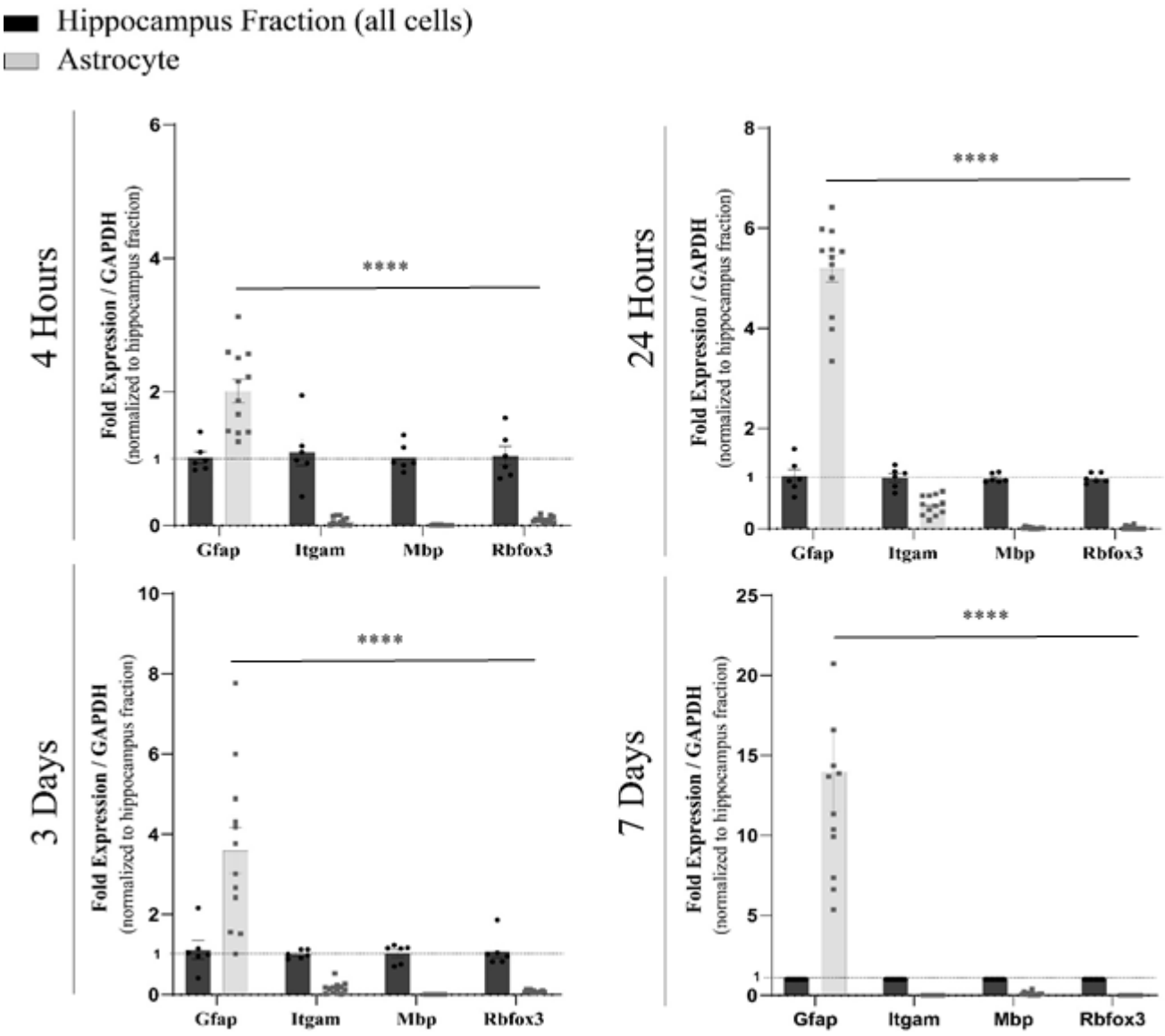

Figure 4.2: Group II: Magnetic-activated cell sorting (MACS) – Hippocampal astrocyte cell isolation. Taqman probes for GFAP (astrocytes), ITGAM (microglia), RBFOX3 (neurons) and MBP (oligodendrocytes) were used to measure gene expression of respective cell types with GAPDH used as a housekeeping gene. A hippocampus fraction with all cells present was collected to be used as an input control for purity test by showing enrichment or depletion of gene expression relative to the "whole hippocampus" fraction. Therefore, our RT-qPCR reveals a purified astrocytes isolation from hippocampus of adult rats by showing enriched expression of GFAP compared to the hippocampus fraction (all cells) with depletion expression of ITGAM, RBFOX3 and MBP genes at all-time points. (n=12/marker; data is represented as normalized by "whole hippocampus fraction"; $^{****}p \leq 0.0001$)

4.3.2 Exploring Hippocampal Astrocytic-Associated DRP1 Protein Levels Post-Single bTBI at Acute and Sub-Acute Stages of the Injury.

Protein extracted from adult rats purified hippocampal astrocytes cells at the acute time point of 4 hours and 24 hours, and at the sub-acute time point of 3 days and 7 days following bTBI were used to perform western blotting analysis to determine if bTBI alters astrocytes-associated DRP1 protein levels. Figure 4.3 depicts results that indicated no significant changes in total DRP1 protein levels between groups at all-time points. Furthermore, although not significant compared to the other time points, DRP1 protein levels at the sub-acute stages of the injury (7 days) were lower.

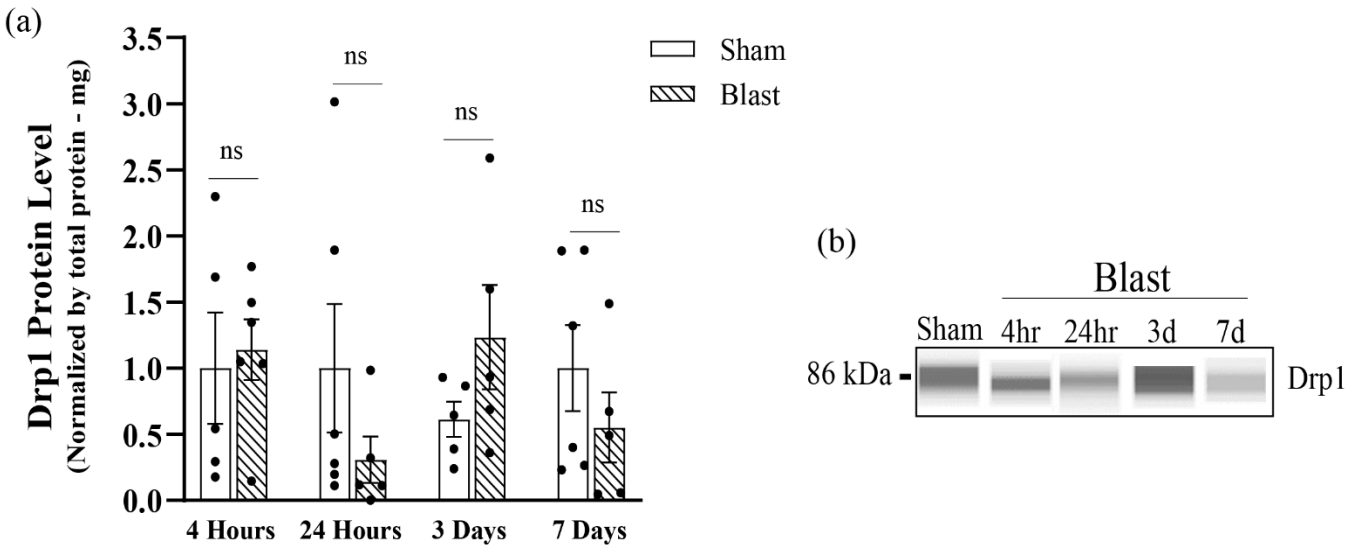

Figure 4.3: Analysis of Total Mitochondrial Fission GTP-DRP1 Protein post single overpressure exposure. Western Blotting was conducted using an automatic capillary-based system (Wes, Protein Simple) to look at relative protein quantification to identify possible fission post-overpressure exposure.
a) There were no significant changes in DRP1 protein levels at 4 hours, 24 hours, 3 days, and 7 days single blast wave exposure. **b)** Only for qualitative visual comparison, digitized bands illustrate how proteins moved through the capillary system on the Wes. (n=6/group; data are mean ± SEM; *p-value represents ≤ 0.05).

4.3.3. Single bTBI Triggers Astrocytic DRP1 translocation to the Mitochondria by Post-Translational Modification with Phosphorylation.

Activation of DRP1 protein by post-translational modification with phosphorylation at serine 616 ($pDRP1^{s616}$) is known to activate DRP1 translocation to the OMM. In contrast, phosphorylation at serine

637 (pDRP1^{s637}) suppresses DRP1 translocation. Therefore, by controlling the translocation of cytosolic DRP1 to the mitochondria, the balance of the pDRP1^{s616}/pDRP1^{s637} ratio leads to the regulation of mitochondrial fission and, consequently, mitochondrial morphology. Results indicated that pDRP1^{s616} levels were significantly increased at 4 hours ($p = 0.0125$) and 7 days ($p = 0.0409$) following bTBI (Figure 4.4 a-c), showing an increase of activated DRP1-mediated mitochondrial fission. In contrast, at 24 hours and 3 days following, levels of pDRP1^{s616} protein were not different to sham levels. Furthermore, there were a significant decrease in the pDRP1^{s616}/pDRP1^{s637} ratio levels across blast groups between the 4 hours and 3 days ($p = 0.0006$) (Figure 4.4 c). In addition, there was an increase in the pDRP1^{s616}/pDRP1^{s637} ratio levels between the 24 hours and 7 days across the blast groups ($p = 0.0596$) (Figure 4.4 c), although not statistically significant. This could indicate a post-injury temporal window within which hippocampal astrocytic mitochondrial presents a possible restoring feedback response during the sub-acute stages of the injury and, if chronic, can lead to the beginning of worst outcomes.

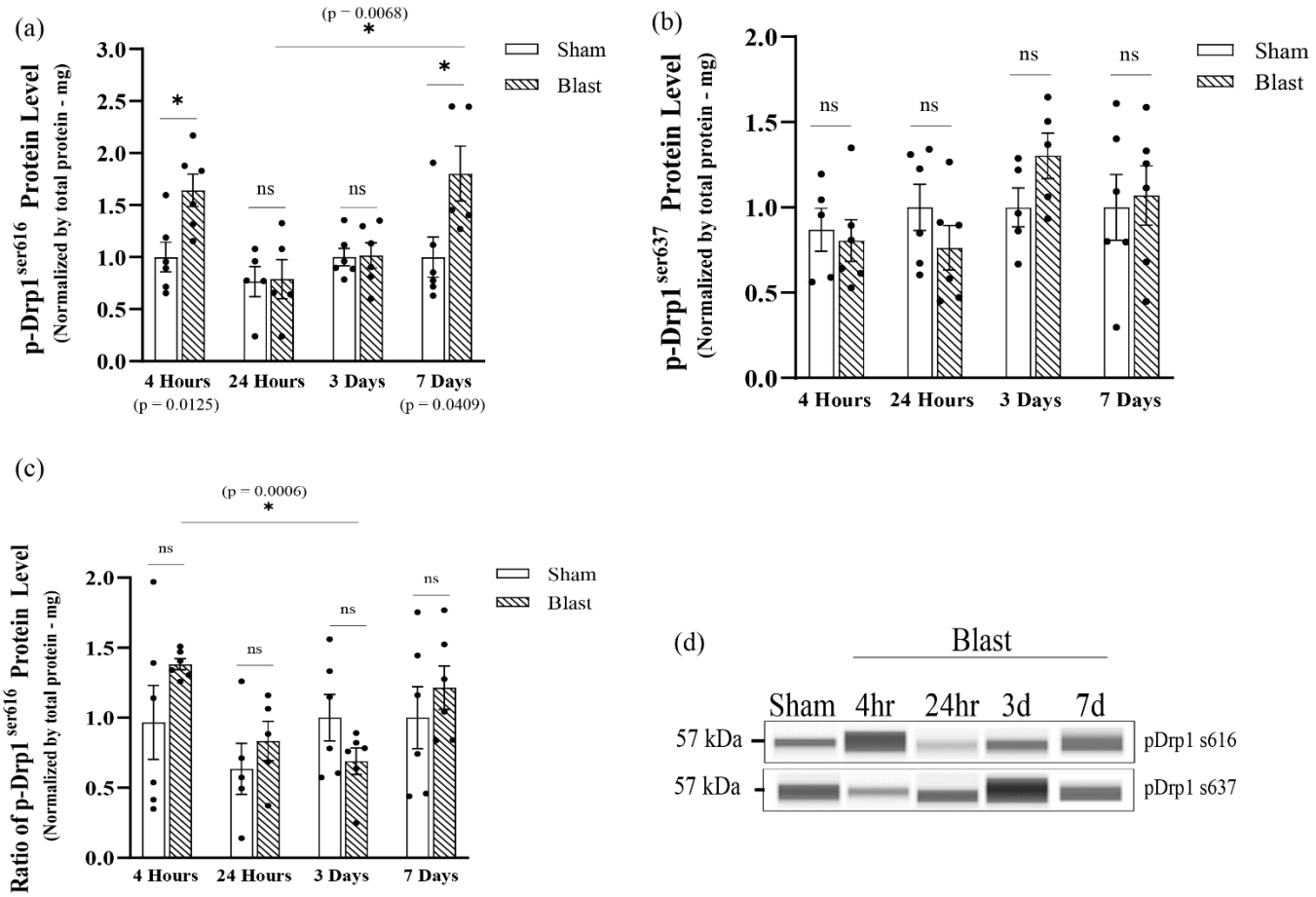

Figure 4.4: Analysis of total DRP1 post-translational modification protein by it phosphorylation at serine 616 and serine 627 post single overpressure exposure. Western Blotting was conducted using an automatic capillary-based system (Wes, Protein Simple) to look at relative protein quantification to identify possible fission post-overpressure exposure. **a)** The total levels of p-DRP1^{616} protein were acutely increased by 4 hours, returned to physiological levels at 24 hours and 3 days and shifted back to an increase at 7 days post single blast wave exposure. **b)** The total levels of p-DRP1^{637} protein were maintained at physiological levels at all-time points. **c)** There were no significant difference in the pDRP1^{s616}/pDRP1^{s637} ratio levels between sham and blast at all-time points. However, there were a difference across blast groups between 4 hours and 3 days with a significant decrease of pDRP1s616/pDRP1s637 ratio levels. **d)** Only for qualitative visual comparison, digitized bands illustrate how proteins moved through the capillary system on the Wes. (n=6/group; data are mean ± SEM; *p-value represents ≤ 0.05).

4.3.4. Single bTBI Induces Hippocampal Astrocyte Reactivity

The results herein focus on characterizing the time course of hippocampal astrocyte reactivity from adult male rats' exposure to a blast wave. To assess the reactive phenotype, protein and fluorescence levels of GFAP were analyzed by western blotting and fluorescence microscopy at 4 hours, 24 hours, 3 days, and 7 days post-single bTBI. Results presented in figure 4.5 indicated a significant increase in total GFAP

protein levels starting at 24 hours (p = 0.0469) which also corresponded with an increase in GFAP fluorescence intensity (p = 0.0082) as well as an increase in GFAP area fraction (p = 0.0064) at 24 hours post-single blast exposure (Figure 4.6). Increased area fraction may indicate the proliferation of astrocytes in the hippocampus. The response was shifted back to physiological (sham) levels at 3 days post-blast injury (Figure 4.5; 4.6). At seven days post-blast exposure, hippocampal astrocytes presented a significant increase in total GFAP protein (p = 0.0311), GFAP fluorescence intensity (p = 0.0078), GFAP area fraction (p = 0.0072) and a further increase in GFAP per cell area (p = 0.0059), presumably, this could signify changes in cytoskeleton by the astrocytes cellular body hypertrophy (Figure 4.5; 4.6). Furthermore, each hippocampal sub-region was analyzed separately for the same data parameters. The results indicated that the total hippocampus data correctly represented a diffuse injury across the hippocampus since a significant difference was observed in each sub-region at 24 hours and 3 days post-blast exposure (Figure 4.7-4.9). Together, those data indicate the starting of astrocyte reactivity phenotype following mild bTBI as upregulation of GFAP is a well-represented marker for astrocyte reactivity in TBI.

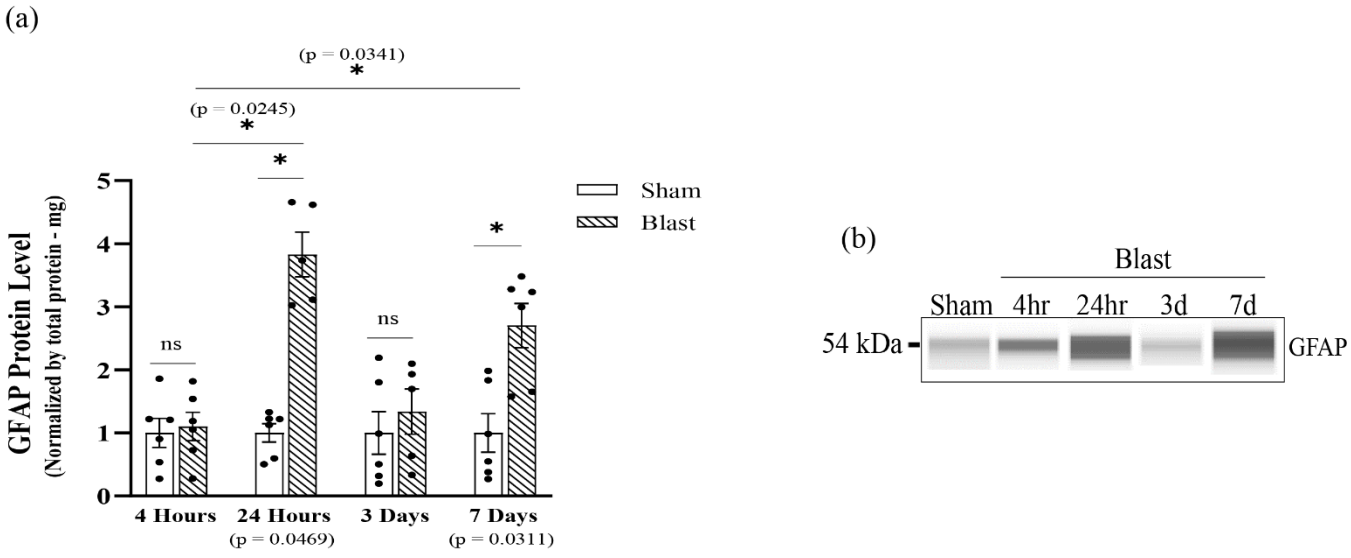

Figure 4.5: Analysis of hippocampal astrocytes total GFAP protein levels were quantified by Western Blotting using an automatic capillary-based system (Wes, Protein Simple).
a) Total GFAP protein levels were increased at 24 hours, returned to physiological levels by 3 days and raised backed up by 7 days post single blast wave exposure. **b)** Digitized bands are representation of how the proteins traveled through the capillary system on the Wes, only for qualitative visual comparison.

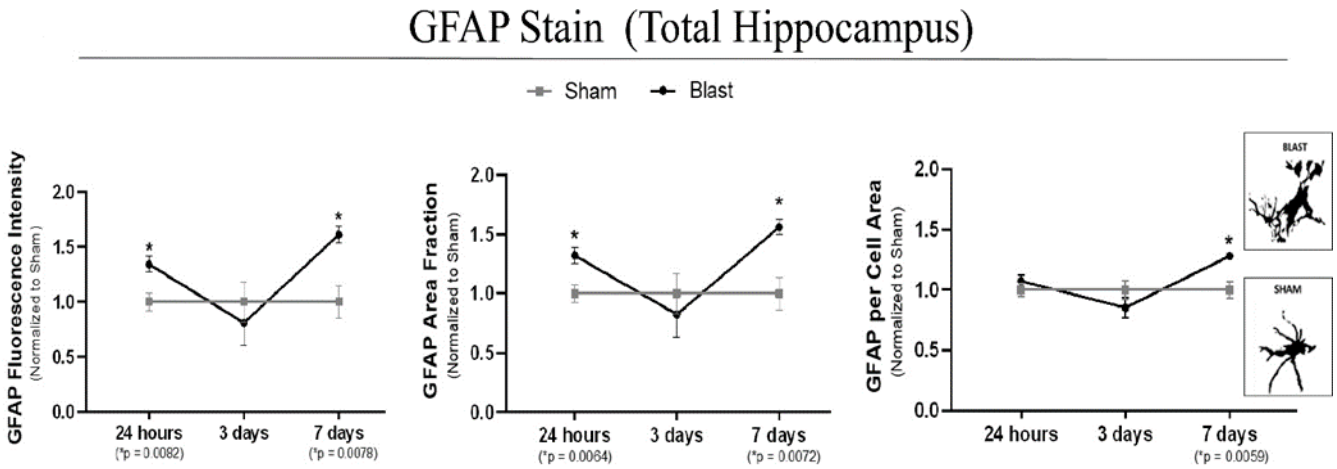

Figure 4.6: To provide a comprehensive analysis of astrocyte reactivity in the adult rodent hippocampus, fluorescence microscope was used to observe changes in GFAP. A total hippocampal expression was acquired by adding the data averages from each sub-region and three parameters were used by ImageJ Software in order to quantify astrocyte reactivity (Integrated density of fluorescence, area fraction and mean are per cell. bTBI leads to an acute and sub-acute increase of astrocyte reactivity with the latest time point presenting a hypertrophic phenotype. A view of individual astrocytes (GFAP) in both sham and single blast animals showed different sizes of cell bodies (soma). (Fluorescence Microscopy group: n=12/group; data are mean ± SEM; *p-value represents ≤ 0.05; ^{ns}p-value represents not significant).

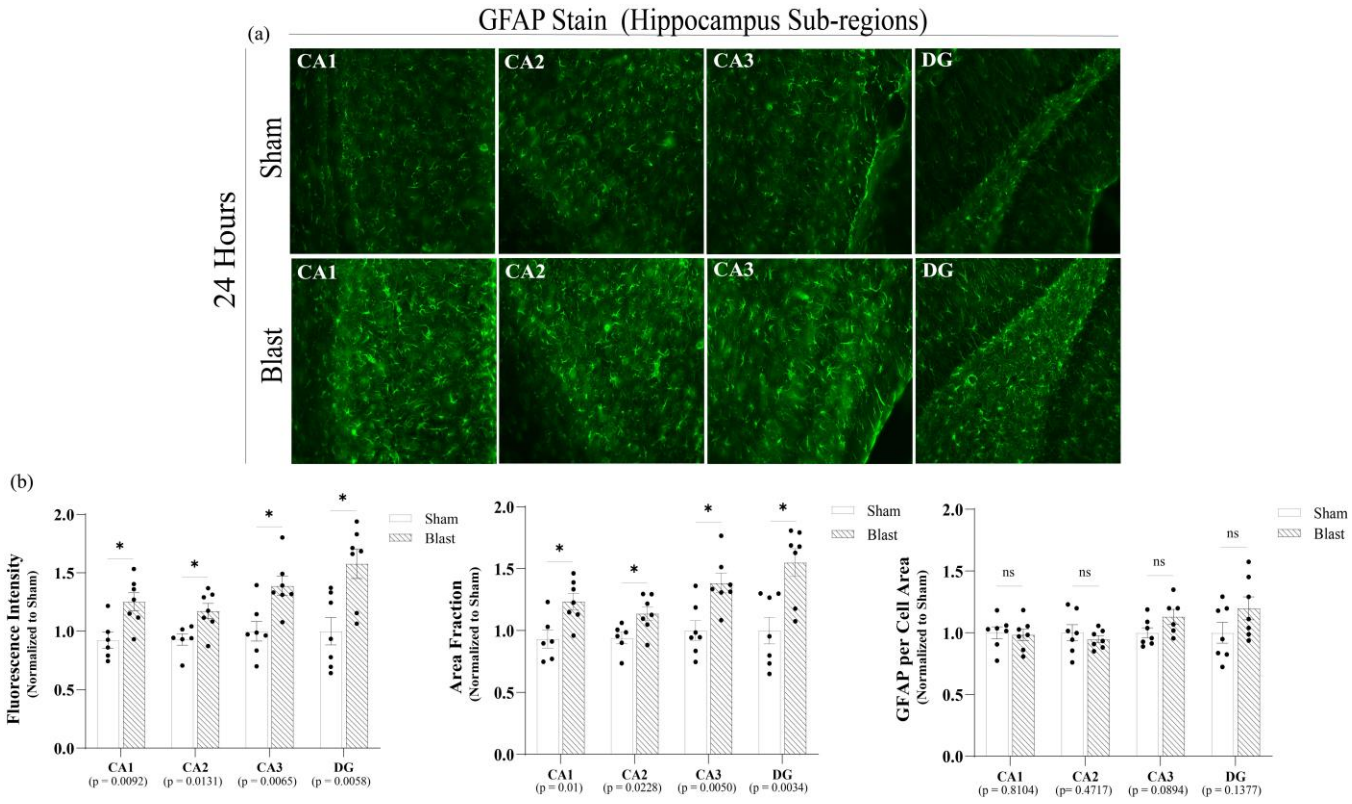

Figure 4.7: Sub-regions of the hippocampus were further analyzed for GFAP to identify if the total hippocampus data correctly represent a diffuse injury across the adult rodent hippocampus at 24 hours post mild blast wave exposure.
a) Representative images of GFAP obtained from 10 weeks old adult male rats. Image was collected from each hippocampal sub-region: Dentate gyrus (DG) and Cornu Ammonis 1, 2, and 3 (CA1, CA2, and CA3).
b) Three parameters were used by ImageJ Software in order to quantify astrocyte reactivity (Integrated density of fluorescence, area fraction and mean are per cell. At 24 hours, blast presented a higher fluorescence intensity across all hippocampal sub-regions compared to sham group, indicating an initial acute reactive phenotype. (Fluorescence Microscopy group: n=7/group; data are mean ± SEM; *p-value represents ≤ 0.05; ^{ns}p-value represents not significant; Scale bar in a = 57µm).

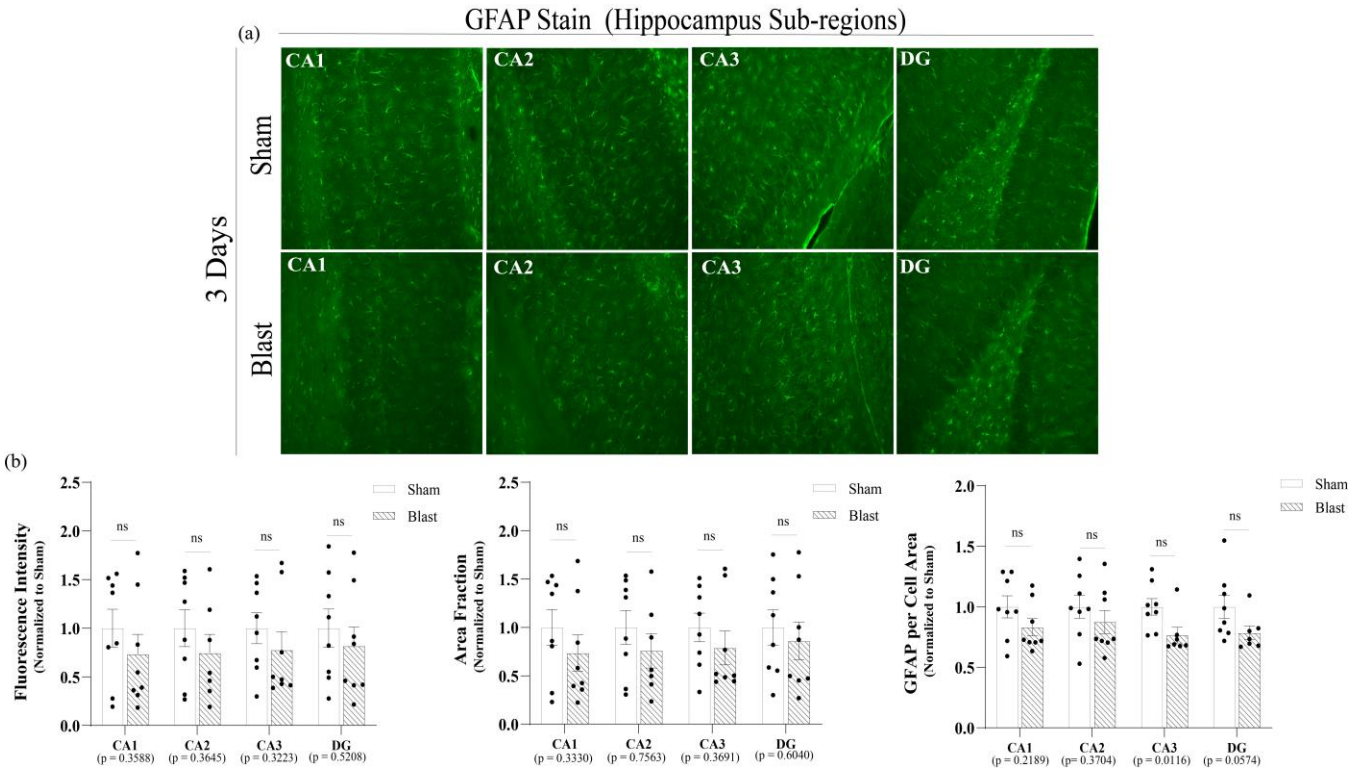

Figure 4.8: Sub-regions of the hippocampus were further analyzed for GFAP to identify if the total hippocampus data correctly represent a diffuse injury across the adult rodent hippocampus at 24 hours post mild blast wave exposure.
a) Representative images of GFAP obtained from 10 weeks old adult male rats. Image was collected from each hippocampal sub-region: Dentate gyrus (DG) and Cornu Ammonis 1, 2, and 3 (CA1, CA2, and CA3). **b)** At 3 days, blast group presented no significant changes compared to sham across all hippocampus sub-regions. (Fluorescence Microscopy group: n=8/group; data are mean ± SEM; *p-value represents ≤ 0.05; ^{ns}p-value represents not significant; Scale bar in a = 57µm).

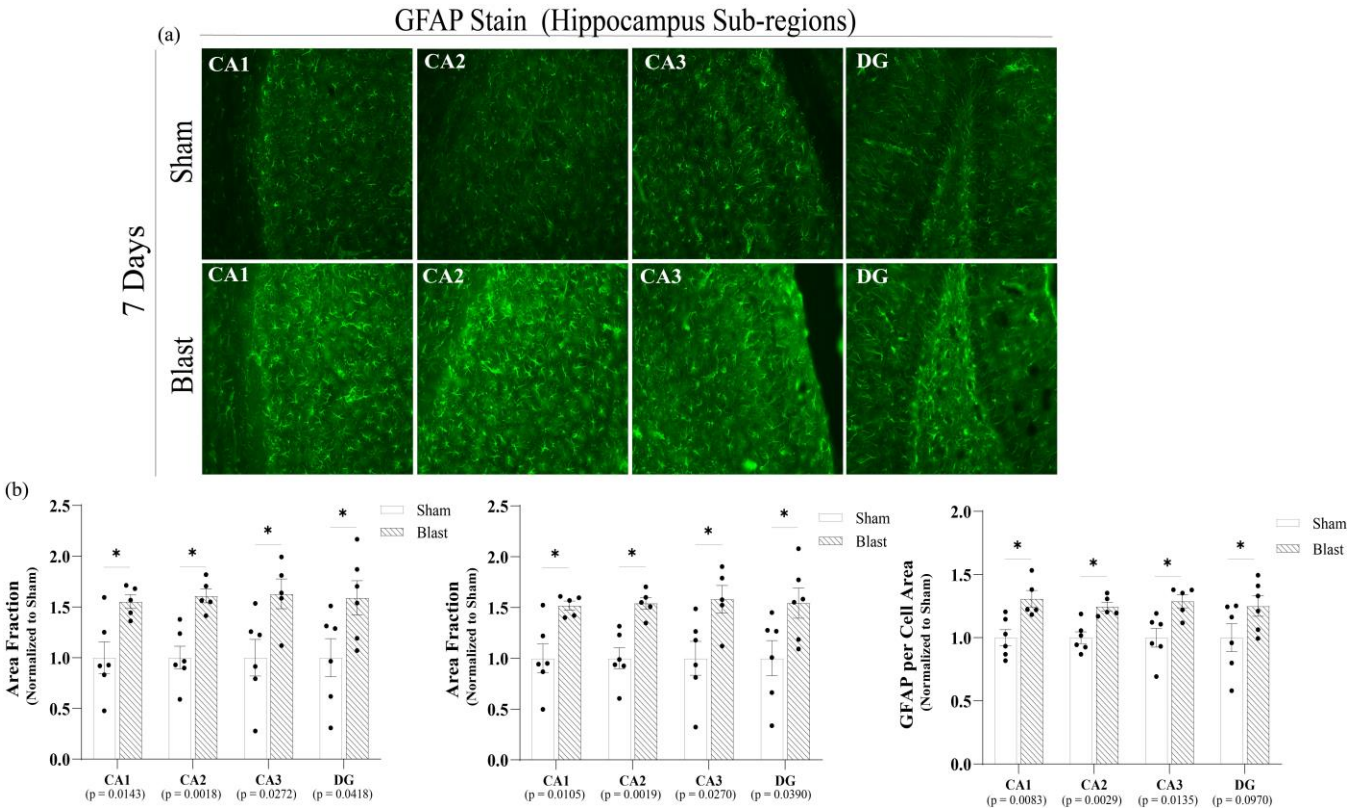

Figure 4.9: Sub-regions of the hippocampus were further analyzed for GFAP to identify if the total hippocampus data correctly represent a diffuse injury across the adult rodent hippocampus at 24 hours post mild blast wave exposure. **a)** Representative images of GFAP obtained from 10 weeks old adult male rats. Image was collected from each hippocampal sub-region: Dentate gyrus (DG) and Cornu Ammonis 1, 2, and 3 (CA1, CA2, and CA3). **b)** At 7 days, blast group presented an increase within all quantified parameters across all hippocampal sub-regions compared to sham. This Indicated a shift back to a reactive phenotype at the sub-acute stages of the injury. (Fluorescence Microscopy group: n=6/group; data are mean ± SEM; *p-value represents ≤ 0.05; ^{ns}p-value represents not significant; Scale bar in a = 57µm).

4.3.5. Optimization of Endogenous Control Gene Expression in Purified Hippocampal Astrocyte Cells post-single bTBI.

A panel of 32 housekeeping genes was tested to optimize a reference gene for usage in the gene expression experiments using a pre-designed endogenous control plate from ThermoFisher (information under *"section 4.2.4"*) (Figure 4.10). These genes are known to be good candidates for experiments looking at relative quantitation of gene expression that wish to customize a housekeeping gene. We chose to run this reference control gene optimization for our purified adult hippocampal astrocytes at 24 hours

and 3 days post bTBI as previous studies conducted in our lab showed that GAPDH may not be optimal under blast conditions. At 24 hours post-single bTBI, our data showed a significant change in gene expression in 23 control genes, with only 9 control genes presenting no changes in their expression (Elf1, Hmbs, Tbp, Elf2b1, Gusb, Tfrc, Gadd45a, PES1, and Mrpll9) (Figure 4.11). In contrast, at 3 days post-single bTBI, our data showed a significant change in gene expression in only 3 control genes (β-actin, Ubc, B2M) (Figure 4.12). and the other 29 control genes presented no changes in their gene expression. Therefore, nine housekeeper genes (Elf1, Hmbs, Tbp, Elf2b1, Gusb, Tfrc, Gadd45a, PES1, and Mrpll9) were identified as good candidates for future RT-qPCR data in bTBI studies.

Table 1

Candidate reference genes analyzed in the study

Gene Symbol	Gene Name	Main Function
18S	Eukaryotic 18S rRNA	Ribosomal Protein
Actb	Beta actin	Actin and Actin related protein
Pgk1	Phosphoglycerate Kinase 1	Carbohydrate Kinase
Ubc	Ubiquitin C	Ubiquitin protein ligase binding
Casc3	Cancer Susceptibility Candidate 3	RNA Binding
Pum1	Pumilio RNA-binding family member 1	RNA metabolism protein
Abl1	ABL proto-oncogene 1, non-receptor tyrosine kinase	Scaffold / Adaptor Protein
Pop4	Processing of precursor 4, ribonuclease P/MRP subunit	RNA Binding
GAPDH	Glyceraldehyde-3-phosphate dehydrogenase	Oxidoreductase / Dehydrogenase
B2m	Beta-2 microglobulin	Major histocompatibility complex protein
Rplp2	Ribosomal protein, large P2	Ribosomal Protein
Ywhaz	Tyrosine 3-monooxygenase/tryptophan 5-monooxygenase activation protein, zeta	Scaffold / Adaptor Protein
Cdkn1a	Cyclin-dependent kinase inhibitor 1A	Kinase Inhibitor
Psmc4	Proteasome 26S subunit, ATPase, 4	Protease
Elf1	E74-like factor 1	Winged helix / transcription factor
Rpl37a_predicted	Ribosomal protein L37a	Ribosomal Protein
Hprt1	Hypoxanthine phosphoribosyltransferase 1	Glycosyltransferase
Hmbs	Hydroxymethylbilane synthase	Deaminase
Tbp	TATA box binding protein	General Transcription Factor
Ppia	Peptidylprolyl isomerase A (cyclophilin A)	Chaperone
Cdkn1b	Cyclin-dependent kinase inhibitor 1B	Kinase Inhibitor
Eif2b1	Eukaryotic translation initiator factor 2B, subunit 1 alpha	Translation Initiation Factor
MT-ATP6	Mitochondrially encoded ATP synthase 6	ATP synthase
Rpl30	Ribosomal protein L30-like	Ribosomal Protein
Gusb	Glucuronidase, beta	Glycosidase
Arbp	Ribosomal protein, large, P0	Ribosomal Protein
Tfrc	Transferrin receptor	Metalloprotease
Ppib	Peptidylprolyl isomerase B	Chaperone
Gadd45a	Growth arrest and DNA-damage-inducible, alpha	Cell Cycle, Regulation of cell cycle
PES1_predicted	Pescadillo ribosomal biogenesis factor 1	RNA Metabolism Protein
Mrpl19	Mitochondrial ribosomal protein L19	Ribosomal Protein
Rps17	Ribosomal protein S17	Ribosomal Protein

Figure 4.10: Table with the 32 candidates endogenous reference genes and their main function.

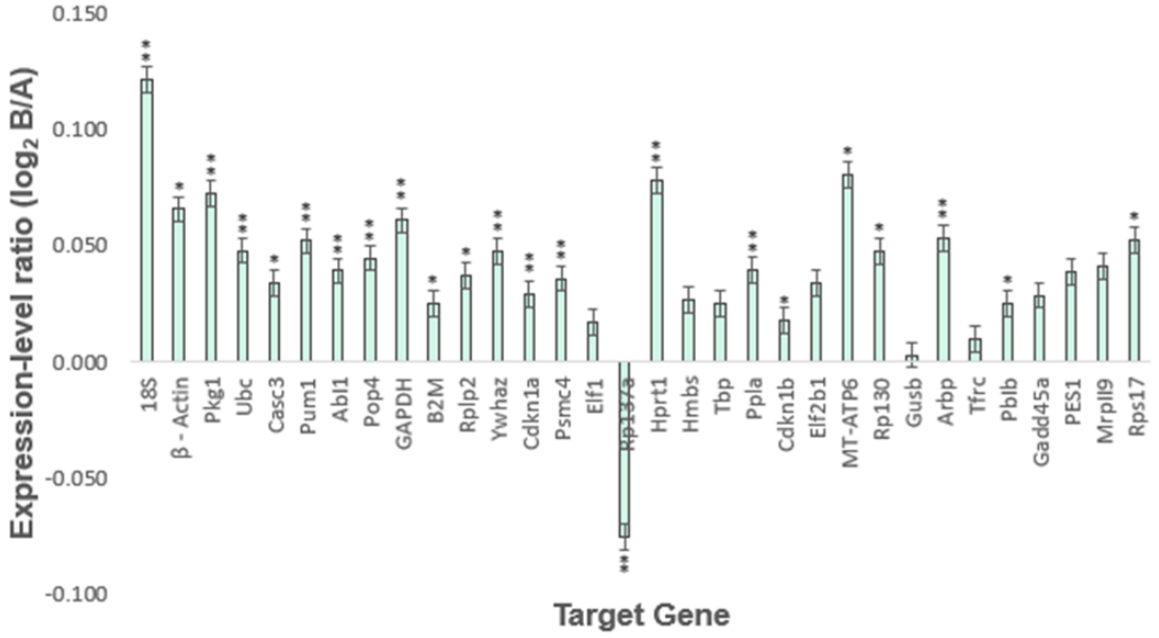

Figure 4.11: Optimization of 32 endogenous reference Gene from hippocampal adult rat astrocytes at 24 hours post mild blast wave exposure. Log2 fold change representing the difference in the levels of expression of 32 reference genes between the 24hrs. post single blast traumatic brain injury (b-TBI) (B) and Sham groups (A) in Adult Primary Rat Astrocytes (Hippocampus) using quantitative real time-PCR.

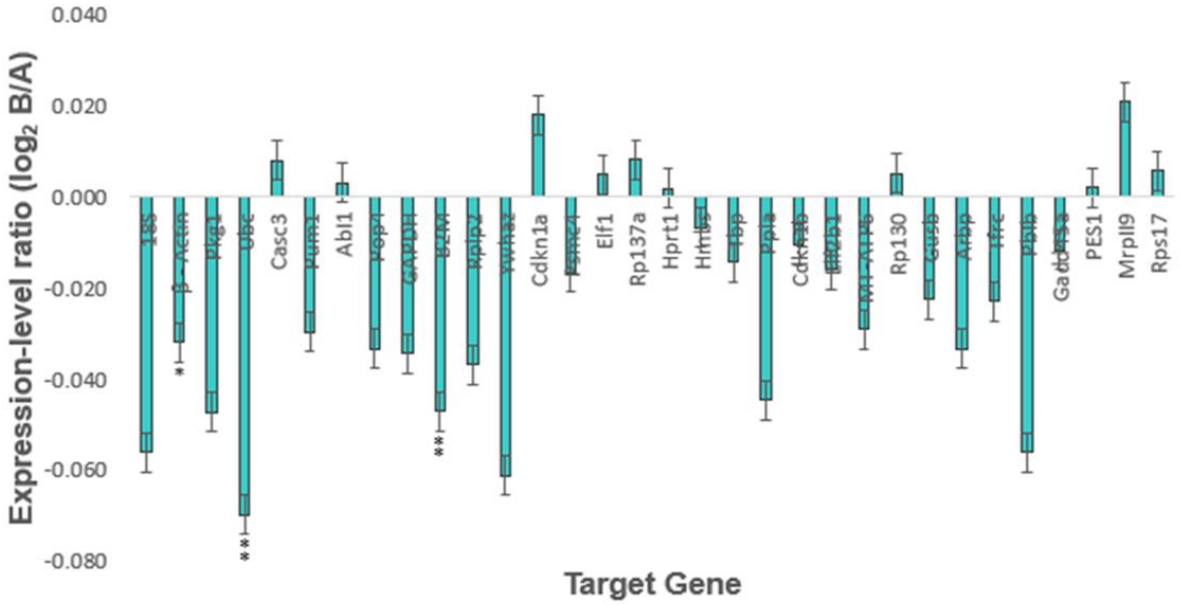

Figure 4.12: Optimization of 32 endogenous reference Gene from hippocampal adult rat astrocytes at 3 days post mild blast wave exposure. Log2 fold change representing the difference in the levels of expression of 32 reference genes between the 3 days post single blast traumatic brain injury (b-TBI) (B) and Sham groups (A) in Adult Primary Rat Astrocytes (Hippocampus) using quantitative real time-PCR.

4.4 Discussion

More people are becoming aware of the importance of better characterizing and comprehending how brain cells react to mechanical trauma, both individually and as a whole. Our *in vitro* model lacked cell-to-cell interactions that further influence astrocyte response to brain injury. Validating the *in vitro* data with our *in vivo* bTBI model is fundamental to understanding how astrocyte mitochondria are affected by primary blast injury mechanics in the native brain tissue. Magnetic bead cell separation gave us a vigorous analysis of non-autonomous astrocyte mitochondrial responses following bTBI. In this study, we were able to characterize the time course from the acute and sub-acute stages of hippocampal astrocytic-associated DRP1-mediated mitochondrial fission and a time-dependent reactive phenotype transition in astrocytes.

Specific Aim 2 presented an astrocytic pro-fission state associated with the activation of DRP1 protein, confirming the study conducted in Specific Aim 1, yet now looking at adult male rat hippocampal astrocytes instead of rat pup astrocytes. Participation of the GTPase DRP1 protein was assessed at four hours, 24 hours, three days, and seven days post-exposure to a blast wave. The results reveal that total DRP1 protein levels do not change at all time points. These findings correlate with an *in vivo* study that looked at mitochondrial dynamic dysfunction following a controlled cortical impact (CCI) injury (Fischer et al., 2016). Fischer and colleagues found that TBI does not alter total hippocampal (homogenized tissue sample) DRP1 protein levels. Instead, it increased the translocation of DRP1 to the mitochondria to initiate fission (Fischer et al., 2016). In addition, just as shown in neuronal mitochondria, dysregulation of the primary protein regulator of mitochondrial fission, DRP1, along with the upregulation in the phosphorylation of DRP1 at the serine 616 site (p-DRP1^{s616}), the activated form of DRP1, are being reported to play a key role in astrocytic mitochondrial dysfunction, favoring fission over fusion post-TBI (Motori et al., 2013; Rahman & Suk, 2020; Shih & Robinson, 2018; Stephen et al., 2014).

Corresponding with those findings, the current study presented that bTBI triggered hippocampal astrocytic DRP1 translocation from the cytoplasm to the mitochondria by post-translational modification with an increase of phosphorylation at the serine 616 site (pDRP1^{s616}). Our results indicated that 4 hours following blast wave exposure, a significant increase in pDRP1^{s616} protein levels occurred. The total level of pDRP1^{s616} protein was restored to sham levels at 24 hours and three days, whereas at seven days, levels of pDRP1^{s616} protein were shifted back to a significant increase compared to the sham group. These results indicated a higher activity of DRP1-mediated mitochondrial fission by its translocation from the cytoplasm to the mitochondrial organelle. In addition, levels of pDRP1^{s637} protein were visibly higher at three days post blast wave exposure compared to all the other time points. This data was further correlated with a significant decrease in the pDRP1s616/pDRP1s637 ratio levels between four hours and three days across the blast groups and presented a non-statistically significant increase in the pDRP1s616/pDRP1s637 ratio levels across blast groups at 24 hours and seven days. Activation of Drp1 is regulated by posttranslational modification, among which phosphorylation of Drp1 can either activate (pDRP1^{s616}) or inhibit (pDRP1^{s637}) its enzymatic activity. Phosphorylation at these two sites exerts opposite effects on mitochondrial morphology. Therefore, by controlling the translocation of cytosolic DRP1 to the mitochondria, the balance of the pDRP1^{s616}/pDRP1^{s637} ratio leads to the regulation of mitochondrial fission and, consequently, mitochondrial morphology.

Astrocytes play an essential role in the healthy brain and proper maintenance of the CNS. However, there is increasing debate over the different functions associated with reactive astrocytes and their response to injury, where they may play a dual role in TBI by contributing to the repair of damaged tissue and the return to homeostasis or leading to deleterious effects by causing scar tissue formation and therefore inhibit neuronal axon growth (Michinaga & Koyama, 2021; Zhou et al., 2020). The degree of astrocyte reactivity can be triggered by different potential insult events, such as the mechanical severity

of TBI and a wide variety of context-dependent intercellular and intracellular signaling molecules associated with early and late stages of TBI (Anderson et al., 2014; Burda et al., 2016; Khakh & Sofroniew, 2015; Matias et al., 2019; Sofroniew, 2020). This study helped characterize the time course of hippocampal astrocyte reactivity from adult male rats' exposure to a mild blast wave. Reactive astrocytes are mainly characterized by morphological changes in molecular signatures such as cellular hypertrophy (body and process), proliferation, and alteration in the intermediate filament protein GFAP. However, those features are not an all-or-none response. Instead, they are finely regulated along a gradient of intensity that can vary from very small to very intense phenotypic changes (Sofroniew, 2015b).

The results showed no changes in total hippocampal astrocytic GFAP protein as early as four hours. At 24 hours post-insult, total GFAP protein levels were higher. Fluorescence microscopy provided the same outcome with increased GFAP fluorescence intensity combined with increased possible astrocytic proliferation in the hippocampal injured area. No cellular body hypertrophy was identified then. GFAP is an important intermediate filament protein responsible for astrocyte cytoskeleton structure. It is believed to play a crucial role in controlling astrocyte motility and form by giving astrocytic processes structural stability (Eng et al., 2000). Furthermore, it is believed that the acute stages of astrocyte proliferation, phenotypes of mild astrocyte reactivity, could present reparative characteristics (Anderson et al., 2014; Sofroniew, 2020; Zhou et al., 2020). Correlated with the astrocytic mitochondrial dynamics data, at three days post-insult, total hippocampal astrocytic GFAP protein was almost returned to physiological (sham) levels, and the same was observed in the microscopy data. Moreover, at seven days post-blast wave exposure, GFAP was shifted back to a higher increase of total protein levels combined with an increase in astrocytic proliferation and changes in the cytoskeleton by presenting astrocytic cellular body hypertrophy. As mentioned, astrocyte reactivity may play a dual role in protective and deleterious actions in TBI. Together, these data indicate the starting of an astrocyte reactivity phenotype

following mild single bTBI as upregulation of GFAP, which is a well-represented marker for astrocyte reactivity in TBI and bTBI (Ekmark-Lewén et al., 2010; Michinaga & Koyama, 2021; Sajja et al., 2016; Schwerin et al., 2021), and it could be the start of an astrocytic protective response acutely after mild bTBI. However, if persisting, it can lead to a phenotypic transition into a severe reactive state, whereas it can distinctly extend into a highly proliferative, scar-forming phenotype due to chronic-state injury (Buffo et al., 2008; Pekny & Nilsson, 2005; Pekny & Pekna, 2014; Silver & Miller, 2004; Sofroniew, 2009; Wanner et al., 2013).

An additional study that was conducted within the Specific Aim 2 was focused on optimization of housekeeping genes for blast experiments. It is necessary to select proper endogenous controls when studying gene expression alterations following bTBI. Endogenous control, commonly known as housekeeping genes, are cellular maintenance genes that regulate basic and ubiquitous cellular functions. These genes are used as an internal control for RT-qPCR reactions to normalize variations in sample input. Unfortunately, changes in gene expression for GAPDH and β-actin have been observed in cells post TBI. Therefore, 32 housekeeping genes known to be good candidates for experiments looking at relative quantitation of gene expression were chosen to run a reference control gene optimization for our purified hippocampal astrocyte cells at 24 hours and three days post single bTBI. The results observed at 24 hours post-single blast wave exposure, a significant upregulation of gene expression in 23 control genes, including GAPDH and β-actin, whereas, at three days post-single blast wave exposure, there was a significant downregulation of gene expression in only three control genes including β-actin. Although many control genes changed at their specific time point between sham and blast groups, including GAPDH and β-actin, nine housekeeper genes (Elf1, Hmbs, Tbp, Elf2b1, Gusb, Tfrc, Gadd45a, PES1, and Mrpll9) were identified as good candidates for future RT-qPCR data in bTBI studies.

In conclusion, Specific Aim 2 characterized the time-dependent course response of astrocytic mitochondrial dynamics and the astrocyte reactive phenotype post mild bTBI with data acquired from the same biological samples. Recent studies highlight the importance of proper astrocytic mitochondrial dynamics in a healthy brain and how altered mitochondrial dynamics could lead to both protective and detrimental astrocyte reactivity phenotypes in CNS degenerative diseases and TBI pathologies (Bantle et al., 2021; Ishii et al., 2017; Rahman & Suk, 2020; Rose et al., 2017; Sarkar et al., 2018; Zehnder et al., 2021). The same insult that triggered an initial reactive phenotype in astrocytes also altered astrocytic mitochondrial dynamics. It is noteworthy that those alterations were first seen in the mitochondria as early as four hours post-single blast wave exposure.

Chapter 5. Conclusion

The text within Chapter 5 are adapted from Dickerson, M.*****, **Guilhaume-Corrêa, F. ***, Strickler, J., & VandeVord, P. J. (2022). ***First co-authorship**. Age-relevant in vitro models may lead to improved translational research for traumatic brain injury. *Current Opinion in Biomedical Engineering*, 100391.

5.1 Summary

I. Specific Aim 1

The study used an *in vitro* bTBI model to characterize astrocyte mitochondrial response to a mechanical insult. The results revealed four key findings in primary cultured cortical astrocytes: 1) Total DRP1 protein levels were not altered post-overpressure mechanical insult. Rather, post-translational modifications such as the phosphorylation at the serine 616 (pDRP1^{s616}) site increased which could indicate DRP1 translocation to the OMM; 2) Mechanical insult induced differential remodeling of the astrocytic mitochondrial network, leading to fragmentation by presenting a higher number of fragmented mitochondria and a lower number of mitochondrial networks; 3) At the sub-acute stages of the injury, astrocytic mitochondrial network integrity returned to physiological (sham) conditions and corresponded with an equal pDRP1^{s616}/ pDRP1^{s637} ratio; and 4) Total GFAP protein levels were not altered at four hours, 24 hours and three days post mechanical insult.

II. Specific Aim 2

The study was conducted using an *in vivo* bTBI model to characterize astrocyte mitochondrial dynamics in response to the primary blast injury mechanics in the brain. The results revealed four key findings in hippocampal astrocytes isolated from adult male rats: 1) Magnetic-activated cell bead separation gave a vigorous analysis of non-autonomous hippocampal astrocytic mitochondrial responses following bTBI. 2) bTBI had no effect on total DRP1 levels during the injury's acute, subacute, and early chronic stages. 3) Activated DRP1 translocated from the cytoplasm to the OMM by the increase of pDRP1^{s616} at four hours and seven days post-blast wave exposure; 4) Post-bTBI, astrocytes presented an upregulation of GFAP protein at 24 hours, by three days there were a shift back to physiological levels which were upregulated again by seven days.

5.2. Discussion

Structurally, astrocytes contain multiple radial processes that form various interfaces with other glia, neurons, and capillary endothelial cells. Their fine processes are close to neuronal cell bodies and synapses, and their endfeet envelop blood vessels (Abbott et al., 2006; Allen & Eroglu, 2017). They also communicate with other astrocytes intercellular via gap junctions, forming a vast interconnected network throughout the brain (Allen & Eroglu, 2017; Li et al., 2019; B. Ma et al., 2016). Astrocytic unique morphology characteristics and architecture arrangement in the brain make them a crucial player in neuronal protection and neuronal degeneration post brain injury. Astrocytes respond to a brain injury by a process called astrocyte reactivity; however, studies are identifying a heterogeneity response within the astrocyte reactive phenotype which is governed by the severity of the injury and intracellular and intercellular molecular signaling (Anderson et al., 2014; Matias et al., 2019; Sofroniew, 2020).

bTBI is a combination of the interplay between the primary mechanical insult and the subsequent secondary biochemical cascade insults. Therefore, initially starting as a mechanical injury, it is critical to comprehend the mechanical insult characteristics and forces that affect the brain, specifically how they affect astrocytes. Astrocytes are mechanically sensitive cells and do respond to mechanical overpressure insult (Hlavac et al., 2015; Ravin et al., 2012, 2016; Sawyer et al., 2017; VandeVord et al., 2008; Zander et al., 2016). Astrocytes have been reported to respond to mechanical insult by mechanosensitive calcium signaling (Blomstrand et al., 1999; Charles et al., 1991; Ostrow & Sachs, 2005; Ravin et al., 2016; Venance et al., 1997). For instance, as demonstrated by an *in vitro* study, a single adult rat astrocyte mechanically stimulated by a stretch-induced insult triggered the propagation of calcium signaling across the astrocyte-astrocyte interconnected network (Ostrow et al., 2000). Astrocytes can further respond to mechanical insults by mechanosensitive cytoskeletal remodeling. An *in vitro* wound healing assay was conducted to understand primary astrocyte migration towards the site of injury (De Pascalis et al., 2018),

a phenotype of astrocyte reactivity. The study observed that upregulation of intermediate filaments such as GFAP, vimentin, and nestin collectively contributed to reactive astrocytes migration. The intermediate filaments helped control the force across the astrocytes-astrocytes network by preventing the generation of traction forces from the "front line" cells from spreading across the neighboring cells and allowing a collective migration of reactive astrocytes towards the injury site (De Pascalis et al., 2018). A fission event has been reported to trigger mitochondrial fragmentation, increasing the mitochondria locomotion towards active zones in migrating cells (Madan et al., 2022). Given that primary astrocytes exhibit oscillating calcium signaling within their astrocytic network, mitochondria's strategic location within the cell is crucial to match the local calcium activity since they help with calcium buffering (Stephen et al., 2014). Acute (4 hours) astrocyte mitochondrial network remodeling was observed in our *in vitro* mild bTBI model by presenting an increase in fragmented mitochondria, and it was followed by an increase in PCNA (proliferation marker) which was later accompanied by the upregulation of GFAP (Hlavac & VandeVord, 2019). Presumably, this phenomenon is occurring to facilitate the organelle locomotion within the astrocyte and across the astrocyte network to allow cytoskeleton plasticity in response to the mechanical insult.

Mitochondrial fission events can also enable damaged mitochondrial dissociation from the network and subsequent degradation of the damaged portion of the mitochondria by mitophagy (mitochondrial quality control) (Chan, 2012; Lemasters, 2005; Pickles et al., 2018; Youle & van der Bliek, 2012). An *in vitro* study reported that astrocytes responded to inflammatory stimuli, a common secondary insult post bTBI, with a prompt autophagic response as a mitochondrial quality control mechanism (Motori et al., 2013). The study went further to knock out astrocytic Atg7, a gene encoding essential autophagic machinery, and found this led to a failure in regenerating mitochondrial integrity and ultimately affecting astrocyte survival. Fission events can increase ROS and consequently trigger an

oxidative stress environment (Balaban et al., 2005; Flippo & Strack, 2017; Glancy et al., 2020; Jezek et al., 2018; Sprenger & Langer, 2019). Published data from our laboratory observed, at 24 hours following insult, an astrocytic pro-oxidative environment was triggered (Hlavac et al., 2020). Even though mitophagy outcomes were not an outcome of the current study, the *in vitro* data showed that 3 days after the mechanical insult, the astrocytic mitochondrial network had been restored, and fewer fragmented mitochondria were present. This finding supports a potential acute autologous astrocytic repair mechanism that would involve removing damaged mitochondria and restoring a healthy mitochondrial network after mechanical overpressure to preserve mitochondrial integrity and prevent the accumulation of additional potentially harmful compounds.

A preclinical study demonstrated in neuronal mitochondria that early mitophagy events are crucial for ongoing neuroprotection after TBI. In this study, mitophagy inhibition led to worse results, confirming the idea that mitochondrial fission served as an early form of cellular protection by clearing damaged mitochondria before the start of apoptotic pathways (Chao et al., 2019). Furthermore, another study looking at neuronal mitochondria response post-TBI demonstrated that giving a mitochondrial drug such as pioglitazone that binds to a specific mitochondrial membrane protein, mitoNEET, at 3 hours post-injury did not help ameliorate neuronal protection. On the other hand, delaying the treatment until 18 hours post-injury did ameliorate ongoing neuronal protection (Hubbard et al., 2021). These researchers hypothesize that the mitochondrial dynamics acutely after TBI are necessary to promote neuronal protection by promoting functional mitochondria in critical phases of secondary TBI insult (Hubbard et al., 2021). Those concepts could be translated to astrocytic mitochondrial dynamics and its role in acute brain injury. For instance, astrocytic activity is linked to neuronal synaptic activity. Enhancing neuronal synaptic activity induced mitochondrial remodeling and migration to astrocyte's fine processes near the neuronal synapses (Agarwal et al., 2017; Bélanger et al., 2011; Lovatt et al., 2007; Stephen et al., 2015). Our *in vivo* model

presented an acute (4 hours) increase of the GTP-DRP1 protein activation by an increase in phosphorylation at the serine 616 sites indicating a pro-fission mediated mechanism. Moreover, this response was followed by upregulation of GFAP combined with an early astrocyte proliferation 24 hours post mild bTBI, presenting a possible "reparative" acute reactive phenotype. An *in vivo* CCI-TBI model assessed the influence of ablating astrocyte reactivity on the volume of cortical tissue underneath the CCI impact site. Ablation of reactive astrocytes was found to aggravate tissue loss following moderate CCI as early as seven days after injury, reaching its highest levels by 28 days after injury. In contrast, severe CCI showed no discernible changes (Myer et al., 2006)**.** Presumably, following mild bTBI, acute mitochondrial fission would allow for easier migration of the mitochondria within the astrocyte, helping with astrocyte cytoskeleton plasticity and calcium buffering requirements to the demands of neuronal signaling. This could help astrocytes to positively respond to the injury since an increase in intracellular calcium can lead to the release of neuroactive substances that can modulate synaptic transmission and plasticity (De Pascalis et al., 2018; Stephen et al., 2014)**.**

As a result, in the case of a mild bTBI, acute mitochondrial fragmentation may present an early beneficial effect on the astrocytes' response to the injury. However, if chronic, mitochondrial fragmentation can have negative consequences such as increased mitochondrial ROS, which activates the NF-kB pathway and results in the release of astrocytic pro-inflammatory mediators (Joshi et al., 2019; Motori et al., 2013). The current *in vivo* data showed a restoration of mitochondrial dynamics three days after mild bTBI. Still, this response was shifted back to a pro-fission mediated mitochondrial fragmentation seven days later due to increased GTP-DRP1 protein activation. Although no quantitative ROS data were analyzed in the current study, there was a non-statistically significant increase in pDRP1s616/pDRP1s637 ratio across the blast groups from three to seven days. An imbalance in favor of a larger $pDRP1^{s616}/pDRP1^{s637}$ ratio has been connected to a disruption in the redox status of astrocytic

mitochondria, which in turn causes a high generation of ROS (Dai et al., 2020; Motori et al., 2013) and ROS is an outcome seen in preclinical bTBI (Cho, Sajja, Vandevord, et al., 2013)**.** Furthermore, these responses were accompanied by astrocyte upregulation of GFAP proteins, proliferation, and cytoskeleton hypertrophy, indicating the start of reactive worsening phenotypes and, as a result, negative bTBI outcomes. Moreover, recent research emphasized the significance of astrocytic balanced fission and fusion events (mitochondrial dynamics) in a healthy brain and the potential repercussions of altered mitochondrial dynamics from both protective and maladaptive astrocyte reactivity patterns in TBI detrimental outcomes (Bantle et al., 2021; Ishii et al., 2017; Rahman & Suk, 2020; Rose et al., 2017; Sarkar et al., 2018; Zehnder et al., 2021). For instance, during cell mitosis, Cyclin-Dependent Kinase 1 (CDK1/cyclin B) or Cyclin Dependent Kinase 5 (CDK5) phosphorylate DRP1 at the serine 616 ($pDRP1^{s616}$) site (Taguchi et al., 2007). CDK5 also plays a role in astrocyte reactivity whereas inhibiting CDK5 activity on injured cultured astrocytes caused a delay in the rearrangement of tubulin, GFAP, and the extension of astrocytic hypertrophic processes (He et al., 2007). In a similar manner, inhibition of CDK5 activity after pilocarpine-induced status epilepticus reduces astrocytic apoptosis and astrocyte reactivity in the dentate gyrus, a hippocampal sub-region; moreover, it attenuated excessive mitochondrial fission by decreasing the levels of $pDRP1^{s616}$ by maintaining the $pDRP1^{s616}$/ $pDRP1^{s637}$ ratio balance (Hyun et al., 2017). In contrast, under physiological conditions, inhibition of CDK5 activity did not affect astrocytic mitochondrial morphology. This work suggests CDK5 may contribute in astrocyte reactivity accompanied by modulations of DRP1-mediated mitochondrial fission (Hyun et al., 2017).

In conclusion, acute astrocytic mitochondrial fission events could present beneficial outcomes in mild bTBI; if chronic, it may be harmful to the astrocytes. Exacerbation of fragmented mitochondrial may intensify astrocyte reactivity, and since astrocytes present an interconnected network with other astrocytes, this could have far-reaching effects in worsening the reactive phenotype. Furthermore, we were able to

characterize the participation of the DRP1 protein in astrocyte mediated-mitochondrial fission, and we were able to demonstrate the same response pattern between our *in vitro* and *in vivo* models. Those results indicated that our *in vitro* bTBI model mimics the pressure and shear stress in the *in vivo* bTBI models. Finally, the current study may point to a possible therapeutically window post-mild bTBI, leading to innovative therapeutic targets to help prevent secondary injury cascades involving mitochondria dynamics dysfunction.

5.3. Limitations

Each specific aim does present potential limitations. These limitations may impact the study's findings and should be considered in the design of future research.

I. Specific Aim 1

1. An *in vitro* model of 2D cortical astrocytes was used for this study.

Since monolayer two-dimensional (2D) *in vitro* platforms involve artificial cell development, their fundamental drawback is that they cannot accurately represent the intrinsic complexity of organ systems. Therefore, the astrocyte morphology may be different compared to the *in vivo* response. Three-dimensional (3D) platforms of primary astrocytes have been reported to preserve the astrocytic heterogeneity morphology, closely mimicking the *in vivo* heterogeneity astrocyte population, despite the fact that a 3-D cell platform still provides artificial elements for cell development (Balasubramanian et al., 2016). Moreover, an astrocyte 2D monolayer bTBI model presented lower cell viability compared to 3D platforms at 24 and 48 hours post mechanical insult (Hlavac et al., 2015)**,** which could be happening because the surrounding environment may affect the cell response to the injury insult. For instance, cells could be experiencing a different shearing force since a 2D platform has cells growing directly in contact with the plastic culture dish, while the 3D platform has the cells cultured in a matrix-embedded

environment. While surrounding may vary, both models have presented similar results with cell viability higher than 94%, indicating that astrocytes survive with minimal cell detachment occurring during the mechanical insult (Hlavac et al., 2015). Furthermore, GFAP expression has been reported to vary between 2D and 3D platforms, with the 2D presenting upregulation by 48 hours which returned to sham levels by 72 hours and 3D showing the opposite responses, seeming to indicate the 3D environment may lead to a delayed response. Although there was a different time-dependent expression of GFAP regulation, the GFAP levels were not significantly different across blast groups from both models at 72 hours (Hlavac et al., 2015). Finally, both *in vitro* platforms presented no changes in their cytoskeleton components (actin and vinculin) at all-time points compared to sham (Hlavac et al., 2015). In conclusion, both models demonstrated high astrocyte viability (survival), cytoskeleton integrity, and similar levels of astrocyte reactivity at the acute stages of the injury. Future work could compare the 3D platform using astrocyte mitochondrial dynamics outcomes to determine if the environment will delay the responses seen in the 2D cultures.

2. Primary astrocytes were obtained from two days postnatal (P2) rat pups.

Depending on the research topic being addressed, there are some limitations when using *in vitro* model of astrocytes isolated from neonatal rodent brains (M. Dickerson et al., 2022). Those limitations should be considered, particularly when used in conjunction with *in vivo* studies addressing detrimental TBI outcomes in the adult brain. It is important to consider the differences between immature and mature astrocytes in the healthy and injured brain. Since astrocytes facilitate the formation of synapses and circuits, their distinctive phenotypic traits (morphology and protein expression patterns) are crucial for neuronal network development (Allen & Eroglu, 2017; Felix et al., 2021; Li et al., 2019). For instance, mature astrocytes exhibit a complex architecture with their peripheral astrocytic processes contacting numerous neuronal synapses and blood vessels, whereas immature astrocytes are distinguished by having

fewer processes (Akdemir et al., 2020). As a result, mature astrocytes are better able to form scar borders after TBI than immature astrocytes. In addition, while immature astrocytes exhibit lower levels of plasma transmembrane protein connexin (Cx), mature astrocytes form a highly interconnected network via Cx, creating gap junctions or hemichannels. Low levels of Cx may be linked to a relatively weak syncytial network and reduced intercellular exchange of ions, metabolites, and neurotransmitters because Cx is essential in forming discrete cell-to-cell coupling (Felix et al., 2021; Zhong et al., 2016). Furthermore, Kir4.1, another plasma membrane found in higher quantity in mature compared to immature astrocytes, plays an important role in astrocyte biophysical properties by maintaining resting membrane potential and extracellular potassium (K^+) homeostasis (Felix et al., 2021; Zhong et al., 2016). Since it has been reported that the Kir4.1 protein is lost following injury (Boni et al., 2020), this protein's level of expression and function plays an important role in astrocyte response following TBI. Furthermore mature astrocytes have higher levels of glutamate transporter 1, a glutamate uptake transporter within the plasma membrane that is important in protecting the brain from extracellular excitotoxicity damage (Felix et al., 2021; Hernandez et al., 2018), which is one of the hallmarks of TBI outcomes. Compared to our *in vivo* model, the current *in vitro* study demonstrated a similar time-dependent pattern response in the astrocytic mitochondrial dynamics. Even though, using immature astrocytes to study adult TBI responses may lead to a biased interpretation of bTBI outcomes. When using age-relevant *in vitro* models, adult mature astrocyte cultures should be considered (Souza et al., 2013), as they may help unravel astrocytes' role in an aged brain following TBI.

II. Specific Aim 2

1. Adult male rats were exposed to a single mild blast-induced TBI.

The three categories of TBI severity are mild, moderate, and severe (Jain & Iverson, 2022). Military personnel are most likely to suffer from mild bTBI (*DOD TBI Worldwide Numbers | Health.Mil*, 2022).

Due to drills or military engagement, the military population is frequently exposed to many blast wave events. Thus, the astrocyte reactivity and mitochondrial dynamics responses could be altered as the severity of the injury is exacerbated by a repetitive mechanical insult. For instance, in the hippocampus of adult rats exposed to a blast injury, our laboratory observed a delayed response of microglia activation starting at two weeks post-injury (Cho, Sajja, Vandevord, et al., 2013). In contrast, astrocyte reactivity started as early as 24 hours post single mild bTBI, as seen in our current and previous data, which was accompanied by neurodegenerations (Sajja et al., 2012). Protein levels of the cytokine IFN-γ, a pro-inflammatory cytokine, were observed within 24 hours and returned to physiological levels by two weeks post single mild bTBI (Cho, Sajja, Vandevord, et al., 2013). Reactive astrocytes are capable of releasing a vast array of chemicals that influence other resident brain cell's function, and an initial pro-inflammatory environment in response to injury could beneficially help reduce cellular damage and so neutralize potential threats to the CNS due to the injury (Allan & Rothwell, 2003; Amor et al., 2010; Lucas et al., 2006; Martino et al., 2002). However, repetitive blast events have led to microglia activation as early as seven days post-injury (M. Dickerson et al., 2022)**,** indicating a smaller post-injury window for possible treatments compared to a single blast due to an increase in the number of blast wave exposure. However, single and repeated blast events both present long-term detrimental cognitive outcomes (M. R. Dickerson et al., 2020; Sajja, Hubbard, & VandeVord, 2015)**,** such as memory and anxiety disorders shown in patients who suffered a bTBI (Agoston, 2017; Chapman & Diaz-Arrastia, 2014; Higgins et al., 2014; Kashdan et al., 2006; Miles et al., 2017; Theeler et al., 2012; Trudeau et al., 1998). Nevertheless, investigation of the changes that occur following a single blast insult is fundamental to understanding the initial biochemical response that contributes to the complex pathology following repetitive injuries. Repetitive mechanical insults have a more dynamic biochemical response rather than an additive effect. Therefore, establishing the molecular response following a single blast exposure is even more critical as

a baseline to understand complex injuries in addition to addressing a clinical need following mild single bTBI injuries.

5.4. Future Work

Comprehensive results from this current study characterized astrocyte dynamic response to a single mild bTBI and further characterized a time-dependent astrocyte reactivity. Future work should explore the potential involvement of early mitochondrial fission events in the acute astrocyte reactive phenotype response post single mild bTBI.

I. Acute mediated-mitochondrial fission event was observed by increased mitochondrial fragmentation, which was less visible three days post-injury. It would be important to examine if this result happened by mitophagy as a mechanism in astrocytes aiding in eliminating damaged mitochondria and therefore initially acting as a positive response post-mechanical overpressure insult. When mitochondria fission occurs, they can be separated into polarized daughter mitochondria, which have a high likelihood of fusing, while depolarized mitochondria are particularly targeted for mitophagy elimination (Chan, 2012; Lemasters, 2005; Pickles et al., 2018). Mitophagy starts with PINK1 accumulation on the OMM, where it recruits Parkin acting as a marker of impaired mitochondria. Parkin will then be activated and initiate ubiquitination of the OMM. Finally, ubiquitin-binding autophagic components such as LC3B identify ubiquitinated mitochondria, promote autophagosome development, and induce mitochondrial clearance (Pickles et al., 2018). Therefore, exploring the PINK1/Parkin-mediated mitophagy and LC3 participation in astrocytes post-acute mild bTBI would help better understand our current study's early fission outcomes.

II. Single mild bTBI presented an increase of ROS formation as early as four hours, which was maintained up to two weeks post-injury (Cho, Sajja, Vandevord, et al., 2013)**,** combined with a significant decrease of glutathione (Sajja et al., 2012). Glutathione is an important antioxidant, and since astrocytes produce more neuronal glutathione than neurons do on a basic level, this suggests that they are better able to detoxify reactive oxygen and nitrogen species under normal circumstances (Aoyama, 2021; Bylicky et al., 2018; McGann & Mandel, 2018; Raps et al., 1989). As a result, it highlights how crucial optimal astrocytic mitochondrial dynamics are in healthy and damaged brains. Current data presented a non-statistically significant increase in pDRP1s616/pDRP1s637 ratio across the blast groups from three to seven days. An imbalance in favor of a larger $pDRP1^{s616}$/$pDRP1^{s637}$ ratio has been connected to a disruption in the redox status of astrocytic mitochondria (Dai et al., 2020; Motori et al., 2013). Future work should explore the effects of ROS such as mitochondrial superoxide and glutathione in acute astrocyte reactive phenotype. Increased mitochondrial ROS can activate the NF-kB pathway and trigger the release of astrocytic pro-inflammatory mediators (Joshi et al., 2019; Motori et al., 2013)**,** and if chronic can present detrimental outcomes.

III. One approach to further test the current study hypothesis would be to block and activate DRP1 enzymatic activity by phosphorylation at serine 616 site (pDRP1s616). Blocking acute DRP1 activity could help determine the role mitochondrial fission plays in astrocyte reactive phenotype post mild bTBI. CDK5 it is one of the kinases that increased DRP1 phosphorylation at serine 616 sites (Taguchi et al., 2007); moreover, after blocking CDK5 activity, a study observed a preserved pDRP1s616/pDRP1s637 ratio and also reduced astrocytes hippocampus reactive and astrocyte apoptosis (Hyun et al., 2017) post pilocarpine-induced status epilepticus.

Furthermore, other studies have shown that inhibiting CDK5 activity in astrocytes provides neuroprotection outcomes (Posada-Duque et al., 2015) by leading to calcium homeostasis in the hippocampus, playing a crucial role in neuronal synaptic plasticity markers (Toro-Fernández et al., 2021). In addition, activating pDRP1s616 by the direct activation of the CDK5 pathway would help to further test the astrocytic mitochondrial fission phenotype and if this phenotype is driven by CDK5-mediated phosphorylation of DRP1 on serine 616 site and further characterize this phosphorylation event and mitochondrial fragmentation are leading to astrocytes reactive phenotype transition. As a result, it would be intriguing to pursue those concept of blocking and activating CDK5 while focusing on a single mild bTBI.

Bibliography

Abbott, N. J., Rönnbäck, L., & Hansson, E. (2006). Astrocyte–endothelial interactions at the blood–brain barrier. *Nature Reviews Neuroscience*, *7*(1), 41–53. https://doi.org/10.1038/nrn1824

Agarwal, A., Wu, P.-H., Hughes, E. G., Fukaya, M., Tischfield, M. A., Langseth, A. J., Wirtz, D., & Bergles, D. E. (2017). Transient Opening of the Mitochondrial Permeability Transition Pore Induces Microdomain Calcium Transients in Astrocyte Processes. *Neuron*, *93*(3), 587-605.e7. https://doi.org/10.1016/j.neuron.2016.12.034

Agoston, D. V. (2017). Modeling the Long-Term Consequences of Repeated Blast-Induced Mild Traumatic Brain Injuries. *Journal of Neurotrauma*, *34*(Suppl 1), S-44-S-52. https://doi.org/10.1089/neu.2017.5317

Akdemir, E. S., Huang, A. Y.-S., & Deneen, B. (2020). Astrocytogenesis: Where, when, and how. *F1000Research*, *9*, F1000 Faculty Rev-233. https://doi.org/10.12688/f1000research.22405.1

Allan, S. M., & Rothwell, N. J. (2003). Inflammation in central nervous system injury. *Philosophical Transactions of the Royal Society B: Biological Sciences*, *358*(1438), 1669–1677. https://doi.org/10.1098/rstb.2003.1358

Allen, N. J., & Eroglu, C. (2017). Cell Biology of Astrocyte-Synapse Interactions. *Neuron*, *96*(3), 697–708. https://doi.org/10.1016/j.neuron.2017.09.056

Amor, S., Puentes, F., Baker, D., & van der Valk, P. (2010). Inflammation in neurodegenerative diseases. *Immunology*, *129*(2), 154–169. https://doi.org/10.1111/j.1365-2567.2009.03225.x

Anderson, M. A., Ao, Y., & Sofroniew, M. V. (2014). Heterogeneity of reactive astrocytes. *Neuroscience Letters*, *565*, 23–29. https://doi.org/10.1016/j.neulet.2013.12.030

Aoyama, K. (2021). Glutathione in the Brain. *International Journal of Molecular Sciences*, *22*(9), 5010. https://doi.org/10.3390/ijms22095010

Arun, P., Abu-Taleb, R., Oguntayo, S., Wang, Y., Valiyaveettil, M., Long, J. B., & Nambiar, M. P. (2013). Acute Mitochondrial Dysfunction after Blast Exposure: Potential Role of Mitochondrial Glutamate Oxaloacetate Transaminase. *Journal of Neurotrauma*, *30*(19), 1645–1651. https://doi.org/10.1089/neu.2012.2834

Bailey, Z. S., Grinter, M. B., & VandeVord, P. J. (2016). Astrocyte Reactivity Following Blast Exposure Involves Aberrant Histone Acetylation. *Frontiers in Molecular Neuroscience*, *9*. https://www.frontiersin.org/articles/10.3389/fnmol.2016.00064

Bakare, A. B., Daniel, J., Stabach, J., Rojas, A., Bell, A., Henry, B., & Iyer, S. (2021). Quantifying Mitochondrial Dynamics in Patient Fibroblasts with Multiple Developmental Defects and Mitochondrial Disorders. *International Journal of Molecular Sciences*, *22*(12), 6263. https://doi.org/10.3390/ijms22126263

Balaban, R. S., Nemoto, S., & Finkel, T. (2005). Mitochondria, Oxidants, and Aging. *Cell*, *120*(4), 483–495. https://doi.org/10.1016/j.cell.2005.02.001

Balan, I. S., Saladino, A. J., Aarabi, B., Castellani, R. J., Wade, C., Stein, D. M., Eisenberg, H. M., Chen, H. H., & Fiskum, G. (2013). Cellular Alterations in Human Traumatic Brain Injury: Changes in Mitochondrial Morphology Reflect Regional Levels of Injury Severity. *Journal of Neurotrauma*, *30*(5), 367–381. https://doi.org/10.1089/neu.2012.2339

Balasubramanian, S., Packard, J. A., Leach, J. B., & Powell, E. M. (2016). Three-Dimensional Environment Sustains Morphological Heterogeneity and Promotes Phenotypic Progression During Astrocyte Development. *Tissue Engineering. Part A*, *22*(11–12), 885–898. https://doi.org/10.1089/ten.tea.2016.0103

Balog, J., Mehta, S. L., & Vemuganti, R. (2016). Mitochondrial fission and fusion in secondary brain damage after CNS insults. *Journal of Cerebral Blood Flow & Metabolism*, *36*(12), 2022–2033. https://doi.org/10.1177/0271678X16671528

Bantle, C. M., Hirst, W. D., Weihofen, A., & Shlevkov, E. (2021). Mitochondrial Dysfunction in Astrocytes: A Role in Parkinson's Disease? *Frontiers in Cell and Developmental Biology*, *8*, 608026. https://doi.org/10.3389/fcell.2020.608026

Bélanger, M., Allaman, I., & Magistretti, P. J. (2011). Brain Energy Metabolism: Focus on Astrocyte-Neuron Metabolic Cooperation. *Cell Metabolism*, *14*(6), 724–738. https://doi.org/10.1016/j.cmet.2011.08.016

Bir, C., Vandevord, P., Shen, Y., Raza, W., & Haacke, E. M. (2012). Effects of variable blast pressures on blood flow and oxygen saturation in rat brain as evidenced using MRI. *Magnetic Resonance Imaging*, *30*(4), 527–534. https://doi.org/10.1016/j.mri.2011.12.003

Blomstrand, F., Khatibi, S., Muyderman, H., Hansson, E., Olsson, T., & Rönnbäck, L. (1999). 5-hydroxytryptamine and glutamate modulate velocity and extent of intercellular calcium signalling in hippocampal astroglial cells in primary cultures. *Neuroscience*, *88*(4), 1241–1253. https://doi.org/10.1016/S0306-4522(98)00351-0

Bolander, R., Mathie, B., Bir, C., Ritzel, D., & VandeVord, P. (2011). Skull Flexure as a Contributing Factor in the Mechanism of Injury in the Rat when Exposed to a Shock Wave. *Annals of Biomedical Engineering*, *39*(10), 2550. https://doi.org/10.1007/s10439-011-0343-0

Boni, J. L., Kahanovitch, U., Nwaobi, S. E., Floyd, C. L., & Olsen, M. L. (2020). DNA methylation: A mechanism for sustained alteration of KIR4.1 expression following central nervous system insult. *Glia*, *68*(7), 1495–1512. https://doi.org/10.1002/glia.23797

Buffo, A., Rite, I., Tripathi, P., Lepier, A., Colak, D., Horn, A.-P., Mori, T., & Götz, M. (2008). Origin and progeny of reactive gliosis: A source of multipotent cells in the injured brain. *Proceedings of the National Academy of Sciences*, *105*(9), 3581–3586. https://doi.org/10.1073/pnas.0709002105

Buffo, A., Rolando, C., & Ceruti, S. (2010). Astrocytes in the damaged brain: Molecular and cellular insights into their reactive response and healing potential. *Biochemical Pharmacology*, *79*(2), 77–89. https://doi.org/10.1016/j.bcp.2009.09.014

Burda, J. E., Bernstein, A. M., & Sofroniew, M. V. (2016). Astrocyte roles in traumatic brain injury. *Experimental Neurology*, *275*, 305–315. https://doi.org/10.1016/j.expneurol.2015.03.020

Burda, J. E., & Sofroniew, M. V. (2014). Reactive Gliosis and the Multicellular Response to CNS Damage and Disease. *Neuron*, *81*(2), 229–248. https://doi.org/10.1016/j.neuron.2013.12.034

Bylicky, M. A., Mueller, G. P., & Day, R. M. (2018). Mechanisms of Endogenous Neuroprotective Effects of Astrocytes in Brain Injury. *Oxidative Medicine and Cellular Longevity*, *2018*, 1–16. https://doi.org/10.1155/2018/6501031

Canchi, S., Sarntinoranont, M., Hong, Y., Flint, J. J., Subhash, G., & King, M. A. (2017). Simulated blast overpressure induces specific astrocyte injury in an ex vivo brain slice model. *PLOS ONE*, *12*(4), e0175396. https://doi.org/10.1371/journal.pone.0175396

Casas, A. I., Geuss, E., Kleikers, P. W. M., Mencl, S., Herrmann, A. M., Buendia, I., Egea, J., Meuth, S. G., Lopez, M. G., Kleinschnitz, C., & Schmidt, H. H. H. W. (2017). NOX4-dependent neuronal autotoxicity and BBB breakdown explain the superior sensitivity of the brain to ischemic damage. *Proceedings of the National Academy of Sciences*, *114*(46), 12315–12320. https://doi.org/10.1073/pnas.1705034114

Cash, A., & Theus, M. H. (2020). Mechanisms of Blood–Brain Barrier Dysfunction in Traumatic Brain Injury. *International Journal of Molecular Sciences*, *21*(9), 3344. https://doi.org/10.3390/ijms21093344

Cernak, I., & Noble-Haeusslein, L. J. (2010). Traumatic brain injury: An overview of pathobiology with emphasis on military populations. *Journal of Cerebral Blood Flow and Metabolism: Official Journal of the International Society of Cerebral Blood Flow and Metabolism*, *30*(2), 255–266. https://doi.org/10.1038/jcbfm.2009.203

Cervantes-Silva, M. P., Cox, S. L., & Curtis, A. M. (2021). Alterations in mitochondrial morphology as a key driver of immunity and host defence. *EMBO Reports*, *22*(9). https://doi.org/10.15252/embr.202153086

Chan, D. C. (2012). Fusion and Fission: Interlinked Processes Critical for Mitochondrial Health. *Annual Review of Genetics*, *46*(1), 265–287. https://doi.org/10.1146/annurev-genet-110410-132529

Chang, C.-R., & Blackstone, C. (2007). Cyclic AMP-dependent Protein Kinase Phosphorylation of Drp1 Regulates Its GTPase Activity and Mitochondrial Morphology *. *Journal of Biological Chemistry*, *282*(30), 21583–21587. https://doi.org/10.1074/jbc.C700083200

Chang, C.-R., & Blackstone, C. (2010). Dynamic regulation of mitochondrial fission through modification of the dynamin-related protein Drp1. *Annals of the New York Academy of Sciences*, *1201*, 34–39. https://doi.org/10.1111/j.1749-6632.2010.05629.x

Chao, H., Lin, C., Zuo, Q., Liu, Y., Xiao, M., Xu, X., Li, Z., Bao, Z., Chen, H., You, Y., Kochanek, P. M., Yin, H., Liu, N., Kagan, V. E., Bayır, H., & Ji, J. (2019). Cardiolipin-Dependent Mitophagy Guides Outcome after Traumatic Brain Injury. *The Journal of Neuroscience: The Official Journal of the Society for Neuroscience*, *39*(10), 1930–1943. https://doi.org/10.1523/JNEUROSCI.3415-17.2018

Chapman, J. C., & Diaz-Arrastia, R. (2014). Military traumatic brain injury: A review. *Alzheimer's & Dementia*, *10*(3S). https://doi.org/10.1016/j.jalz.2014.04.012

Charles, A. C., Merrill, J. E., Dirksen, E. R., & Sandersont, M. J. (1991). Intercellular signaling in glial cells: Calcium waves and oscillations in response to mechanical stimulation and glutamate. *Neuron*, *6*(6), 983–992. https://doi.org/10.1016/0896-6273(91)90238-U

Cheng, G., Kong, R., Zhang, L., & Zhang, J. (2012). Mitochondria in traumatic brain injury and mitochondrial-targeted multipotential therapeutic strategies: Mitochondria in traumatic brain injury. *British Journal of Pharmacology*, *167*(4), 699–719. https://doi.org/10.1111/j.1476-5381.2012.02025.x

Cho, H. J., Sajja, V. S. S. S., VandeVord, P. J., & Lee, Y. W. (2013). Blast induces oxidative stress, inflammation, neuronal loss and subsequent short-term memory impairment in rats. *Neuroscience*, *253*, 9–20. https://doi.org/10.1016/j.neuroscience.2013.08.037

Cho, H. J., Sajja, V. S. S. S., Vandevord, P. J., & Lee, Y. W. (2013). Blast induces oxidative stress, inflammation, neuronal loss and subsequent short-term memory impairment in rats. *Neuroscience*, *253*, 9–20. https://doi.org/10.1016/j.neuroscience.2013.08.037

Clark, R. E., & Squire, L. R. (2013). Similarity in form and function of the hippocampus in rodents, monkeys, and humans. *Proceedings of the National Academy of Sciences of the United States of America*, *110*(Suppl 2), 10365–10370. https://doi.org/10.1073/pnas.1301225110

Cullen, D. K., Simon, C. M., & LaPlaca, M. C. (2007). Strain rate-dependent induction of reactive astrogliosis and cell death in three-dimensional neuronal-astrocytic co-cultures. *Brain Research*, *1158*, 103–115. https://doi.org/10.1016/j.brainres.2007.04.070

Dai, C.-Q., Guo, Y., & Chu, X.-Y. (2020). Neuropathic Pain: The Dysfunction of Drp1, Mitochondria, and ROS Homeostasis. *Neurotoxicity Research*, *38*(3), 553–563. https://doi.org/10.1007/s12640-020-00257-2

De Pascalis, C., Pérez-González, C., Seetharaman, S., Boëda, B., Vianay, B., Burute, M., Leduc, C., Borghi, N., Trepat, X., & Etienne-Manneville, S. (2018). Intermediate filaments control collective migration by restricting traction forces and sustaining cell–cell contacts. *Journal of Cell Biology*, *217*(9), 3031–3044. https://doi.org/10.1083/jcb.201801162

Desagher, S., Glowinski, J., & Premont, J. (1996). Astrocytes protect neurons from hydrogen peroxide toxicity. *The Journal of Neuroscience*, *16*(8), 2553–2562. https://doi.org/10.1523/JNEUROSCI.16-08-02553.1996

Detmer, S. A., & Chan, D. C. (2007). Functions and dysfunctions of mitochondrial dynamics. *Nature Reviews Molecular Cell Biology*, *8*(11), 870–879. https://doi.org/10.1038/nrm2275

Dewan, M. C., Rattani, A., Gupta, S., Baticulon, R. E., Hung, Y.-C., Punchak, M., Agrawal, A., Adeleye, A. O., Shrime, M. G., Rubiano, A. M., Rosenfeld, J. V., & Park, K. B. (2019). Estimating the global incidence of traumatic brain injury. *Journal of Neurosurgery*, *130*(4), 1080–1097. https://doi.org/10.3171/2017.10.JNS17352

Di Giovanni, S., Movsesyan, V., Ahmed, F., Cernak, I., Schinelli, S., Stoica, B., & Faden, A. I. (2005). Cell cycle inhibition provides neuroprotection and reduces glial proliferation and scar formation

after traumatic brain injury. *Proceedings of the National Academy of Sciences of the United States of America*, *102*(23), 8333–8338. https://doi.org/10.1073/pnas.0500989102

Dickerson, M., Guilhaume-Corrêa, F., Strickler, J., & VandeVord, P. J. (2022). Age-relevant in vitro models may lead to improved translational research for traumatic brain injury. *Current Opinion in Biomedical Engineering*, *22*, 100391. https://doi.org/10.1016/j.cobme.2022.100391

Dickerson, M. R., Bailey, Z. S., Murphy, S. F., Urban, M. J., & VandeVord, P. J. (2020). Glial Activation in the Thalamus Contributes to Vestibulomotor Deficits Following Blast-Induced Neurotrauma. *Frontiers in Neurology*, *11*, 618. https://doi.org/10.3389/fneur.2020.00618

Dieckman, L. M. (2012). *"PCNA Structure and Function: Insights from Structures of PCNA Complexes and Post-translationally Modified PCNA," in The Eukaryotic Replisome: A Guide to Protein Structure and Function: Vol. The Eukaryotic Replisome: a Guide to Protein Structure and Function*. ed. S. MacNeil.

DOD TBI Worldwide Numbers | Health.mil. (2022, July 11). https://health.mil/Military-Health-Topics/Centers-of-Excellence/Traumatic-Brain-Injury-Center-of-Excellence/DOD-TBI-Worldwide-Numbers

Dong, P., & Cremer, O. (2011). Limitations of the use of the Glasgow Coma Scale in intensive care patients with non-neurological primary disease: A search for alternatives. *Critical Care*, *15*(Suppl 1), P506. https://doi.org/10.1186/cc9926

Duchen, M. R. (2000). Mitochondria and calcium: From cell signalling to cell death. *The Journal of Physiology*, *529 Pt 1*, 57–68. https://doi.org/10.1111/j.1469-7793.2000.00057.x

Edwards, R., Eaglesfield, R., & Tokatlidis, K. (2021). The mitochondrial intermembrane space: The most constricted mitochondrial sub-compartment with the largest variety of protein import pathways. *Open Biology*, *11*(3), 210002. https://doi.org/10.1098/rsob.210002

Ekmark-Lewén, S., Lewén, A., Israelsson, C., Li, G. L., Farooque, M., Olsson, Y., Ebendal, T., & Hillered, L. (2010). Vimentin and GFAP responses in astrocytes after contusion trauma to the murine brain. *Restorative Neurology and Neuroscience*, *28*(3), 311–321. https://doi.org/10.3233/RNN-2010-0529

Eng, L. F., Ghirnikar, R. S., & Lee, Y. L. (2000). Glial fibrillary acidic protein: GFAP-thirty-one years (1969-2000). *Neurochemical Research*, *25*(9–10), 1439–1451. https://doi.org/10.1023/a:1007677003387

Escartin, C., Galea, E., Lakatos, A., O'Callaghan, J. P., Petzold, G. C., Serrano-Pozo, A., Steinhäuser, C., Volterra, A., Carmignoto, G., Agarwal, A., Allen, N. J., Araque, A., Barbeito, L., Barzilai, A., Bergles, D. E., Bonvento, G., Butt, A. M., Chen, W.-T., Cohen-Salmon, M., … Verkhratsky, A. (2021). Reactive astrocyte nomenclature, definitions, and future directions. *Nature Neuroscience*, *24*(3), 312–325. https://doi.org/10.1038/s41593-020-00783-4

Farkas, O., & Povlishock, J. T. (2007). Cellular and subcellular change evoked by diffuse traumatic brain injury: A complex web of change extending far beyond focal damage. *Progress in Brain Research*, *161*, 43–59. https://doi.org/10.1016/S0079-6123(06)61004-2

Felix, L., Stephan, J., & Rose, C. R. (2021). Astrocytes of the early postnatal brain. *European Journal of Neuroscience*, *54*(5), 5649–5672. https://doi.org/10.1111/ejn.14780

Fievisohn, E., Bailey, Z., Guettler, A., & VandeVord, P. (2018). Primary Blast Brain Injury Mechanisms: Current Knowledge, Limitations, and Future Directions. *Journal of Biomechanical Engineering*, *140*(2). https://doi.org/10.1115/1.4038710

Fischer, T. D., Hylin, M. J., Zhao, J., Moore, A. N., Waxham, M. N., & Dash, P. K. (2016). Altered Mitochondrial Dynamics and TBI Pathophysiology. *Frontiers in Systems Neuroscience*, *10*. https://doi.org/10.3389/fnsys.2016.00029

Fitzgerald, M., Tan, T., Rosenfeld, J. V., Noonan, M., Tee, J., Ng, E., Mathew, J., Broderick, S., Kim, Y., Groombridge, C., Udy, A., & Mitra, B. (2022). An initial Glasgow Coma Scale score of 8 or less does not define severe brain injury. *Emergency Medicine Australasia*, *34*(3), 459–461. https://doi.org/10.1111/1742-6723.13937

Flippo, K. H., & Strack, S. (2017). Mitochondrial dynamics in neuronal injury, development and plasticity. *Journal of Cell Science*, *130*(4), 671–681. https://doi.org/10.1242/jcs.171017

Ganpule, S., Alai, A., Plougonven, E., & Chandra, N. (2013). Mechanics of blast loading on the head models in the study of traumatic brain injury using experimental and computational approaches. *Biomechanics and Modeling in Mechanobiology*, *12*(3), 511–531. https://doi.org/10.1007/s10237-012-0421-8

Giacomello, M., Pyakurel, A., Glytsou, C., & Scorrano, L. (2020). The cell biology of mitochondrial membrane dynamics. *Nature Reviews Molecular Cell Biology*, *21*(4), 204–224. https://doi.org/10.1038/s41580-020-0210-7

Glancy, B., Kim, Y., Katti, P., & Willingham, T. B. (2020). The Functional Impact of Mitochondrial Structure Across Subcellular Scales. *Frontiers in Physiology*, *11*, 541040. https://doi.org/10.3389/fphys.2020.541040

Gollihue, J. L., & Norris, C. M. (2020). Astrocyte mitochondria: Central players and potential therapeutic targets for neurodegenerative diseases and injury. *Ageing Research Reviews*, *59*, 101039. https://doi.org/10.1016/j.arr.2020.101039

Hamby, M. E., Coppola, G., Ao, Y., Geschwind, D. H., Khakh, B. S., & Sofroniew, M. V. (2012). Inflammatory Mediators Alter the Astrocyte Transcriptome and Calcium Signaling Elicited by Multiple G-Protein-Coupled Receptors. *The Journal of Neuroscience*, *32*(42), 14489–14510. https://doi.org/10.1523/JNEUROSCI.1256-12.2012

Hampton, C. E., Thorpe, C. N., Sholar, C. A., Rzigalinski, B. A., & VandeVord, P. J. (2013). A novel bridge wire model of blast traumatic brain injury—Biomed 2013. *Biomedical Sciences Instrumentation*, *49*, 312–319.

Hampton, C. E., & Vandevord, P. J. (2012). Vibrational frequency response to impact loading of skull models. *Biomedical Sciences Instrumentation*, *48*, 157–164.

Hao, Z. Y., Zhong, Y., Ma, Z. J., Xu, H. Z., Kong, J. Y., Wu, Z., Wu, Y., Li, J., Lu, X., Zhang, N., & Wang, C. (2020). Abnormal resting-state functional connectivity of hippocampal subfields in patients with major depressive disorder. *BMC Psychiatry*, *20*(1), 71. https://doi.org/10.1186/s12888-020-02490-7

He, Y., Li, H.-L., Xie, W.-Y., Yang, C.-Z., Yu, A. C. H., & Wang, Y. (2007). The presence of active Cdk5 associated with p35 in astrocytes and its important role in process elongation of scratched astrocyte. *Glia*, *55*(6), 573–583. https://doi.org/10.1002/glia.20485

Hernandez, A., Tan, C., Plattner, F., Logsdon, A. F., Pozo, K., Yousuf, M. A., Singh, T., Turner, R. C., Lucke-Wold, B. P., Huber, J. D., Rosen, C. L., & Bibb, J. A. (2018). Exposure to mild blast forces induces neuropathological effects, neurophysiological deficits and biochemical changes. *Molecular Brain*, *11*(1), 64. https://doi.org/10.1186/s13041-018-0408-1

Higgins, D. M., Kerns, R. D., Brandt, C. A., Haskell, S. G., Bathulapalli, H., Gilliam, W., & Goulet, J. L. (2014). Persistent Pain and Comorbidity Among Operation Enduring Freedom/Operation Iraqi Freedom/Operation New Dawn Veterans. *Pain Medicine*, *15*(5), 782–790. https://doi.org/10.1111/pme.12388

Hlavac, N. (2018). *Attributes of Astrocyte Response to Mechano-stimulation by High-rate Overpressure; Doctoral dissertation*. Virginia Tech.

Hlavac, N., Guilhaume-Corrêa, F., & VandeVord, P. J. (2020). Mechano-stimulation initiated by extracellular adhesion and cationic conductance pathways influence astrocyte activation. *Neuroscience Letters*, *739*, 135405. https://doi.org/10.1016/j.neulet.2020.135405

Hlavac, N., Miller, S., Grinter, M., & VandeVord, P. (2015). Two and Three-Dimensional in Vitro Models of Blast-Induced Neurotrauma. *Biomedical Sciences Instrumentation*, *51*, 439–445.

Hlavac, N., & VandeVord, P. J. (2019). Astrocyte Mechano-Activation by High-Rate Overpressure Involves Alterations in Structural and Junctional Proteins. *Frontiers in Neurology*, *10*, 99. https://doi.org/10.3389/fneur.2019.00099

Hoitzing, H., Johnston, I. G., & Jones, N. S. (2015). What is the function of mitochondrial networks? A theoretical assessment of hypotheses and proposal for future research. *BioEssays*, *37*(6), 687–700. https://doi.org/10.1002/bies.201400188

Holt, L. M., Stoyanof, S. T., & Olsen, M. L. (2019). Magnetic Cell Sorting for In Vivo and In Vitro Astrocyte, Neuron, and Microglia Analysis. *Current Protocols in Neuroscience*, *88*(1). https://doi.org/10.1002/cpns.71

Hubbard, W. B., Spry, M. L., Gooch, J. L., Cloud, A. L., Vekaria, H. J., Burden, S., Powell, D. K., Berkowitz, B. A., Geldenhuys, W. J., Harris, N. G., & Sullivan, P. G. (2021). Clinically relevant mitochondrial-targeted therapy improves chronic outcomes after traumatic brain injury. *Brain*, *144*(12), 3788–3807. https://doi.org/10.1093/brain/awab341

Hyun, H.-W., Min, S.-J., & Kim, J.-E. (2017). CDK5 inhibitors prevent astroglial apoptosis and reactive astrogliosis by regulating PKA and DRP1 phosphorylations in the rat hippocampus. *Neuroscience Research*, *119*, 24–37. https://doi.org/10.1016/j.neures.2017.01.006

Ishii, T., Takanashi, Y., Sugita, K., Miyazawa, M., Yanagihara, R., Yasuda, K., Onouchi, H., Kawabe, N., Nakata, M., Yamamoto, Y., Hartman, P. S., & Ishii, N. (2017). Endogenous reactive oxygen species cause astrocyte defects and neuronal dysfunctions in the hippocampus: A new model for aging brain. *Aging Cell*, *16*(1), 39–51. https://doi.org/10.1111/acel.12523

Jackson, J. G., & Robinson, M. B. (2018). Regulation of mitochondrial dynamics in astrocytes: Mechanisms, consequences, and unknowns. *Glia*, *66*(6), 1213–1234. https://doi.org/10.1002/glia.23252

Jacobson, J., & Duchen, M. R. (2004). Interplay between mitochondria and cellular calcium signalling. *Molecular and Cellular Biochemistry*, *256–257*(1–2), 209–218. https://doi.org/10.1023/b:mcbi.0000009869.29827.df

Jain, S., & Iverson, L. M. (2022). Glasgow Coma Scale. In *StatPearls*. StatPearls Publishing. http://www.ncbi.nlm.nih.gov/books/NBK513298/

Jezek, J., Cooper, K., & Strich, R. (2018). Reactive Oxygen Species and Mitochondrial Dynamics: The Yin and Yang of Mitochondrial Dysfunction and Cancer Progression. *Antioxidants*, *7*(1), 13. https://doi.org/10.3390/antiox7010013

Joshi, A. U., Minhas, P. S., Liddelow, S. A., Haileselassie, B., Andreasson, K. I., Dorn, G. W., & Mochly-Rosen, D. (2019). Fragmented mitochondria released from microglia trigger A1 astrocytic response and propagate inflammatory neurodegeneration. *Nature Neuroscience*, *22*(10), 1635–1648. https://doi.org/10.1038/s41593-019-0486-0

Karve, I. P., Taylor, J. M., & Crack, P. J. (2016). The contribution of astrocytes and microglia to traumatic brain injury. *British Journal of Pharmacology*, *173*(4), 692–702. https://doi.org/10.1111/bph.13125

Kashatus, J. A., Nascimento, A., Myers, L. J., Sher, A., Byrne, F. L., Hoehn, K. L., Counter, C. M., & Kashatus, D. F. (2015). Erk2 Phosphorylation of Drp1 Promotes Mitochondrial Fission and MAPK-Driven Tumor Growth. *Molecular Cell*, *57*(3), 537–551. https://doi.org/10.1016/j.molcel.2015.01.002

Kashdan, T. B., Julian, T., Merritt, K., & Uswatte, G. (2006). Social anxiety and posttraumatic stress in combat veterans: Relations to well-being and character strengths. *Behaviour Research and Therapy*, *44*(4), 561–583. https://doi.org/10.1016/j.brat.2005.03.010

Kato, H., Takahashi, A., & Itoyama, Y. (2003). Cell cycle protein expression in proliferating microglia and astrocytes following transient global cerebral ischemia in the rat. *Brain Research Bulletin*, *60*(3), 215–221. https://doi.org/10.1016/S0361-9230(03)00036-4

Keating, C. E., & Cullen, D. K. (2021). Mechanosensation in traumatic brain injury. *Neurobiology of Disease*, *148*, 105210. https://doi.org/10.1016/j.nbd.2020.105210

Khakh, B. S., & Sofroniew, M. V. (2015). Diversity of astrocyte functions and phenotypes in neural circuits. *Nature Neuroscience*, *18*(7), 942–952. https://doi.org/10.1038/nn.4043

Knott, A. B., Perkins, G., Schwarzenbacher, R., & Bossy-Wetzel, E. (2008). Mitochondrial fragmentation in neurodegeneration. *Nature Reviews Neuroscience*, *9*(7), 505–518. https://doi.org/10.1038/nrn2417

Kochanek, P. M., Dixon, C. E., Shellington, D. K., Shin, S. S., Bayır, H., Jackson, E. K., Kagan, V. E., Yan, H. Q., Swauger, P. V., Parks, S. A., Ritzel, D. V., Bauman, R., Clark, R. S. B., Garman, R. H., Bandak, F., Ling, G., & Jenkins, L. W. (2013). Screening of Biochemical and Molecular Mechanisms of Secondary Injury and Repair in the Brain after Experimental Blast-Induced Traumatic Brain Injury in Rats. *Journal of Neurotrauma*, *30*(11), 920–937. https://doi.org/10.1089/neu.2013.2862

Kuriakose, M., Younger, D., Ravula, A. R., Alay, E., Rama Rao, K. V., & Chandra, N. (2019). Synergistic Role of Oxidative Stress and Blood-Brain Barrier Permeability as Injury Mechanisms in the Acute Pathophysiology of Blast-induced Neurotrauma. *Scientific Reports*, *9*(1), 7717. https://doi.org/10.1038/s41598-019-44147-w

LaPlaca, M. C., Cullen, D. K., McLoughlin, J. J., & Cargill, R. S. (2005). High rate shear strain of three-dimensional neural cell cultures: A new in vitro traumatic brain injury model. *Journal of Biomechanics*, *38*(5), 1093–1105. https://doi.org/10.1016/j.jbiomech.2004.05.032

Law, J., Ibarguen-Vargas, Y., Belzung, C., & Surget, A. (2016). Decline of hippocampal stress reactivity and neuronal ensemble coherence in a mouse model of depression. *Psychoneuroendocrinology*, *67*, 113–123. https://doi.org/10.1016/j.psyneuen.2016.01.028

Lemasters, J. J. (2005). Selective Mitochondrial Autophagy, or Mitophagy, as a Targeted Defense Against Oxidative Stress, Mitochondrial Dysfunction, and Aging. *Rejuvenation Research*, *8*(1), 3–5. https://doi.org/10.1089/rej.2005.8.3

Leonardi, A. D. C., Bir, C. A., Ritzel, D. V., & VandeVord, P. J. (2011). Intracranial pressure increases during exposure to a shock wave. *Journal of Neurotrauma*, *28*(1), 85–94. https://doi.org/10.1089/neu.2010.1324

Levi, L., Guilburd, J. N., Lemberger, A., Soustiel, J. F., & Feinsod, M. (1990). Diffuse axonal injury: Analysis of 100 patients with radiological signs. *Neurosurgery*, *27*(3), 429–432.

Li, J., Khankan, R. R., Caneda, C., Godoy, M. I., Haney, M. S., Krawczyk, M. C., Bassik, M. C., Sloan, S. A., & Zhang, Y. (2019). Astrocyte-to-astrocyte contact and a positive feedback loop of growth factor signaling regulate astrocyte maturation. *Glia*, *67*(8), 1571–1597. https://doi.org/10.1002/glia.23630

Liesa, M., Palacín, M., & Zorzano, A. (2009). Mitochondrial Dynamics in Mammalian Health and Disease. *Physiological Reviews*, *89*(3), 799–845. https://doi.org/10.1152/physrev.00030.2008

Lifshitz, J., Friberg, H., Neumar, R., Raghupathi, R., Welsh, F., Janmey, P., Saatman, K., Wieloch, T., Grady, M., & McIntosh, T. (2003). Structural and functional damage sustained by mitochondria after traumatic brain injury in the rat: Evidence for differentially sensitive populations in the cortex and hippocampus. *Journal of Cerebral Blood Flow and Metabolism : Official Journal of the International Society of Cerebral Blood Flow and Metabolism*, *23*(2), 219–231. https://doi.org/10.1097/00004647-200302000-00009

Lima, A. R., Santos, L., Correia, M., Soares, P., Sobrinho-Simões, M., Melo, M., & Máximo, V. (2018). Dynamin-Related Protein 1 at the Crossroads of Cancer. *Genes*, *9*(2), 115. https://doi.org/10.3390/genes9020115

Lovatt, D., Sonnewald, U., Waagepetersen, H. S., Schousboe, A., He, W., Lin, J. H.-C., Han, X., Takano, T., Wang, S., Sim, F. J., Goldman, S. A., & Nedergaard, M. (2007). The transcriptome and metabolic gene signature of protoplasmic astrocytes in the adult murine cortex. *The Journal of Neuroscience: The Official Journal of the Society for Neuroscience*, *27*(45), 12255–12266. https://doi.org/10.1523/JNEUROSCI.3404-07.2007

Lucas, S.-M., Rothwell, N. J., & Gibson, R. M. (2006). The role of inflammation in CNS injury and disease. *British Journal of Pharmacology*, *147*(Suppl 1), S232–S240. https://doi.org/10.1038/sj.bjp.0706400

Ma, B., Buckalew, R., Du, Y., Kiyoshi, C. M., Alford, C. C., Wang, W., McTigue, D. M., Enyeart, J. J., Terman, D., & Zhou, M. (2016). Gap junction coupling confers isopotentiality on astrocyte syncytium. *Glia*, *64*(2), 214–226. https://doi.org/10.1002/glia.22924

Ma, M. W., Wang, J., Dhandapani, K. M., & Brann, D. W. (2018). Deletion of NADPH oxidase 4 reduces severity of traumatic brain injury. *Free Radical Biology and Medicine*, *117*, 66–75. https://doi.org/10.1016/j.freeradbiomed.2018.01.031

Ma, M. W., Wang, J., Dhandapani, K. M., Wang, R., & Brann, D. W. (2018). NADPH oxidases in traumatic brain injury – Promising therapeutic targets? *Redox Biology*, *16*, 285–293. https://doi.org/10.1016/j.redox.2018.03.005

Madan, S., Uttekar, B., Chowdhary, S., & Rikhy, R. (2022). Mitochondria Lead the Way: Mitochondrial Dynamics and Function in Cellular Movements in Development and Disease. *Frontiers in Cell and Developmental Biology*, *9*, 781933. https://doi.org/10.3389/fcell.2021.781933

Mahmoud, S., Gharagozloo, M., Simard, C., & Gris, D. (2019). Astrocytes Maintain Glutamate Homeostasis in the CNS by Controlling the Balance between Glutamate Uptake and Release. *Cells*, *8*(2), 184. https://doi.org/10.3390/cells8020184

Martino, G., Adorini, L., Rieckmann, P., Hillert, J., Kallmann, B., Comi, G., & Filippi, M. (2002). Inflammation in multiple sclerosis: The good, the bad, and the complex. *The Lancet Neurology*, *1*(8), 499–509. https://doi.org/10.1016/S1474-4422(02)00223-5

Matias, I., Morgado, J., & Gomes, F. C. A. (2019). Astrocyte Heterogeneity: Impact to Brain Aging and Disease. *Frontiers in Aging Neuroscience*, *11*, 59. https://doi.org/10.3389/fnagi.2019.00059

McGann, J. C., & Mandel, G. (2018). Neuronal activity induces glutathione metabolism gene expression in astrocytes. *Glia*, *66*(9), 2024–2039. https://doi.org/10.1002/glia.23455

McGlinchey, R. E., Milberg, W. P., Fonda, J. R., & Fortier, C. B. (2017). A methodology for assessing deployment trauma and its consequences in OEF/OIF/OND veterans: The TRACTS longitudinal prospective cohort study. *International Journal of Methods in Psychiatric Research*, *26*(3). https://doi.org/10.1002/mpr.1556

Meshrkey, F., Cabrera Ayuso, A., Rao, R. R., & Iyer, S. (2021). Quantitative analysis of mitochondrial morphologies in human induced pluripotent stem cells for Leigh syndrome. *Stem Cell Research*, *57*, 102572. https://doi.org/10.1016/j.scr.2021.102572

Meythaler, J. M., Peduzzi, J. D., Eleftheriou, E., & Novack, T. A. (2001). Current concepts: Diffuse axonal injury–associated traumatic brain injury. *Archives of Physical Medicine and Rehabilitation*, *82*(10), 1461–1471. https://doi.org/10.1053/apmr.2001.25137

Michinaga, S., & Koyama, Y. (2021). Pathophysiological Responses and Roles of Astrocytes in Traumatic Brain Injury. *International Journal of Molecular Sciences*, *22*(12), 6418. https://doi.org/10.3390/ijms22126418

Miles, S. R., Harik, J. M., Hundt, N. E., Mignogna, J., Pastorek, N. J., Thompson, K. E., Freshour, J. S., Yu, H. J., & Cully, J. A. (2017). Delivery of mental health treatment to combat veterans with psychiatric diagnoses and TBI histories. *PLOS ONE*, *12*(9), e0184265. https://doi.org/10.1371/journal.pone.0184265

Moss, W. C., King, M. J., & Blackman, E. G. (2009). Skull Flexure from Blast Waves: A Mechanism for Brain Injury with Implications for Helmet Design. *Physical Review Letters*, *103*(10), 108702. https://doi.org/10.1103/PhysRevLett.103.108702

Motori, E., Puyal, J., Toni, N., Ghanem, A., Angeloni, C., Malaguti, M., Cantelli-Forti, G., Berninger, B., Conzelmann, K.-K., Götz, M., Winklhofer, K. F., Hrelia, S., & Bergami, M. (2013). Inflammation-Induced Alteration of Astrocyte Mitochondrial Dynamics Requires Autophagy for Mitochondrial Network Maintenance. *Cell Metabolism*, *18*(6), 844–859. https://doi.org/10.1016/j.cmet.2013.11.005

Munoz-Ballester, C., Mahmutovic, D., Rafiqzad, Y., Korot, A., & Robel, S. (2022). Mild Traumatic Brain Injury-Induced Disruption of the Blood-Brain Barrier Triggers an Atypical Neuronal Response. *Frontiers in Cellular Neuroscience*, *16*. https://www.frontiersin.org/articles/10.3389/fncel.2022.821885

Myer, D. J., Gurkoff, G. G., Lee, S. M., Hovda, D. A., & Sofroniew, M. V. (2006). Essential protective roles of reactive astrocytes in traumatic brain injury. *Brain*, *129*(10), 2761–2772. https://doi.org/10.1093/brain/awl165

Needham, C. E., Ritzel, D., Rule, G. T., Wiri, S., & Young, L. (2015). Blast Testing Issues and TBI: Experimental Models That Lead to Wrong Conclusions. *Frontiers in Neurology*, *6*. https://www.frontiersin.org/articles/10.3389/fneur.2015.00072

Newmeyer, D. D., & Ferguson-Miller, S. (2003). Mitochondria: Releasing Power for Life and Unleashing the Machineries of Death. *Cell*, *112*(4), 481–490. https://doi.org/10.1016/S0092-8674(03)00116-8

Osellame, L. D., Blacker, T. S., & Duchen, M. R. (2012). Cellular and molecular mechanisms of mitochondrial function. *Best Practice & Research. Clinical Endocrinology & Metabolism*, *26*(6), 711–723. https://doi.org/10.1016/j.beem.2012.05.003

Ostrow, L. W., Langan, T. J., & Sachs, F. (2000). Stretch-induced endothelin-1 production by astrocytes. *Journal of Cardiovascular Pharmacology*, *36*(5 Suppl 1), S274-277. https://doi.org/10.1097/00005344-200036051-00081

Ostrow, L. W., & Sachs, F. (2005). Mechanosensation and endothelin in astrocytes—Hypothetical roles in CNS pathophysiology. *Brain Research Reviews*, *48*(3), 488–508. https://doi.org/10.1016/j.brainresrev.2004.09.005

Otera, H., Ishihara, N., & Mihara, K. (2013). New insights into the function and regulation of mitochondrial fission. *Biochimica et Biophysica Acta (BBA) - Molecular Cell Research*, *1833*(5), 1256–1268. https://doi.org/10.1016/j.bbamcr.2013.02.002

Pekny, M., & Nilsson, M. (2005). Astrocyte activation and reactive gliosis. *Glia*, *50*(4), 427–434. https://doi.org/10.1002/glia.20207

Pekny, M., & Pekna, M. (2014). Astrocyte reactivity and reactive astrogliosis: Costs and benefits. *Physiological Reviews*, *94*(4), 1077–1098. https://doi.org/10.1152/physrev.00041.2013

Pekny, M., Pekna, M., Messing, A., Steinhäuser, C., Lee, J.-M., Parpura, V., Hol, E. M., Sofroniew, M. V., & Verkhratsky, A. (2016). Astrocytes: A central element in neurological diseases. *Acta Neuropathologica*, *131*(3), 323–345. https://doi.org/10.1007/s00401-015-1513-1

Perez-Catalan, N. A., Doe, C. Q., & Ackerman, S. D. (2021). The role of astrocyte-mediated plasticity in neural circuit development and function. *Neural Development*, *16*(1), 1. https://doi.org/10.1186/s13064-020-00151-9

Pernas, L., & Scorrano, L. (2016). Mito-Morphosis: Mitochondrial Fusion, Fission, and Cristae Remodeling as Key Mediators of Cellular Function. *Annual Review of Physiology*, *78*, 505–531. https://doi.org/10.1146/annurev-physiol-021115-105011

Pickles, S., Vigié, P., & Youle, R. J. (2018). Mitophagy and Quality Control Mechanisms in Mitochondrial Maintenance. *Current Biology*, *28*(4), R170–R185. https://doi.org/10.1016/j.cub.2018.01.004

Povlishock, J. T., & Katz, D. I. (2005). Update of Neuropathology and Neurological Recovery After Traumatic Brain Injury. *The Journal of Head Trauma Rehabilitation*, *20*(1), 76–94.

Qi, X., Disatnik, M.-H., Shen, N., Sobel, R. A., & Mochly-Rosen, D. (2011). Aberrant mitochondrial fission in neurons induced by protein kinase Cδ under oxidative stress conditions in vivo. *Molecular Biology of the Cell*, *22*(2), 256–265. https://doi.org/10.1091/mbc.E10-06-0551

Rahman, M. H., & Suk, K. (2020). Mitochondrial Dynamics and Bioenergetic Alteration During Inflammatory Activation of Astrocytes. *Frontiers in Aging Neuroscience*, *12*, 614410. https://doi.org/10.3389/fnagi.2020.614410

Raps, S. P., Lai, J. C. K., Hertz, L., & Cooper, A. J. L. (1989). Glutathione is present in high concentrations in cultured astrocytes but not in cultured neurons. *Brain Research*, *493*(2), 398–401. https://doi.org/10.1016/0006-8993(89)91178-5

Ravin, R., Blank, P. S., Busse, B., Ravin, N., Vira, S., Bezrukov, L., Waters, H., Guerrero-Cazares, H., Quinones-Hinojosa, A., Lee, P. R., Fields, R. D., Bezrukov, S. M., & Zimmerberg, J. (2016). Blast shockwaves propagate Ca2+ activity via purinergic astrocyte networks in human central nervous system cells. *Scientific Reports*, *6*, 25713. https://doi.org/10.1038/srep25713

Ravin, R., Blank, P. S., Steinkamp, A., Rappaport, S. M., Ravin, N., Bezrukov, L., Guerrero-Cazares, H., Quinones-Hinojosa, A., Bezrukov, S. M., & Zimmerberg, J. (2012). Shear Forces during Blast, Not Abrupt Changes in Pressure Alone, Generate Calcium Activity in Human Brain Cells. *PLOS ONE*, *7*(6), e39421. https://doi.org/10.1371/journal.pone.0039421

Rose, J., Brian, C., Pappa, A., Panayiotidis, M. I., & Franco, R. (2020). Mitochondrial Metabolism in Astrocytes Regulates Brain Bioenergetics, Neurotransmission and Redox Balance. *Frontiers in Neuroscience*, *14*, 536682. https://doi.org/10.3389/fnins.2020.536682

Rose, J., Brian, C., Woods, J., Pappa, A., Panayiotidis, M. I., Powers, R., & Franco, R. (2017). Mitochondrial dysfunction in glial cells: Implications for neuronal homeostasis and survival. *Toxicology*, *391*, 109–115. https://doi.org/10.1016/j.tox.2017.06.011

Sajja, V. S. S. S., Ereifej, E. S., & VandeVord, P. J. (2014). Hippocampal vulnerability and subacute response following varied blast magnitudes. *Neuroscience Letters*, *570*, 33–37. https://doi.org/10.1016/j.neulet.2014.03.072

Sajja, V. S. S. S., Galloway, M. P., Ghoddoussi, F., Thiruthalinathan, D., Kepsel, A., Hay, K., Bir, C. A., & VandeVord, P. J. (2012). Blast-induced neurotrauma leads to neurochemical changes and neuronal degeneration in the rat hippocampus: BLAST EFFECT ON HIPPOCAMPUS LEADS TO NEUROCHEMICAL CHANGES. *NMR in Biomedicine*, *25*(12), 1331–1339. https://doi.org/10.1002/nbm.2805

Sajja, V. S. S. S., Hlavac, N., & VandeVord, P. J. (2016). Role of Glia in Memory Deficits Following Traumatic Brain Injury: Biomarkers of Glia Dysfunction. *Frontiers in Integrative Neuroscience*, *10*. https://doi.org/10.3389/fnint.2016.00007

Sajja, V. S. S. S., Hubbard, W. B., Hall, C. S., Ghoddoussi, F., Galloway, M. P., & VandeVord, P. J. (2015). Enduring deficits in memory and neuronal pathology after blast-induced traumatic brain injury. *Scientific Reports*, *5*, 15075. https://doi.org/10.1038/srep15075

Sajja, V. S. S. S., Hubbard, W. B., & VandeVord, P. J. (2015). Subacute Oxidative Stress and Glial Reactivity in the Amygdala are Associated with Increased Anxiety Following Blast Neurotrauma. *Shock (Augusta, Ga.)*, *44 Suppl 1*, 71–78. https://doi.org/10.1097/SHK.0000000000000311

Säljö, A., Bolouri, H., Mayorga, M., Svensson, B., & Hamberger, A. (2010). Low-Level Blast Raises Intracranial Pressure and Impairs Cognitive Function in Rats: Prophylaxis with Processed Cereal Feed. *Journal of Neurotrauma*, *27*(2), 383–389. https://doi.org/10.1089/neu.2009.1053

Sarkar, S., Malovic, E., Harischandra, D. S., Ngwa, H. A., Ghosh, A., Hogan, C., Rokad, D., Zenitsky, G., Jin, H., Anantharam, V., Kanthasamy, A. G., & Kanthasamy, A. (2018). Manganese exposure induces neuroinflammation by impairing mitochondrial dynamics in astrocytes. *NeuroToxicology*, *64*, 204–218. https://doi.org/10.1016/j.neuro.2017.05.009

Sawyer, T. W., Lee, J. J., Villanueva, M., Wang, Y., Nelson, P., Song, Y., Fan, C., Barnes, J., & McLaws, L. (2017). The Effect of Underwater Blast on Aggregating Brain Cell Cultures. *Journal of Neurotrauma*, *34*(2), 517–528. https://doi.org/10.1089/neu.2016.4430

Schreiner, B., Romanelli, E., Liberski, P., Ingold-Heppner, B., Sobottka-Brillout, B., Hartwig, T., Chandrasekar, V., Johannssen, H., Zeilhofer, H. U., Aguzzi, A., Heppner, F., Kerschensteiner, M., & Becher, B. (2015). Astrocyte Depletion Impairs Redox Homeostasis and Triggers Neuronal Loss in the Adult CNS. *Cell Reports*, *12*(9), 1377–1384. https://doi.org/10.1016/j.celrep.2015.07.051

Schwerin, S. C., Chatterjee, M., Hutchinson, E. B., Djankpa, F. T., Armstrong, R. C., McCabe, J. T., Perl, D. P., & Juliano, S. L. (2021). Expression of GFAP and Tau Following Blast Exposure in the Cerebral Cortex of Ferrets. *Journal of Neuropathology & Experimental Neurology*, *80*(2), 112–128. https://doi.org/10.1093/jnen/nlaa157

Serasinghe, M. N., & Chipuk, J. E. (2017). Mitochondrial Fission in Human Diseases. *Handbook of Experimental Pharmacology*, *240*, 159–188. https://doi.org/10.1007/164_2016_38

Shih, E. K., & Robinson, M. B. (2018). Role of Astrocytic Mitochondria in Limiting Ischemic Brain Injury? *Physiology*, *33*(2), 99–112. https://doi.org/10.1152/physiol.00038.2017

Siedhoff, H. R., Chen, S., Song, H., Cui, J., Cernak, I., Cifu, D. X., DePalma, R. G., & Gu, Z. (2022). Perspectives on Primary Blast Injury of the Brain: Translational Insights Into Non-inertial Low-Intensity Blast Injury. *Frontiers in Neurology*, *12*, 818169. https://doi.org/10.3389/fneur.2021.818169

Silver, J., & Miller, J. H. (2004). Regeneration beyond the glial scar. *Nature Reviews Neuroscience*, *5*(2), 146–156. https://doi.org/10.1038/nrn1326

Smirnova, E., Griparic, L., Shurland, D.-L., & van der Bliek, A. M. (2001). Dynamin-related Protein Drp1 Is Required for Mitochondrial Division in Mammalian Cells. *Molecular Biology of the Cell*, *12*(8), 2245–2256.

Sofroniew, M. V. (2009). Molecular dissection of reactive astrogliosis and glial scar formation. *Trends in Neurosciences*, *32*(12), 638–647. https://doi.org/10.1016/j.tins.2009.08.002

Sofroniew, M. V. (2015a). Astrogliosis. *Cold Spring Harbor Perspectives in Biology*, *7*(2), a020420. https://doi.org/10.1101/cshperspect.a020420

Sofroniew, M. V. (2015b). Astrogliosis. *Cold Spring Harbor Perspectives in Biology*, *7*(2), a020420. https://doi.org/10.1101/cshperspect.a020420

Sofroniew, M. V. (2020). Astrocyte Reactivity: Subtypes, States, and Functions in CNS Innate Immunity. *Trends in Immunology*, *41*(9), 758–770. https://doi.org/10.1016/j.it.2020.07.004

Sofroniew, M. V., & Vinters, H. V. (2010). Astrocytes: Biology and pathology. *Acta Neuropathologica*, *119*(1), 7–35. https://doi.org/10.1007/s00401-009-0619-8

Souza, D. G., Bellaver, B., Souza, D. O., & Quincozes-Santos, A. (2013). Characterization of Adult Rat Astrocyte Cultures. *PLOS ONE*, *8*(3), e60282. https://doi.org/10.1371/journal.pone.0060282

Sprenger, H.-G., & Langer, T. (2019). The Good and the Bad of Mitochondrial Breakups. *Trends in Cell Biology*, *29*(11), 888–900. https://doi.org/10.1016/j.tcb.2019.08.003

Sridharan, P., Vásquez-Rosa, E., Shin, M.-K., Franke, K. Z., Koh, Y. J., Qi, X., & Pieper, A. (2021). Role of Mitochondrial Fission-Fusion Dynamics in Progressive Neurodegeneration and Memory Deficit After Traumatic Brain Injury. *Biological Psychiatry*, *89*(9), S119–S120. https://doi.org/10.1016/j.biopsych.2021.02.309

Stephen, T.-L., Gupta-Agarwal, S., & Kittler, J. T. (2014). Mitochondrial dynamics in astrocytes. *Biochemical Society Transactions*, *42*(5), 1302–1310. https://doi.org/10.1042/BST20140195

Stephen, T.-L., Higgs, N. F., Sheehan, D. F., Al Awabdh, S., López-Doménech, G., Arancibia-Carcamo, I. L., & Kittler, J. T. (2015). Miro1 Regulates Activity-Driven Positioning of Mitochondria within Astrocytic Processes Apposed to Synapses to Regulate Intracellular Calcium Signaling. *The Journal of Neuroscience*, *35*(48), 15996–16011. https://doi.org/10.1523/JNEUROSCI.2068-15.2015

Susin, S. A., Lorenzo, H. K., Zamzami, N., Marzo, I., Snow, B. E., Brothers, G. M., Mangion, J., Jacotot, E., Costantini, P., Loeffler, M., Larochette, N., Goodlett, D. R., Aebersold, R., Siderovski, D. P., Penninger, J. M., & Kroemer, G. (1999). Molecular characterization of mitochondrial apoptosis-inducing factor. *Nature*, *397*(6718), 441–446. https://doi.org/10.1038/17135

Swanson, T. M., Isaacson, B. M., Cyborski, C. M., French, L. M., Tsao, J. W., & Pasquina, P. F. (2017). Traumatic Brain Injury Incidence, Clinical Overview, and Policies in the US Military Health System Since 2000. *Public Health Reports*, *132*(2), 251–259. https://doi.org/10.1177/0033354916687748

Taguchi, N., Ishihara, N., Jofuku, A., Oka, T., & Mihara, K. (2007). Mitotic Phosphorylation of Dynamin-related GTPase Drp1 Participates in Mitochondrial Fission *. *Journal of Biological Chemistry*, *282*(15), 11521–11529. https://doi.org/10.1074/jbc.M607279200

Theeler, B. J., Flynn, F. G., & Erickson, J. C. (2012). Chronic Daily Headache in U.S. Soldiers After Concussion. *Headache: The Journal of Head and Face Pain*, *52*(5), 732–738. https://doi.org/10.1111/j.1526-4610.2012.02112.x

Toklu, H. Z., Yang, Z., Oktay, S., Sakarya, Y., Kirichenko, N., Matheny, M. K., Muller-Delp, J., Strang, K., Scarpace, P. J., Wang, K. K. W., & Tümer, N. (2018). Overpressure blast injury-induced oxidative stress and neuroinflammation response in rat frontal cortex and cerebellum. *Behavioural Brain Research*, *340*, 14–22. https://doi.org/10.1016/j.bbr.2017.04.025

Torres-Ceja, B., & Olsen, M. L. (2022). A closer look at astrocyte morphology: Development, heterogeneity, and plasticity at astrocyte leaflets. *Current Opinion in Neurobiology*, *74*, 102550. https://doi.org/10.1016/j.conb.2022.102550

Trudeau, D. L., Anderson, J., Hansen, L. M., Shagalov, D. N., Schmoller, J., Nugent, S., & Barton, S. (1998). Findings of Mild Traumatic Brain Injury in Combat Veterans With PTSD and a History of Blast Concussion. *The Journal of Neuropsychiatry and Clinical Neurosciences*, *10*(3), 308–313. https://doi.org/10.1176/jnp.10.3.308

Tsushima, K., Bugger, H., Wende, A. R., Soto, J., Jenson, G. A., Tor, A. R., McGlauflin, R., Kenny, H. C., Zhang, Y., Souvenir, R., Hu, X. X., Sloan, C. L., Pereira, R. O., Lira, V. A., Spitzer, K. W., Sharp, T. L., Shoghi, K. I., Sparagna, G. C., Rog-Zielinska, E. A., … Abel, E. D. (2018). Mitochondrial Reactive Oxygen Species in Lipotoxic Hearts Induce Post-Translational Modifications of AKAP121, DRP1, and OPA1 That Promote Mitochondrial Fission. *Circulation Research*, *122*(1), 58–73. https://doi.org/10.1161/CIRCRESAHA.117.311307

Valente, A. J., Maddalena, L. A., Robb, E. L., Moradi, F., & Stuart, J. A. (2017). A simple ImageJ macro tool for analyzing mitochondrial network morphology in mammalian cell culture. *Acta Histochemica*, *119*(3), 315–326. https://doi.org/10.1016/j.acthis.2017.03.001

VandeVord, P. J., Leung, L. Y., Hardy, W., Mason, M., Yang, K. H., & King, A. I. (2008). Up-regulation of reactivity and survival genes in astrocytes after exposure to short duration overpressure. *Neuroscience Letters*, *434*(3), 247–252. https://doi.org/10.1016/j.neulet.2008.01.056

Venance, L., Stella, N., Glowinski, J., & Giaume, C. (1997). Mechanism Involved in Initiation and Propagation of Receptor-Induced Intercellular Calcium Signaling in Cultured Rat Astrocytes.

Journal of Neuroscience, *17*(6), 1981–1992. https://doi.org/10.1523/JNEUROSCI.17-06-01981.1997

Voskuhl, R. R., Peterson, R. S., Song, B., Ao, Y., Morales, L. B. J., Tiwari-Woodruff, S., & Sofroniew, M. V. (2009). Reactive Astrocytes Form Scar-Like Perivascular Barriers to Leukocytes during Adaptive Immune Inflammation of the CNS. *Journal of Neuroscience*, *29*(37), 11511–11522. https://doi.org/10.1523/JNEUROSCI.1514-09.2009

Wallace, D. C. (2005). A Mitochondrial Paradigm of Metabolic and Degenerative Diseases, Aging, and Cancer: A Dawn for Evolutionary Medicine. *Annual Review of Genetics*, *39*, 359. https://doi.org/10.1146/annurev.genet.39.110304.095751

Walther, D. M., & Rapaport, D. (2009). Biogenesis of mitochondrial outer membrane proteins. *Biochimica et Biophysica Acta (BBA) - Molecular Cell Research*, *1793*(1), 42–51. https://doi.org/10.1016/j.bbamcr.2008.04.013

Wang, C., Pahk, J. B., Balaban, C. D., Miller, M. C., Wood, A. R., & Vipperman, J. S. (2014). Computational Study of Human Head Response to Primary Blast Waves of Five Levels from Three Directions. *PLoS ONE*, *9*(11), e113264. https://doi.org/10.1371/journal.pone.0113264

Wanner, I. B., Anderson, M. A., Song, B., Levine, J., Fernandez, A., Gray-Thompson, Z., Ao, Y., & Sofroniew, M. V. (2013). Glial Scar Borders Are Formed by Newly Proliferated, Elongated Astrocytes That Interact to Corral Inflammatory and Fibrotic Cells via STAT3-Dependent Mechanisms after Spinal Cord Injury. *Journal of Neuroscience*, *33*(31), 12870–12886. https://doi.org/10.1523/JNEUROSCI.2121-13.2013

Xie, J., Hong, E., Ding, B., Jiang, W., Zheng, S., Xie, Z., Tian, D., & Chen, Y. (2020). Inhibition of NOX4/ROS Suppresses Neuronal and Blood-Brain Barrier Injury by Attenuating Oxidative Stress After Intracerebral Hemorrhage. *Frontiers in Cellular Neuroscience*, *14*. https://www.frontiersin.org/articles/10.3389/fncel.2020.578060

Yi, J.-H., & Hazell, A. S. (2006). Excitotoxic mechanisms and the role of astrocytic glutamate transporters in traumatic brain injury. *Neurochemistry International*, *48*(5), 394–403. https://doi.org/10.1016/j.neuint.2005.12.001

Youle, R. J., & van der Bliek, A. M. (2012). Mitochondrial Fission, Fusion, and Stress. *Science (New York, N.Y.)*, *337*(6098), 1062–1065. https://doi.org/10.1126/science.1219855

Yu, R., Lendahl, U., Nistér, M., & Zhao, J. (2020). Regulation of Mammalian Mitochondrial Dynamics: Opportunities and Challenges. *Frontiers in Endocrinology*, *11*. https://www.frontiersin.org/articles/10.3389/fendo.2020.00374

Zander, N. E., Piehler, T., Banton, R., & Benjamin, R. (2016). Effects of repetitive low-pressure explosive blast on primary neurons and mixed cultures. *Journal of Neuroscience Research*, *94*(9), 827–836. https://doi.org/10.1002/jnr.23786

Zehnder, T., Petrelli, F., Romanos, J., De Oliveira Figueiredo, E. C., Lewis, T. L., Déglon, N., Polleux, F., Santello, M., & Bezzi, P. (2021). Mitochondrial biogenesis in developing astrocytes regulates astrocyte maturation and synapse formation. *Cell Reports*, *35*(2), 108952. https://doi.org/10.1016/j.celrep.2021.108952

Zhong, S., Du, Y., Kiyoshi, C. M., Ma, B., Alford, C. C., Wang, Q., Yang, Y., Liu, X., & Zhou, M. (2016). Electrophysiological behavior of neonatal astrocytes in hippocampal stratum radiatum. *Molecular Brain*, *9*(1). https://doi.org/10.1186/s13041-016-0213-7

Zhou, Y., Shao, A., Yao, Y., Tu, S., Deng, Y., & Zhang, J. (2020). Dual roles of astrocytes in plasticity and reconstruction after traumatic brain injury. *Cell Communication and Signaling*, *18*(1), 62. https://doi.org/10.1186/s12964-020-00549-2